UiT The Arctic University of Norway

Faculty of Bioscience, Fisheries and Economics
Department of Arctic and Marine Biology

Are Hooded seals (*Cystophora cristata*) endowed with mechanisms for non-shivering thermogenesis within the skeletal muscle?

Matthew Chiu
BIO-3950 Master thesis in Biology
June 2022

Photo by Marie Aas Westvick

Table of Contents

Foreword

Then God said, “Let us make mankind in our image, in our likeness, so that they may rule over the fish in the sea and the birds in the sky, over the livestock and all the wild animals, and over all the creatures that move along the ground.” ~Genesis 1:26

“It's surely our responsibility to do everything within our power to create a planet that provides a home not just for us, but for all life on Earth.” ~David Attenborough

Acknowledgements

Firstly, I would like to thank my supervisors, Lars Folkow, Shona Wood and Chiara Ciccone, for your help, guidance and most of all your patience. Without you, the work produced here would not have been realized.

The support of my friends has been much appreciated and I wish to nurture and strengthen the bonds made during our two years together. Except you Matt Coyle… we got some things to sort out buddy..

Thank you, Rina, for all the lunches and dinners you made me when I didn't have time to think about anything else. Thank you for your love and support.

Mum and Dad, thank you for your love and care, I dedicate this work to you. Hope you are proud.

Lastly, I thank God. Thank you for giving me the strength and power to move on and on, to never quit. Thank you for your grace, the friendships you put in my life and… the loves.

I hope I never do western blots again…

Abstract

Hooded seals (*Cystophora cristata*) are marine mammals and are characterised as an "Arctic seal" species due to their close association to the pack ice. Their relationship with the ice and water creates challenges in maintaining an internal body temperature of ~37°C. In homeothermic animals, like the hooded seal, shivering is used for thermogenesis, however this can rapidly fatigue skeletal muscle. Other mechanisms of thermogenesis have been found which do not employ the use of shivering thermogenesis and are termed non-shivering thermogenesis (NST) mechanisms. A common area of NST study is the thermogenic mechanism found in brown adipose tissue (BAT). The presence of BAT in mammals is common, particularly in the neonatal life stages where surface area to volume ratio is high and is noticeably present in other seal species e.g. harp seals, which share the same distribution and environmental hardships as hooded seals. However, the presence of BAT has not been reported in hooded seals. Studies in other species have shown that in the absence of BAT, skeletal muscle tissue can be utilised in a non-shivering mechanism using an interaction between Sarcolipin (Sln) and Ca^{2+} ATPase (SERCA) transport protein that produces futile cycling of Ca^{2+}, as well as through a decreased efficiency in mitochondrial processes known as mitochondrial proton LEAK.

Within this study I set out to find whether hooded seals utilise these skeletal muscle based, non-shivering thermogenesis mechanisms and whether those mechanisms are most likely to be found in the neonatal life stages compared to later life stages. *In silico* DNA sequence comparisons of Sln, and the SERCA isoforms, SERCA1a and SERCA2a across 10 mammals including marine mammals from the suborder *Pinnipedia* revealed that these proteins were highly conserved providing proof of principle that a Sln-SERCA NST mechanism could exist. To identify these proteins in hooded seals, western blotting of skeletal muscle samples taken from *M. longissimus dorsi (M. long)* and *Psoas major (P. major)* from adult (n=5) and neonatal (n=4) hooded seals was attempted. SERCA2a was found to be present at high levels in both muscle groups with a significantly higher expression in the neonatal life stage but only in the muscle *M. long* ($p=0.042$). It was not possible to determine the amount of Sln and SERCA1a by western blotting, therefore there is not enough evidence to determine whether there is a Sln-SERCA NST mechanism and further work is required. However, the

significantly high expression of SERCA2a within the neonatal life stage of hooded seals may relate to an increased shivering capacity rather than an NST mechanism.

The detection of mitochondrial LEAK was carried out by tissue respirometry using skeletal muscle samples from juvenile hooded seals (n=6). A high mitochondrial LEAK was found in *M. long* and *P. major* but was shown not to be linked to a non-shivering thermogenesis mechanism. This high mitochondrial LEAK may be associated to an inherent mechanism used to decrease the production of harmful reactive oxygen species in this deep-diving marine mammal. In conclusion, the thick blubber layer, shivering and heat conservation mechanisms already present in hooded seals may be sufficient to maintain body temperature without the addition of a NST mechanism.

Key words: Hooded seal, skeletal muscle, non-shivering thermogenesis, NST, Sarcolipin, SERCA, mitochondria, LEAK.

Introduction

Hooded seals (*Cystophora cristata;* Fig.1) are classed as a marine mammal, from the family *Phocidae* and are hence considered "true seals" which belong to one of the three suborders of the seal line, *Pinnipedia*. Although hooded seals have a fur coat, they are not to be confused with fur seals which belong to the sub order *Otariidae*. Hooded seals are also one of the six species characterised as "Arctic seals" (Blix, 2005). These Arctic seals all share similar traits and behaviour which provide an advantage in living in the Arctic;

I. They give birth and breed on the pack ice.
II. Have a significant blubber layer which provides them with insulation (Scholander et al., 1950;Irving, 1973) .
III. Arctic seal pups have a lanugo fur, however hooded seal pups shed their lanugo fur *in utero* (Kvadsheim and Aarseth, 2002).
IV. Lactation period for the pups is extremely short, ranging from a few days to weeks, depending on the species of Arctic seal (Bowen et al., 1985).
V. Their milk is high in fat, resulting in a nutritious source high in energy (Oftedal, 1984).
VI. The lactation is always followed by breeding and moulting.
VII. Arctic seals all have a delayed implantation (Sandell, 1990).

Figure 1 Adult female Hooded seal (right) and her pup (left). *Photo taken by Marie Westvik.*

The name “hooded seal” is derived from the inflation of the nasal cavity which is something only present in the males. The nasal cavity is inflated during times of excitement and appears on top of the head, resembling a “hood” (Fig.2A). Male seals can also inflate their nasal septum, through the nostrils appearing as a red bladder and therefore sometimes referred to as the “bladder-nose seal” (Fig.2B). The display is used primarily during the mating season as a way to entice females as well as a form of showing aggression to other males (Blix, 2005).

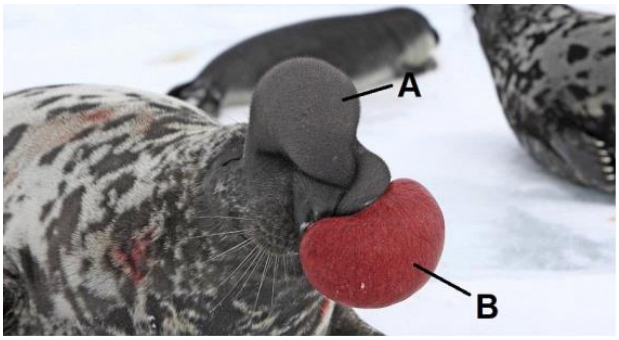

Figure 2. The nasal cavity of a male hooded seal. *(**A**) nasal cavity (**B**) nasal septum. Photo by: Sylvain Cordier*

Their distribution includes much of the North Atlantic and areas within the Arctic oceans (Folkow and Blix, 1995) with populations stocks of two regions: the Northeast (NE) Atlantic and Northwest (NW) Atlantic stocks (Sergeant, 1974) (Fig.3).

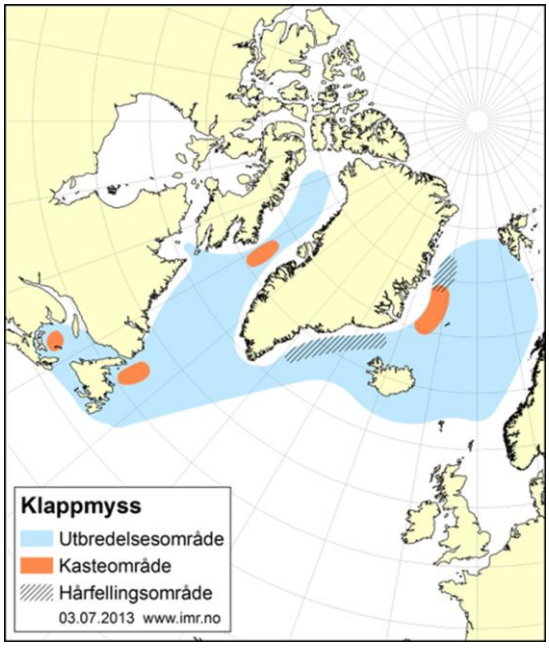

Figure 3 Distribution of hooded seals within the Atlantic Ocean. *Blue areas denote general distribution of both Northeast and Northwest atlantic stocks. Orange areas denote breeding areas. Dashed areas denote moulting areas. Image from:(Gjertsen et al., 2019), based on data from Folkow et al. (1996), DFO, Canada and the Greenland Institute of Natural Resources.*

The Northeast Atlantic stock (ca. 76,000) consist of hooded seals which breed on ice floes off the coast of Greenland, west of Jan Mayen known as the "West ice" (Folkow et al., 1996;ICES, 2019). The Northwest Atlantic stock (ca. 600,000) consists of Hooded seals which breed in the Davis Strait, the Gulf of St. Lawrence and Newfoundland, also known as the "Front"(Sergeant, 1974;Folkow et al., 1996;Hammill and Stenson, 2006).

Hooded seals mainly feed on pelagic amphipods (*Parathemisto spp.*), squid (*Gonatus fabricii*), polar cod (*Boreogadus saida*) and capelin (*Mallotus villosus*). The contribution of these species to their diet changes with seasons, with squid and capelin being the dominant prey during the winter and polar cod being more dominant in the summer (Haug et al., 2004). Larger demersal fishes such as Greenland halibut (*Reinhardtius spp.*), redfish (*Sebastes spp.*), cod (*Gadus morhua*) and wolfish (*Anarhichas minor*) are also considered to be important prey species (Kapel, 2000).

Hooded seals reach sexual maturity roughly between 4-6 and 3-5 years for males and females respectively; populations in both the Northwest and Northeast Atlantic stocks breed and give birth in pack ice within the Arctic circle during late March (Rasmussen, 1960;Folkow et al., 1996;Coltman et al., 2007). Pups are born during the spring period towards the end of March and are born without their lanugo fur which has been shed in utero. Instead, they have fur with a distinct blue-grey hue on the dorsal side and white hue on the ventral side and are termed "bluebacks" due to their pelage (Fig.1). Once born the pups feed on fat enriched milk constituting to 61% fat for 4 days and gaining up to 7kg per day from an initial weight of just 22kg (Bowen et al., 1987;Oftedal et al., 1988). Upon weaning, pups are left unaccompanied by the mother as she leaves to mate (Rasmussen, 1960). The weaned pup is then closely associated with the pack ice, undergoing roughly 4 weeks fasting and exploiting the snow and ice as a source of freshwater (Bowen et al., 1987;Schots et al., 2017). During this fast, pups learn and familiarize themselves with the marine habitat and develop diving capabilities quite rapidly, reaching depths >100m at just 3 weeks of age (Folkow et al., 2010). After the fast has ended, pups from the NE Atlantic stock migrate off the ice floes and into open water off the coast of Greenland and towards the north of Iceland moving towards feeding grounds (Fig.4B) and following similar patterns of adult hooded seals from the "West ice" stock (Folkow et al., 1996;Folkow et al., 2010)(Fig.4A). After one full year these pups are now considered juveniles and undergo an annual moult, shedding their distinctive blue-grey coat

progressively for black/brown spots on a silver/grey background. Once sexually mature they will then join their adult predecessors upon the ice floes to seek a mate and successful females will then return 11 months later to give birth (Kovacs, 2009).

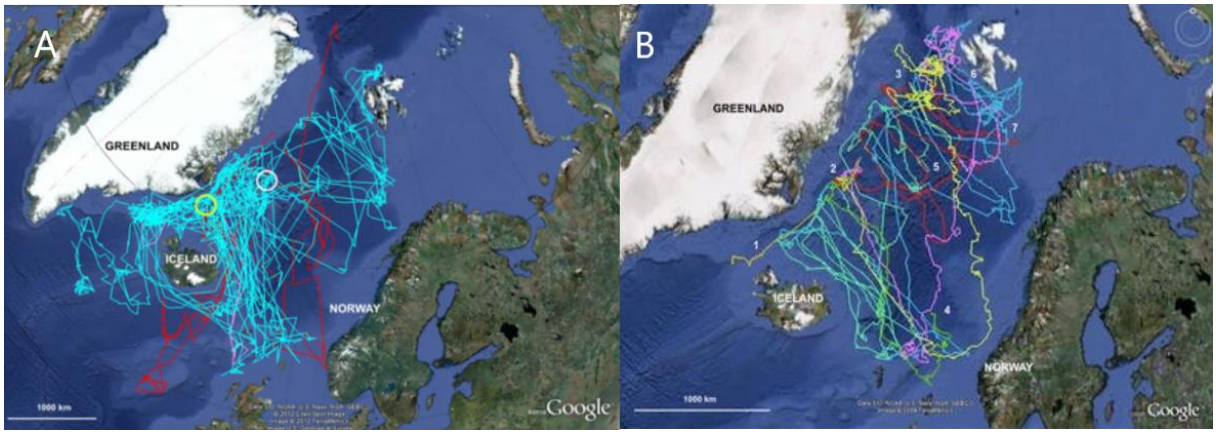

***Figure 4**. **Tracking of hooded seals from the "West ice" population**. **A**=Migration of adult hooded seals. Showing the movement of 15 hooded seals between July 1992-March 1993 (Blue lines). Violet lines indicate continued tracking of 6 seals post breeding in March 1993. Red lines indicate 4 seals tagged during breeding in March 1993 until the moult. White circle indicates place of general tagging. Yellow circle indicates tagging site of seals during breeding (Blix et al., 2013). **B**=Distribution of 7 hooded seal pups post wean tracked by Argos satellite tags (Folkow et al., 2010).*

Thermoregulation

Hooded seals are homeotherms and reside in a habitat which can reach temperatures to well below 0°C with average winter temperatures reaching down to -30°C (Labe, 2022). Sea surface temperatures are warmer at roughly -1.8°C (Timmermans and Labe, 2021). However, these seals are marine mammals and spend a considerable amount of time in the water which has an increased thermal conductivity of 25x that of air (Schmidt-Nielsen, 1997). Hooded seals have therefore evolved a multitude of physiological mechanisms as well as morphological characteristics to combat this harsh environment. The most notable of all being a prominent insulating blubber layer where its insulating properties do not change either in air or in water, making it a perfect insulator for marine mammals (Scholander et al., 1950;Blix and Steen, 1979).

In the following section I will review heat conservation and thermogenic mechanisms that are typical of homeotherms living in an arctic environment and have already been described in hooded seals.

Heat conservation mechanisms

Vasoconstriction

Vasoconstriction is a general mechanism found in all homeotherms where the constriction of blood vessels minimises heat loss. To conserve heat, homeotherms constrict blood vessels limiting blood flow to the skin and appendages. In hooded seals, the limited blood flow to the skin "short circuits" the blood flow and a larger proportion of blood circulates through the arteriovenous shunt keeping warm blood behind the insulative blubber layer (Fig.5). Vasoconstriction can also occur in the appendages reducing the blood flow and essentially decreasing the surface area of heat loss (Bartholomew and Wilke, 1956;Irving and Hart, 1957;Kvadsheim and Folkow, 1997;Davis, 2019).

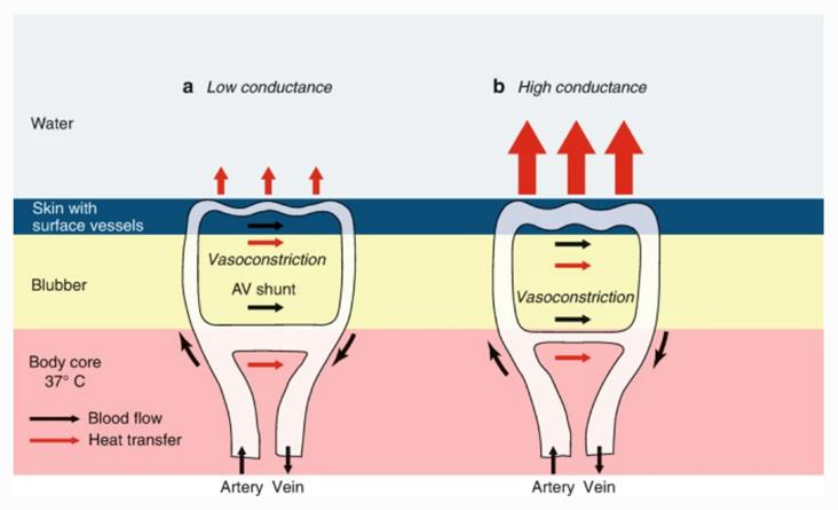

Figure 5*. *Vasoconstriction minimises heat loss. *Constriction and vasodilation of arterioles and arteriovenous (AV) shunts can regulate heat in marine mammals. Constriction reduces blood flow to the skin allowing the insulative properties of blubber to take effect. Dilation bypasses the blubber layer to allow excess heat to be released. (Davis, 2019)*

Counter-current heat exchange

Vasoconstriction is further included in the form of counter-current heat exchange systems in the outlying appendages, where the arterioles and venules are arranged in parallel to each other. Counter-current heat exchange is also present in other homeothermic animals which experience cold stress such as reindeer (*Rangifer tarandus*) and ptarmigan (*Lagopus spp*)(Johnson, 1968;Johnsen et al., 1985). However, in hooded seals constriction of smooth muscle within certain arterioles and arteriovenous vessels of their flippers results in a blood pathway which allows for an exchange of heat between the warm, outgoing arterial blood and

the cold incoming venous blood, keeping heat closer to the body core which minimises heat lost to the environment (Fig.6)(Scholander and Schevill, 1955;Mitchell and Myers, 1968;Blix et al., 2010). The parallel blood vessels are often split into a complex system known as “rete mirabile” to massively increase surface area and maximise heat transfer (Scholander, 1957).

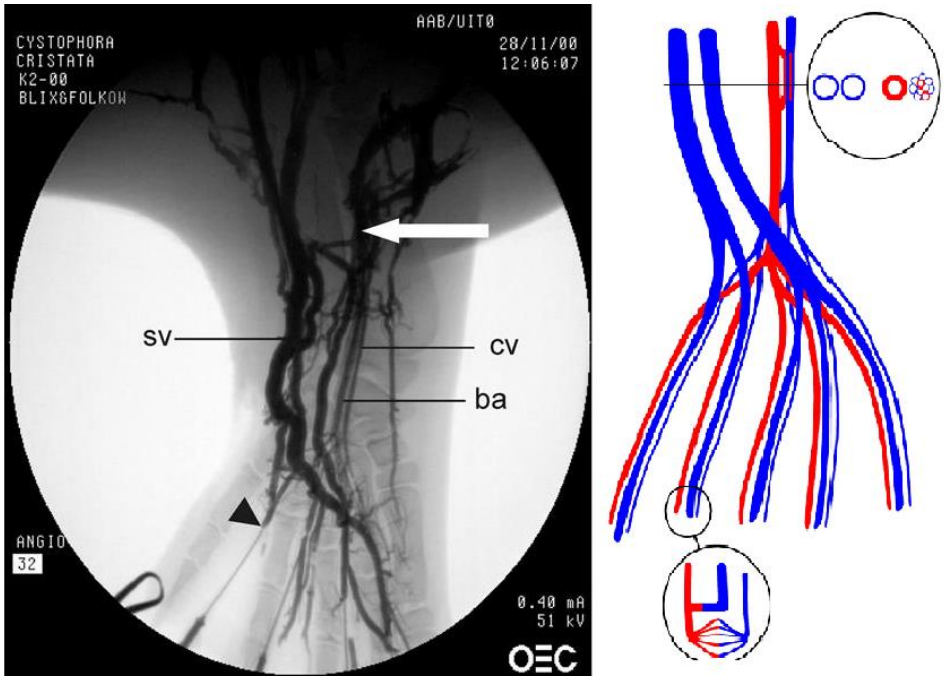

Figure 6. Counter-current heat exchange present in hooded seal foreflipper*. Left panel: An angiogram (left) and schematic drawing (right) of the superficial veins (sv) of a hooded seal foreflipper with the brachial artery (ba) and deep central veins (cv). The white arrow (left) indicates location of a counter-current heat exchanger and a cross-section is shown on the schematic (right). (Blix et al., 2010)*

Nasal Heat Exchange

Heat is not only lost to the environment through the body surfaces but can also be lost through the simple act of breathing. Inhaled air must be heated to body temperature as well as fully saturated with water, creating humid conditions like that of the alveolar spaces within the lung cavity and so due to the processes of convection and evaporation, heat and water is lost from the nasal cavity and once the warm and humid air leaves the nasal cavity and into the atmosphere it is non recoverable (Jackson and Schmidt-Nielsen, 1964). The nasal cavity within seals is made up of dorsal and ventral nasal conchae which house a complex mucosal rete. The arterial nasal concha rete runs in a counter current fashion to the venous rete (Folkow et al., 1988). This counter-current system reduces the amount of heat and water lost

upon exhalation, with the site of recovery being in the nasal cavity before it reaches the atmosphere. Due to the counter-current vasculature, the nasal cavity remains cold when cold air is inhaled; upon exhalation the warm and humid air comes into contact with the cold nasal mucosa and the warm air deposits heat back into the nasal cavity and the water condenses. This mechanism is termed the Nasal heat exchange (NHE)(Folkow et al., 1988;Blix, 2005). In grey seals (*Halichoerus grypus*), this mechanism has the potential to reduce heat loss and water loss by 66% and 80% respectively, the efficiency of which is controlled by sympathetic nervous input to key vessels of the nasal mucosal vasculature; this mechanism is thought to be common in phocid seals (Folkow and Blix, 1987;Folkow et al., 1988;Folkow, 1992).

Surface area and heat loss

Commonly known to all is the relationship between surface area (SA) and volume, where an increase per unit of volume SA increases 2/3 the power (Meeh, 1879). This relationship shows that smaller objects have a higher SA per unit volume compared to larger objects. Even more known is the relationship of SA and heat loss where an increase in SA increases the rate of heat loss (Berman, 2003). This is due to more surfaces being exposed to the surrounding environment allowing the rate of heat transfer through mechanisms such as convection and radiation to increase. In general, seals have a lower surface area to volume ratio (~23%) compared to terrestrial mammals (Innes et al., 1990). However hooded seal pups, and any new-born, are smaller and hence have a larger SA:V ratio compared to adults. To combat this, hooded seal pups are born with a relatively significant blubber layer compared to other species in the same environment such as the harp seal (Blix and Steen, 1979;Kvadsheim and Aarseth, 2002). Researchers have suggested that the already existing blubber layer is sufficient for keeping pups insulated but only when briefly submerged in cold seawater (Lydersen et al., 1997). The insulative blubber also diminishes throughout the 4 week fast, losing roughly 1.2kg/day during the first week and on average 0.4kg/day throughout the entirety of the fast (Bowen et al., 1987). During the fasting period, pups stay closely associated with the pack ice and although already insulated with blubber, may experience thermoregulatory stress due to the factors mentioned above.

Furthermore, new-born and juvenile animals may not have developed the adult capacity to thermoregulate. Hansen and Lavigne (1997) have shown a link between age and the thermal neutral zone in harbour seals where earlier life stages results in a reduced thermal neutral zone

(TNZ) compared to later life stages, possibly due to poor vasomotor control at birth (Lapierre et al., 2004). This pattern may also be present in hooded seals, resulting in a reliance on other thermoregulatory processes to maintain internal body temperatures.

Thermogenesis

The mechanisms which limit heat loss within the hooded seal are fairly well characterised in literature (Folkow et al., 1988;Folkow, 1992;Blix, 2005;Blix et al., 2010). However, despite these mechanisms the challenges of being a new-born hooded seal may require additional measures. In this section, I will discuss thermogenic mechanisms that are commonly found in homeotherms and discuss any evidence of their use in hooded seals.

Basal metabolic rate and Skeletal Muscle

The basal metabolic rate is the rate at which the body utilises energy to maintain basal functions such as breathing and maintaining internal body temperature (in homeotherms). Due to its very definition, heat production and metabolic rate are tightly linked and a direct measurement of metabolic rate was first described by Lavoisier and Laplace in 1777 with their ice calorimeter. Skeletal muscle is known to be a major contributor to the basal metabolic rate and is the largest organ in the body contributing between 45%-55% of body mass in humans (Zurlo et al., 1990;Janssen et al., 2000) and 20%-30% in phocid seals (Burns et al., 2007). The first law of thermodynamics states that "energy cannot be created or destroyed, merely transformed or transferred from one form to another". The energy used to drive all life forms comes in the form of adenosine triphosphate (ATP).

Mitochondria are the powerhouse of the cell, phosphorylating adenosine diphosphate (ADP) to ATP. The production of ATP is done by transforming energy through a series of oxidation and reduction reactions (Glycolysis and Krebs Cycle) which produce NADH and $FADH_2$. These two molecules donate their H^+ ions to complex I and II resulting in a transfer of electrons through the electron transport chain with O_2 being the final electron acceptor (Fig.7). This flow of electrons provides the energy necessary for complex I,III and IV to pump protons across the inner mitochondrial membrane which creates a proton electrochemical gradient. The proton gradient is then used to power the protein ATP synthase creating ATP by phosphorylating ADP, this final step is called Oxidative phosphorylation (Mitchell, 1961;Chinnery and Schon, 2003). All forms of work done by skeletal muscle

produce heat through the hydrolysis of ATP and the interactions of actin-myosin, and most modes of contraction are inefficient so only a fraction of the potential energy available is used as work with the rest being liberated as heat (Hill, 1922). Endotherms and subsequently homeotherms utilise this liberated heat to maintain stable internal body temperatures and may also activate shivering to further increase thermogenesis, should temperatures reach below the lower critical limit of the TNZ.

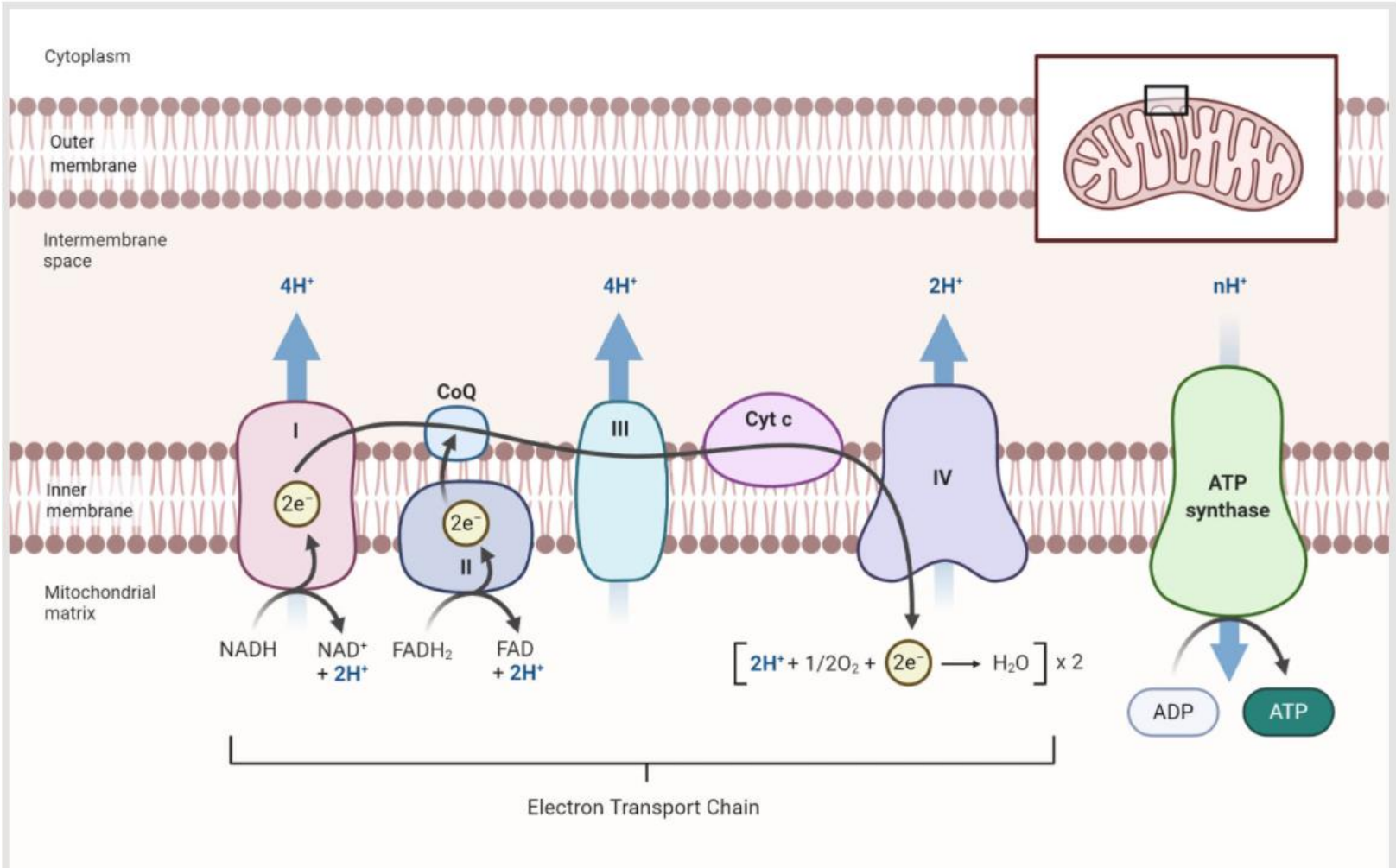

Figure 7. Mitochondrial processes and the production of ATP. *Using products from glycolysis and the Krebs cycle (NADH, FADH), electrons flow across the mitochondrial inner membrane with O_2 as a final electron acceptor. The flow of electrons provide energy for protein complexes I,III and IV to pump protons (H^+) into the intermembrane space, creating a electrochemical gradient which is then utilised by ATP synthase to create ATP. Image created by biorender.com*

Shivering Thermogenesis

In homeotherms, behavioural mechanisms such as seeking shelter or reducing the surface area as well as the physiological mechanisms mentioned earlier are usually among the first line of defence when combating cold stress, in order to reduce heat loss. However, when that proves to be insufficient in maintaining thermal balance, they resort to thermogenesis, one mechanism of which is to adopt skeletal muscle through the act of shivering. To better describe the process of shivering I will introduce the basic structure and function of muscle.

Muscle Structure

Skeletal muscle consists of bundles of muscle fibre cells within a cell membrane called Sarcolemma. The sarcolemma itself has invaginations of tubes termed transverse tubules or t-tubules which penetrate the muscle fibres transversely, hence their names. The muscle fibres themselves are made of multiple myofibrils that are in cased in a secondary membrane called the sarcoplasmic reticulum (SR). The SR is a network of tubules which are distributed throughout the muscle fibres and contains a solution with a relatively high store of Ca^{2+} ions due to Ca^{2+} ATPase transport proteins (SERCA) maintaining an ion gradient between the cytosol and SR space (MacLennan et al., 1997). Myofibrils themselves house two kinds of myofilaments, a thick filament named myosin and a thin filament named actin. The interaction between these two myofilaments produces the contraction of muscle (Fig.8).

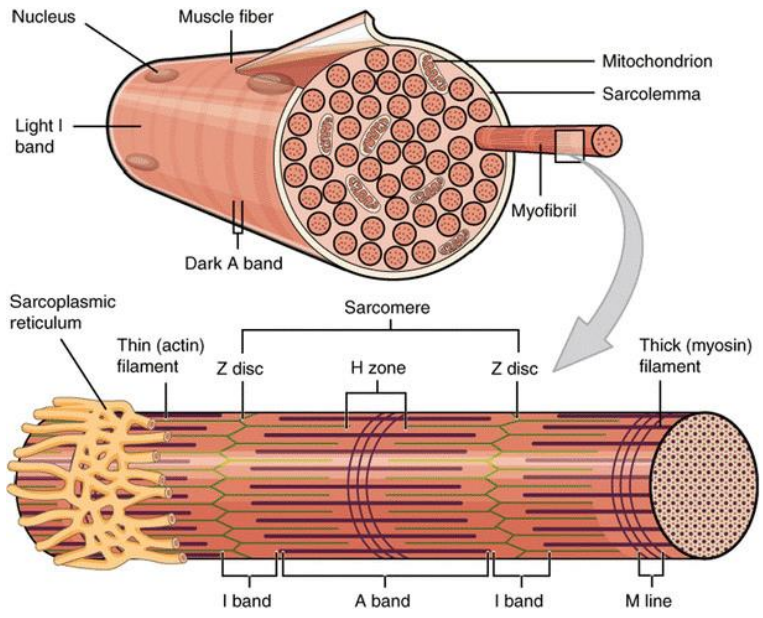

***Figure 8. The hierarchical structure of skeletal muscle**. Muscle fibres encased in a sarcolemma, consist of multiple myofibrils and mitochondria. Myofibrils are encased in a sarcoplasmic reticulum which are a source of Ca^{2+} ions, allowing the thin and thick filaments to interact and cause a contraction. (Oliver et al., 2016) Reproduced from Anatomy and Physiology under Creative Commons Attribution License 4.0 from OpenStax. Copyright 2016*

Muscle Contraction and Role of Ca^{2+}

Actin filaments are wound with regulatory proteins called tropomyosin and troponin which prevent the interaction between itself and myosin. Tropomyosin covers the myosin binding-site and can only be moved through the activation of troponin which can only occur through the presence and binding of Ca^{2+}.

Myosin filaments possess myosin heads/cross bridges which bind to actin creating a pulling action. This action is called the cross-bridge cycle and undergoes multiple cycles in a single contraction. This cycle requires the hydrolysis of ATP. When Ca^{2+} is present and bound to troponin the cross-bridge tightly binds to actin and the myosin head pulls the actin filament.

Contraction can thus, only happen through the presence of Ca^{2+} the release of which is controlled by neural excitation and is termed excitation-contraction coupling. Once action potentials are triggered in the myocyte, they will propagate down the t-tubules into the interior of the myocyte and cause a ryanodine receptor to open which releases the needed Ca^{2+} ions from the SR (Fig.9). Released Ca^{2+} ions now in the cytosol are actively transported back into the SR by way of the Ca^{2+} pump, SERCA (Ebashi and Endo, 1968;Huxley, 1974;Dumonteil et al., 1993).

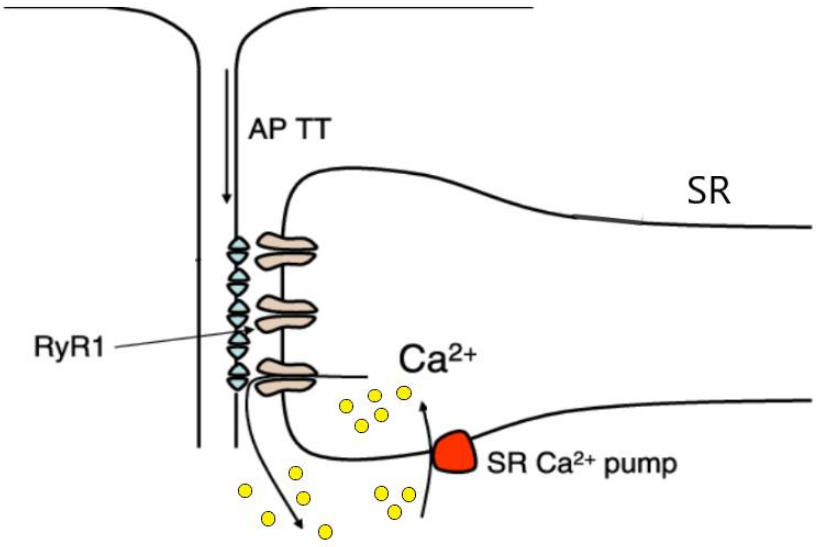

Figure 9 Excitation contraction coupling. *An action potential (AP) propagates down a t-tubule and which causes ryanodine receptors (RyR1) to open, releasing Ca^{2+} into the cytosol where it can bind to Troponin. Ca^{2+} can then be actively transported by the SR Ca^{2+} (SERCA) pump (Allen et al., 2008).*

Shivering is a non-voluntary and random form of muscle contraction taking advantage of the heat produced by the hydrolysis of ATP molecules during cross-bridge cycles as well as the through the active transport of Ca^{2+} ions into the SR (Dumonteil et al., 1993;Hohtola, 2004). During intense periods of shivering, skeletal muscle can account for 90% of O_2 uptake in the body as a whole. Since O_2 is the final electron acceptor in oxidative phosphorylation it can be used as a proxy for heat production (Stainsby and Lambert, 1979;Zurlo et al., 1990). Hooded seal juveniles have been known to exhibit shivering when exposed to low ambient temperatures (Kvadsheim et al., 2005). However, shivering under long term conditions can cause muscle fatigue due to insufficient release of Ca^{2+} ions from the SR (Aydin et al., 2008). Such muscle fatigue may increase the chances of predation with predators that utilise an "endurance-exhaustion" technique where prey are chased to the point of exhaustion (Guinet et al., 2007)

Non-shivering thermogenesis (NST)

Due to the disadvantageous effects of long-term shivering have on the muscle, non-shivering thermogenesis has evolved to maintain thermal balance (Aydin et al., 2008;Periasamy et al., 2017). Non-shivering thermogenesis (NST) is where thermogenesis occurs without the employment of contracting muscle hydrolysing ATP. The most known non-shivering thermogenesis mechanism takes place in the form of brown adipose tissue (BAT).

Brown Adipose Tissue (BAT)

BAT contains small lipid pockets and is incredibly rich in mitochondria in comparison to white adipose tissue (Hull, 1966;Cinti, 2001). A defining feature of BAT mitochondria is the presence of an uncoupling protein (UCP1) which is situated within the inner membrane (Aquila et al., 1985;Nedergaard and Cannon, 1992). In BAT mitochondria, H^+ ions flow through UCP1 which generates heat instead of ATP as would occur in mitochondria lacking UCP1 (Fig.10)(Cannon and Vogel, 1977). This process is known as uncoupling. This thermogenic mechanism is common in small rodents and hibernators and is typically distributed in the interscapular and perirenal regions (Cannon and Nedergaard, 2004). BAT is also utilised in new-born animals such as lambs, reindeer and muskox, atrophying a few weeks after birth as the animal increases in body size and lowers in SA:V (Brück and Wünnenberg, 1966;Gemmell et al., 1972;Casteilla et al., 1989;Soppela et al., 1991).

BAT has been observed in harp seals pups which experience the same environmental hardships as hooded seal pups (Grav et al., 1974). Harp seal pups rely heavily on BAT in early life to maintain thermal balance and survive (Grav and Blix, 1976) and yet hooded seals have not evolved such a mechanism and do not have the capacity to generate heat through BAT (Blix and Steen, 1979;Blix, 2005;Pearson et al., 2011). The birth weights are quite different between hooded and harp pups, with harps being significantly smaller, therefore they can benefit from a BAT based thermogenic mechanism, whereas BAT thermogenesis may not be necessary in the larger hooded seal pup (Blix and Steen, 1979;Pearson et al., 2011).

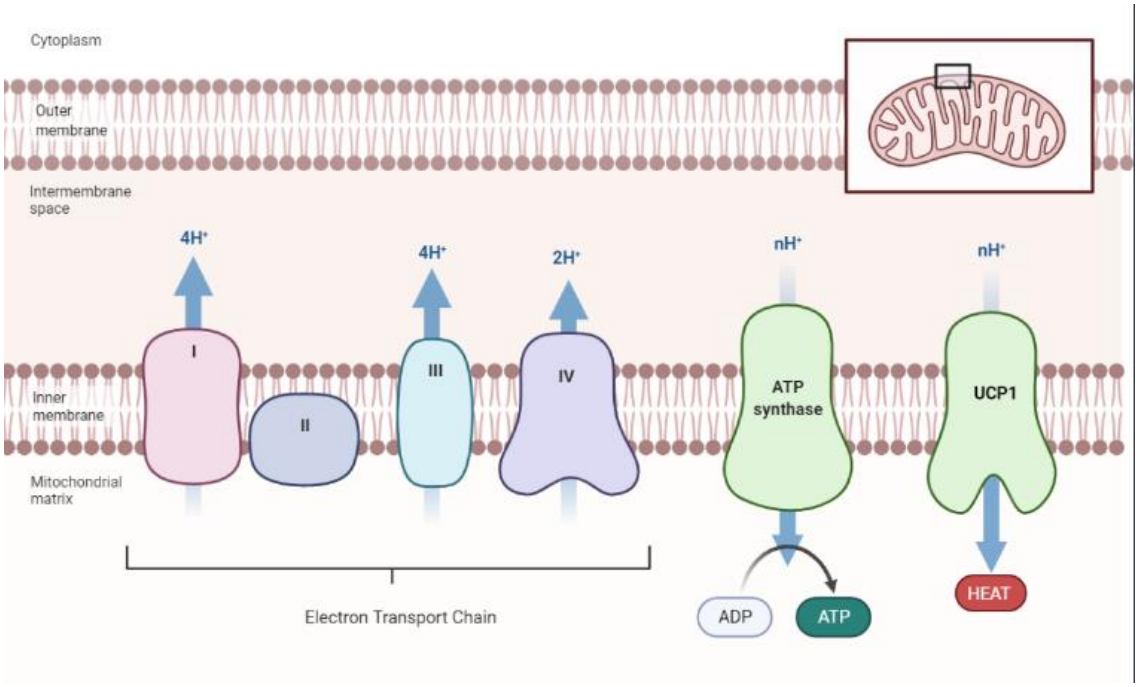

Figure 10 Uncoupled respiration with the presence of UCP1 generates heat*. The energy stored in the H^+ ion gradient produced by the electron transport chain is usually used to synthesis ATP using ATP synthase. But this process can be uncoupled and instead the ion gradient is used to produce heat using UCP1. Produced using biorender.com*

Non-shivering thermogenesis in skeletal muscle

Non-shivering mechanisms do not only occur in fat tissue but can be present in the skeletal muscle. Studies have shown that in fur seals and other species, skeletal muscle can contribute to maintaining thermal balance (Grav and Blix, 1979;Bal et al., 2012;Nowack et al., 2019). The study of muscle NST, specifically work focusing on Ca^{2+} cycling has been around since the 1980s when Barré and Nedergaard (1987) noticed changes in Ca^{2+} cycling without the

observation of shivering in Muscovy ducklings (*Anas barbariae*). This led them to believe that an NST was present in the skeletal muscle through the use of the SERCA pump.

Sln-SERCA Interaction

The SERCA pump can be regulated by two small proteins Phospholamban (Plb) and Sarcolipin (Sln) (Bhupathy et al., 2007). However, phospholamban does not seem to be involved in thermogenesis within the skeletal muscle and only affects SERCA at low Ca^{2+} concentration (Odermatt et al., 1996;Sahoo et al., 2013;Shaikh et al., 2016). Whereas Sln has a more substantial role in muscle thermogenesis (Bal et al., 2012).

Sln was first discovered by MacLennan (1974) terming it as a proteolipid. It was only in the early 1990s when Wawrzynow et al. (1992) mapped the complete 31 amino acid sequence that the name Sarcolipin was given.

Sln regulates SERCA through direct binding to the transmembrane protein within the phospholipid bilayer and decreases the maximum velocity (V_{max}) of Ca^{2+} reuptake (Asahi et al., 2003;Shaikh et al., 2016). Its regulation of SERCA is unique in that although there is a reduction of V_{max} of Ca^{2+}, ATP hydrolysis remains unchanged leading to the conclusion that in the presence of Sln there is an uncoupling between Ca^{2+} transport and the hydrolysis of ATP (Smith et al., 2002;Mall et al., 2006). Otherwise known as futile cycling, this allows for the continuation of ATP hydrolysis producing heat (Fig.11)(Periasamy et al., 2017).

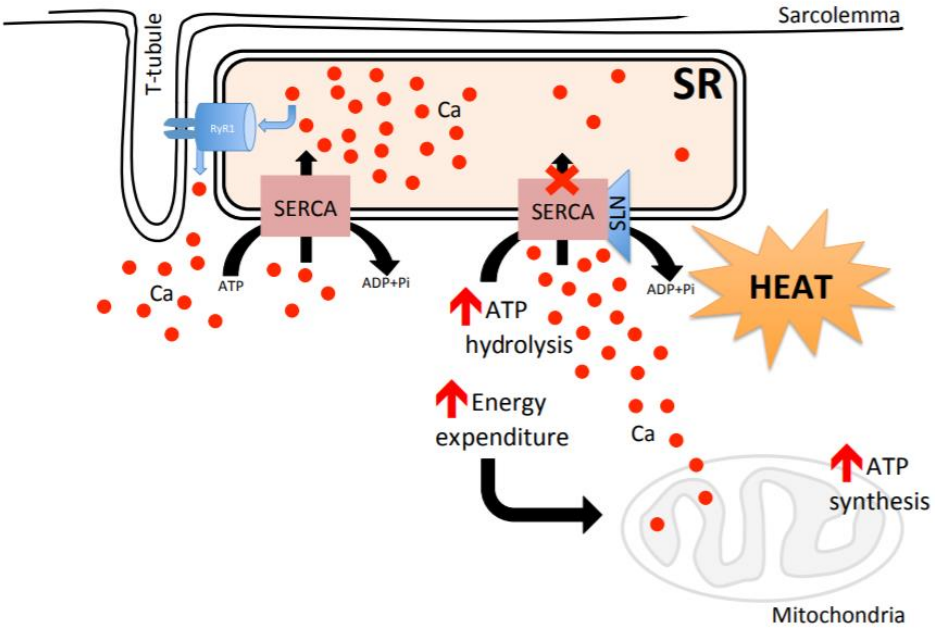

Figure 11 The non-shivering mechanism produced by the Sln-SERCA interaction. *The futile cycling of Ca^{2+} ions in the cytosol of skeletal muscle ultimately increases hydrolysis of ATP, producing heat. (Periasamy et al., 2017)*

A recent study has shown that Sln is essential in the generation of non-shivering thermogenesis through SERCA with an experiment on knockout mice (Bal et al., 2012). The ability to express Sln and uncoupling protein UCP1 (and therefore BAT thermogenesis) was removed. The Sln/UCP1 knockout mice were not able to maintain internal body temperature when put under cold stress. However, when Sln was reintroduced the ability to maintain internal body temperature was regained, even in the absence of UCP1, demonstrating the presence and importance of muscle based NST (Bal et al., 2012).

When comparing gene and protein sequence of the Sln protein, it has been shown that it is highly conserved across multiple species in land and marine mammals (Fig.12)(Rowland et al., 2015). No seals were included in that analysis but it seems possible that the hooded seal may possess the necessary proteins to produce heat through a Sln-SERCA interaction in the skeletal muscle.

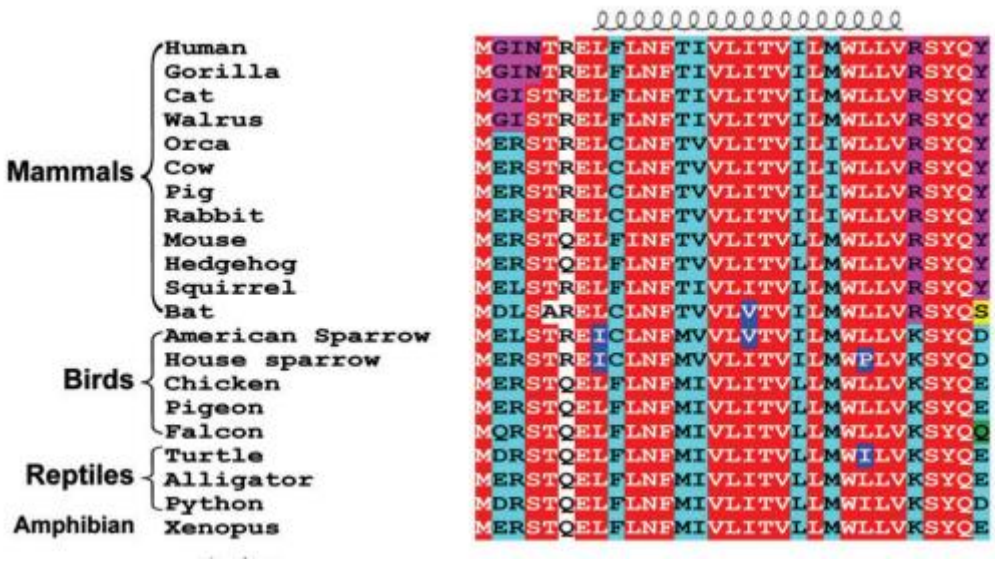

Figure 12 The amino acid sequence of Sln in Mammals, birds, reptiles and amphibians. *(Rowland et al., 2015)*

Sarcoplasmic-endoplasmic reticulum Calcium ATPase (SERCA)

As stated earlier the SERCA pump is essential in the re-uptake of Ca^{2+} ions during skeletal muscle activation. In doing so it allows muscle to relax by taking up ions from the cytosol and restoring ions to the SR ready for muscle contraction (Periasamy and Kalyanasundaram, 2007).

SERCA has 3 different major forms; SERCA1, SERCA2 and SERCA3, with SERCA3 appearing in non-muscle tissues (Bobe et al., 2005). Both SERCA1 and SERCA2 are associated with different skeletal muscle fibre types.

Skeletal muscle fibre types are categorised, depending on the rate at which the muscle consumes ATP and hence the speed of contraction (Barany, 1967). At the beginning of muscle fibre composition research, two major forms of muscle types were described; red muscle which is high in myoglobin and mitochondria and undergoes oxidative metabolism, white muscle which is low in myoglobin, less innervated with capillaries and rely on non-oxidative forms of metabolism (Needham, 1926). As research progressed, muscle fibre tying expanded the notion that there are 4 major muscle types; type 1, type 2a, type 2b and type 2x with type 2x being an intermediary between 2a and 2b muscle types (Guth and Samaha, 1969;Larsson et al., 1991;Schiaffino and Reggiani, 2011).

Type 1 muscle fibres are the slow oxidative muscle types and have the characteristics of red muscle stated earlier and are termed slow oxidative fibres as the rate at which cross-bridge cycling and Ca^{2+} re-uptake occurs is slow (Hill et al., 2017).

Type 2a muscle fibres are much faster in the rate of cross-bridge cycles and Ca^{2+} re-uptake leading to a reduced contractile time. Although the rate of ATP consumed is larger than type 1 muscle fibres, type 2a still uses oxidative metabolism to provide ATP and are hence termed fast oxidative fibres.

Type 2b has the fastest contractile time and can produce the most power, receives all its energy from glycolysis (without the use of O_2) and fatigues the quickest.

Both type 2a and type 1 muscle fibres due to their mode of metabolism allows them to have a steady supply of oxygen and therefore ATP, making them ideal candidates as sites for muscle NST (Periasamy et al., 2017).

The three major SERCA forms can be spliced further into multiple isoforms. SERCA1 is typically expressed in type 2b, fast twitch fibres, and is spliced into ‘SERCA1a’ and ‘SERCA1b’ isoforms. The SERCA1a is usually expressed in adult skeletal muscle whereas SERCA1b is expressed in neonatal tissue (Brandl et al., 1986; 1987). SERCA2 has three isoforms 2a, 2b and 2c; SERCA2a is typically expressed in type 1 and 2a oxidative muscle

fibres (MacLennan et al., 1985;Zarain-Herzberg et al., 1990). SERCA2b and 2c are less associated with skeletal muscle as 2b is expressed in low levels in all muscle tissue including smooth muscle and 2c is reported to be in cardiac muscle (Dally et al., 2006). The relationships mentioned here between the SERCA isoforms and skeletal muscle fibre types were observed in rabbits however is thought to be the same in all mammalian skeletal tissue (Periasamy and Kalyanasundaram, 2007). Therefore, the forms that are most likely to be involved in thermogenesis are SERCA1 and SERCA2 due to their close association to skeletal muscle with the SERCA2a isoform being of particular interest as it is present in type 1 and type 2a oxidative fibres.

Mitochondrial Proton Leak (LEAK)

As stated earlier the flow of electrons across the electron transport chain provides energy for complexes I,III and IV to pump H^+ across the inner mitochondrial membrane producing an electrochemical gradient which powers the protein ATP synthase (Fig. 7 & Fig. 10). However, this process as with all forms of energy conversion is not 100% efficient and H^+ ions have the potential to leak back through the inner mitochondrial membrane space uncoupled from ATP synthase. This is termed mitochondrial proton leak (LEAK) and occurs in all eukaryotic cells (Cadenas, 2018). This LEAK can be regulated through uncoupling proteins (inducible LEAK) as seen in BAT or unregulated (basal LEAK) where H^+ ions move through the inner mitochondrial membrane itself (Fig.13)(Busiello et al., 2015).

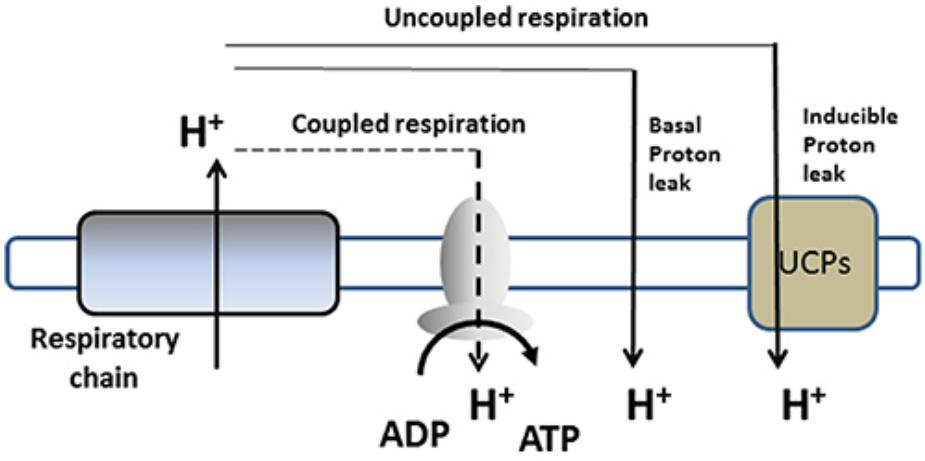

Figure 13. Uncoupled mitochondrial respiration. *Protons (H^+) can leak through different pathways within the inner mitochondrial membrane. Reproduced from Busiello et al., 2015.*

The presence of LEAK in all eukaryotic cells is on the account of its effect on the rate of reactive oxygen species (ROS) production. ROS are the toxic by-products of aerobic respiration which include the oxygen free radicals, superoxide anion free radical ($O_2^{\cdot -}$) and hydroxyl radicals (˙OH); as well as nonradical oxidants, hydrogen peroxide (H_2O_2) and singlet oxygen ($^1O_2$). These ROS when left unattended, termed oxidative stress, can be detrimental to DNA structure, cell life and are known to contribute to aging (Osiewacz and Scheckhuber, 2006;Zorov et al., 2012). The production of these ROS within the mitochondria have been linked to the electrochemical H^+ gradient produced by the electron transport chain, where a high gradient equates to an increase in ROS production (Korshunov et al., 1997). The presence of LEAK, uncoupling oxidative respiration, reduces the proton gradient and in doing so reduces the production of ROS (Brand, 2000).

LEAK increases the rate of respiration and can account for up to 25% of the basal metabolic rate, showing a reduced efficiency for the production of ATP in mitochondria (Rolfe and Brand, 1996). A markedly reduced efficiency can lead to thermogenic hypermetabolism as has been observed in sea otters (*Enhydra lutis*) the smallest marine mammal (Wright et al., 2021). Wright et al. (2021), have shown that up to 40% of the potential energy produced by skeletal muscle respiration in sea otters is contributed to the thermogenic demand of the animal which led to the conclusion that basal LEAK in muscle is an important NST mechanism allowing the sea otter to occupy an aquatic lifestyle, despite their small size.

Loose coupling of muscle mitochondria (LEAK) has also been found in northern fur seal (*Callorhinus ursinus*) skeletal muscle indicating that a LEAK based NST mechanism could be present in the skeletal muscle of seals (Grav and Blix, 1979). In addition, the notion that marine mammal basal metabolic rate is higher than terrestrial mammals of the same size (Irving, 1973;Williams et al., 2001), although disputed (Lavigne et al., 1986), may support the presence of a NST in the form of LEAK.

Hypothesis

Therefore, in this study I hypothesise that the hooded seal uses skeletal muscle-based, non-shivering thermogenesis (NST) mechanisms, and that those mechanisms are most likely to be present in the neonatal life stage compared to later life stages due to new-borns having a higher surface area:volume ratio increasing their exposure to the cold environment.

Specifically, I will test the following aims:

I. Whether hooded seals express sarcolipin and SERCA in skeletal muscle.
II. If the amount of sarcolipin or SERCA protein differ between muscle groups.
III. Whether ethe amount of sarcolipin or SERCA protein decreases with age as other thermoregulatory mechanisms develop.
IV. Whether an increased mitochondrial proton leak (LEAK) is present within skeletal muscle of hooded seals, which could generate heat.

Material and Methods

Sample Collection and Processing

Adult (n=5) hooded seals, hooded seal pups (n=4)(Table.1) were live-captured between 21st March 2021 and 6th April in the "West Ice" off Greenland (i.e. on the pack-ice of the Greenland Sea at 72°24' N, 14°15' W) during a research cruise with the RV Helmer Hanssen. The 14-day research cruise was part of the Arctic Biology course (BIO-2310) offered by the Department of Arctic and Marine Biology at University of Tromsø providing knowledge of the adaptive physiology of hooded and harp seals. Muscle samples were collected opportunistically from animals that were euthanized for other research purposes. Harp and hooded seal pups were live captured on the ice by slowly approaching on foot across the ice floes. They could then easily be grabbed and placed in a burlap sack and brought on board. The pups were then euthanised by competent persons, by use of approved euthanasia procedures by use of hakapik in accordance with Norwegian sealing regulations (Nærings- og fiskeridepartementet, 2022), or by using an i.v. injection of a lethal dose of barbiturate (15-20 mg·kg-1; Euthasol, 400mg·ml^{-1}, Le Vet B.V., Oudewater, Netherlands) via a catheter (Secalon 16G/1.70x130mm, Argon Medical Devices, Argon Critical Care systems, Singapore) inserted into the extradural intravertebral vein after prior sedation with an intramuscular injection of Zoletil Forte Vet (~1mg·kg^{-1}; 100mg·ml^{-1}, Virbac, Carros Cedex, France). Adult hooded seals were used for post-mortem sampling of intact brains and were therefore euthanized under a separate protocol which was approved by the Norwegian Food Safety Authority (NFSA, FOTS permit No. 22451). Seals were live-captured with hoop nets upon the ice floes and were sedated with an intramuscular injection of Zoletil Forte Vet (~2-2.5 mg·kg^{-1}). The adult seals were brought onboard the vessel, where they were intubated and ventilated with isoflurane in air (4-5%; Baxter AS, Oslo, Norway) until fully anaesthetized, at which point they were bled to death by cutting of the carotid arteries/jugular veins. All animal captures were approved by the Department of Fisheries, Hunting and Agriculture, Government of Greenland (permit no. 2021-80).

Table 1. Summary of Hooded seals used in the present study and the muscle groups sampled.

Species	ID	Sex	Body mass (Kg)	Life stage	M. longissimus dorsi	M. intercostal externa	Psoas major
Hooded seal	K1-21	Male	200	Adult	X	X	X
Hooded seal	K3-21	Male	32.86	2-3 days	X	X	X
Hooded seal	K4-21	Female	33.36	2-3 days	X	X	X
Hooded seal	K8-21	Female	161	Adult	X	X	X
Hooded seal	K8b-21	Female	19.84	Newborn	X	X	X
Hooded seal	K9-21	Female	165	Adult	X	X	X
Hooded seal	K10-21	Female	149	Adult	X	X	X
Hooded seal	K10b-21	Female	32	2-3 days	X	X	X
Hooded seal	K11-21	Female	27	2 days	X	X	X
Live Seals							
Hooded Seal	K2-21	Male	62	7-8 Months	X		
Hooded Seal	K6-21	Male	69	7-8 Months	X		
Hooded Seal	K7-21	Female	66	7-8 Months	X		X
Hooded Seal	K9b-21	Male	69	7-8 Months	X		X
Hooded Seal	K12-21	Female	70	7-8 Months	X		
Hooded Seal	K13-21	Female	63	7-8 Months	X		X
ID Key							

Skeletal muscle samples were cut roughly from the *m. longissimus dorsi (M.long), m. psoas major (P.major)* and *m.intercostal externa* (Fig.14, highlighted). Both *M.long* and *P.major* are relatively active muscle groups as they are recruited during aquatic locomotion with *M.long* being one of the largest muscle groups within phocid seals (Howell, 1929) while *Intercostal externa* muscles have been known to already contribute to shivering thermogenesis (Duron, 1973). All muscle groups are considered to be oxidative fibres which are suitable conditions to allow for NST (Han et al., 1993;Burns et al., 2010). Due to the function and oxidative capacity of these muscle groups they were the target muscle groups within this study.

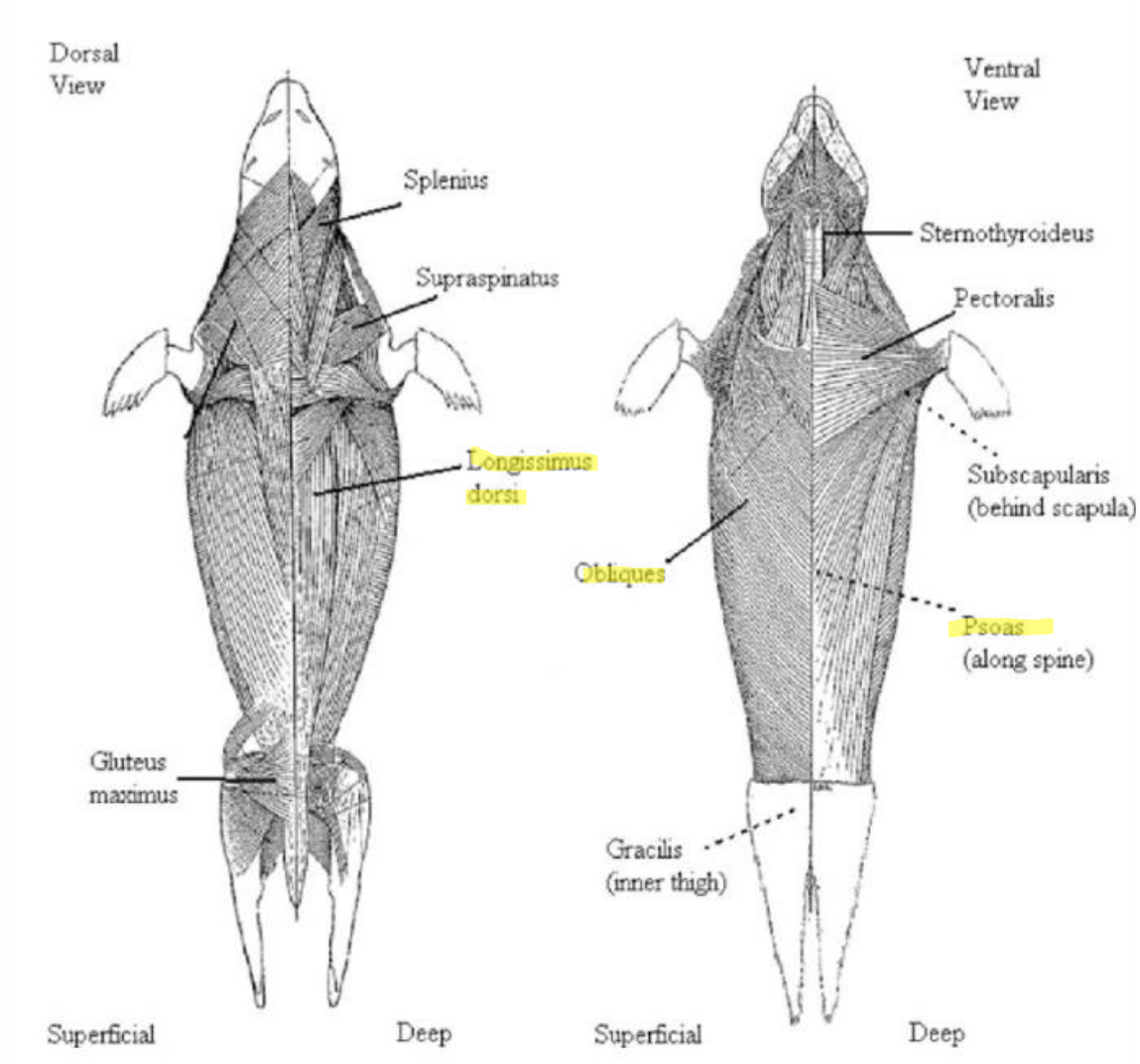

***Figure 14 Anatomy and musculature of a seal**. Dorsal and ventral views of a seal showing the location of Longissimus dorsi and Psoas major skeletal muscles. The Psoas major muscle is not clearly shown as it runs close to the spine, connecting the lower lumbar to the hip. Obliques indicate the location of the intercostal externa. (Howell, 1929).*

These samples were placed into petri dishes with phosphate buffer solution (PBS, Cat.No: 10010023, Thermo Fisher Scientific, Massachusetts, USA) on ice and brought into the lab. The samples were then precisely cut by scalpel and transferred into cryotubes. Samples were preserved in liquid nitrogen and remained in the medium for the remainder of the research cruise (2 weeks). On return to Tromsø, samples stored in liquid nitrogen were removed and transferred to an ultra freezer (-80°C) for later analysis.

Live seal pups (n=6, Table 1) were also captured and brought back from the West Ice to the approved research facility at the Department of Arctic and Marine Biology (AMB), by permit (FOTS ID 22751) from the NFSA. Later, these seals were sedated and then culled using the adult protocol stated above, for collection of fresh tissue samples for use in a range of research projects, this one included. Longissimus dorsi (n=6) and Psoas major (n=3) muscle groups were sampled and immediately analysed using Oroboros instruments (See Tissue respirometry).

DNA comparison of target proteins

To assess whether Sln and SERCA exist within seals, the DNA which codes for Sln, SERCA1 and SERCA2 must be cross-referenced to a seal. The genome for hooded seals has not been fully mapped, the closest relative with a full genome to allow for comparison is the Weddell seal (*Leptonychotes weddellii*) another member of the phocid family.

The Weddell seal genome was downloaded through the National Center for Biotechnology Information's (NCBI) assembly database (National Library of Medicine (US), 2004). A BLAST database was created using the seal genome, which was used to compare DNA.

Sln is a relatively small protein with 31 amino acids. The DNA sequence for the human Sln gene was found using the genome database, Ensembl (https://www.ensembl.org release 106)(Cunningham et al., 2021) and inserted into the DNA editor software ApE (https://jorgensen.biology.utah.edu/wayned/ape/)(Davis and Jorgensen, 2022). The DNA sequence was then copied from ApE and translated into the amino acid sequence using Expasy translation tool (https://web.expasy.org/translate/)(Gasteiger et al., 2005). The Expasy translation tool highlighted the specific amino acid sequence of Sln which allowed for the extraction of the specific DNA sequence of Sln within the software ApE, disregarding non-coding DNA. This sequence was blasted against the Weddell seal genome which allowed for

the cross-reference of human and Weddell seal DNA specific for the coding of Sln. The Weddell seal DNA was then copied and translated into Expasy. The translated DNA sequence of Weddell seal as well as human Sln could then be compared for correspondence in the sequence alignment tool, Clustal Omega (https://www.ebi.ac.uk/Tools/msa/clustalo/) (Sievers et al., 2011), with a percent identity matrix.

The steps above were repeated for mouse, dog, walrus, grey seal, ferret, cow, orca and the naked mole rat to better understand how well Sln is conserved in multiple species as well as to compare the data shown by Rowland et al., 2015. The same procedure was repeated for SERCA1 and SERCA2.

Protein Extraction

Muscle samples which were flash frozen in liquid nitrogen and then transferred to -80°C were then ready for homogenisation.

Prior to the development of this protocol, a tissue ruptor (TissueRuptor II, Cat. No: 9002756, Qiagen, Hilden, Germany) was used to homogenise muscle samples however this was deemed too time consuming and inefficient given the number of samples needed to be processed (Appendix A).

While working on ice, 170-180mg of the 33 flash frozen samples were taken from the cryotubes and placed in a centrifuge tube along with one 0.5g ball bearing the function of which was to pulverise the frozen samples. Centrifuge tubes were then placed back into the -80°C so that samples remained frozen. During this time radioimmunoprecipitation assay (RIPA) buffer was prepared (100ml; 5M NaCl (3ml), 1M Tris-HCL at pH 8 (5ml), Triton-x-100 (1ml), 10% Sodium deoxycholate (5ml) and de-ionised H_2O), adding 100x Holt protease inhibitor at 10µl/ml (Cat.No: 87786, Thermo Fisher Scientific, Massachusetts, USA).

Samples were then placed from the -80°C into a tissue lyser (Tissuelyser II, Qiagen, Hilden, Germany), the holders of which had been in a freezer at -20°C to keep cold and ran for 2 minutes at a frequency of 30/s. One ml of RIPA buffer with the added protease inhibitor was then pipetted into each centrifuge tube and then ran for a further 1 minute within the tissue lyser. The contents were then observed to determine homogenisation and then ran for another 1 minute.

Samples were then transferred to a rocker (IKA® Rocker 2D basic, IKA, Staufen, Germany) and agitated for 2 hours at 4°C. Once completed samples were centrifuged (Himac CT15RE, Hitachi Koki Co.,Ltd, Minato, Tokyo) at 16000g for 20 minutes at 4°C. The supernatant was collected and transferred to a clean tube.

Protein Quantification

Protein quantification was done by Bicinchoninic acid assay (BCA). BCA assays take advantage of the reduction of the cupric ion (Cu^{2+}) to cuprous ion (Cu^{+}) in the presence of protein, also known as a biuret reaction. Bicinchoninic acid is a reagent for Cu^{+} and a purple-coloured product is given dependent on the amount of protein present. This reaction is nearly linear with increasing protein concentrations at absorbance 572nm (Smith et al., 1985). A common protein of known concentration, in this case bovine serum albumin, can be introduced to the BCA and Cu^{2+} and upon measuring absorbance will provide a standard curve which can be used to compare to unknown protein samples to determine their concentration. Using the information provided by the BCA analysis the amount of protein utilised, in this case for Western Blots, can be standardised.

Pierce™ BCA Protein Assay Kit (Cat. No. 23227, Thermo Fisher Scientific, Massachusetts, USA) was used for the protein quantification, this kit included reagent A which contains the BCA component, reagent B containing the Cu^{2+} component and ampules of bovine serum albumin at a concentration of 2mg/ml.

Reagent A and B are mixed in a ratio of 50:1 respectively to form the working reagent (WR). The amount of WR used is dependent on the number of albumin standards, unknown samples, how many replicates are needed and how much will be added to each sample.

In this BCA assay a 96 well microplate was used, and 9 Albumin standards were prepared using RIPA lysis buffer in descending concentration (Table. 2). Homogenate samples of *M. longissimus dorsi* and *Psoas major* muscle groups (N=22) were assessed in this protein assay (Appendix B). Each standard and sample were replicated twice and 200µl of working reagent was used for each sample.

***Table 2 Dilution series of a BCA analysis**. Showing the preparations of the Albumin standards and their final concentrations. Diluent (RIPA lysis buffer) and BSA (Bovine Serum Albumin)*

Dilution Scheme for Standard Test Tube Protocol and Microplate Procedure (Working Range = 20–2,000 µg/mL)			
Vial	**Volume of Diluent (µL)**	**Volume and Source of BSA (µL)**	**Final BSA Concentration (µg/mL)**
A	0	300 of Stock	2000
B	125	375 of Stock	1500
C	325	325 of Stock	1000
D	175	175 of vial B dilution	750
E	325	325 of vial C dilution	500
F	325	325 of vial E dilution	250
G	325	325 of vial F dilution	125
H	400	100 of vial G dilution	25
I	400	0	0 = Blank

Albumin standard and protein samples were pipetted (25µl) into the microwell plate and 200µl of the WR was added. The microplate was then added to a microplate reader (Glomax Explorer Multimode Microplate Reader, Promega, Wisconsin, USA) and a pre-programmed protocol called 'BCA Protein Assay with incubation' was selected. Under this protocol, the microwell plate was then shook for 30 seconds and incubated for 30 minutes at 37°C. The plate was then cooled to room temperature and the absorbance was measured at 562nm.

To calculate the standard curve (Fig. 15), averages of the absorbance of albumin standards from vials A to I (Table 2) were calculated and the blank was subtracted to disregard any background from the WR and RIPA buffer.

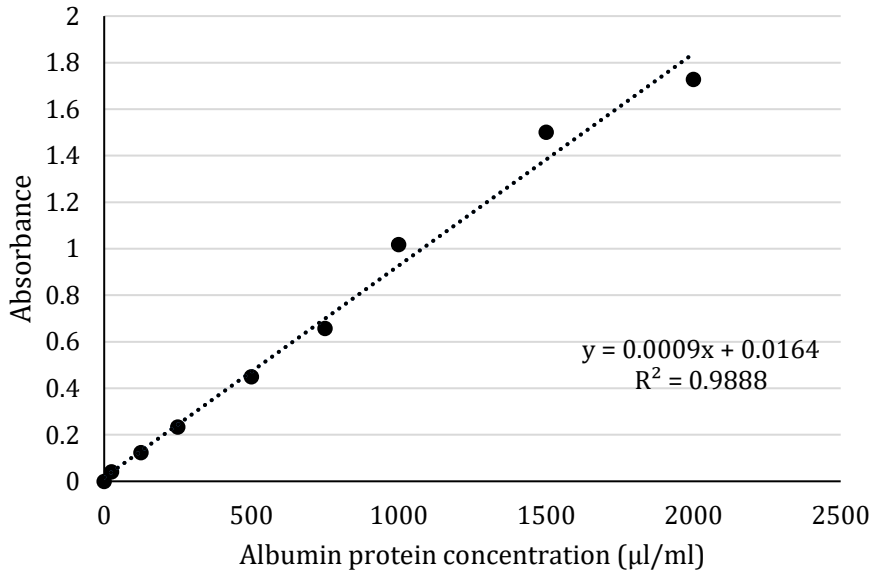

***Figure 15. The standard curve of bovine serum albumin**. Provided using BCA assay. Absorbance at 562nm.*

Western Blotting

Western blotting is a form of electrophoresis, allowing to separate protein molecules based on size or electrical charge through a protein gel. The separated proteins can then be electrophoretically transferred onto a nitrocellulose membrane (Towbin et al., 1979) and be inoculated by a primary antibody in order to bind to the target protein. Then a secondary antibody is inoculated which binds to the primary antibody. The secondary antibody is conjugated with horseradish peroxidase (HRP) which catalyses the oxidation of luminol when hydrogen peroxide is present. Luminol is an organic compound that when oxidised, emits light and is a form of chemiluminescence. The light emitted from the chemiluminescence is then exposed to a single emulsion film within a dark room which is then developed. The amount of signal can be quantified to give a semi-quantitative measure of the amount of target protein present, after appropriate normalisation for the total amount of protein loaded. Within this protocol only *M.long* and *P. major* was used as all three muscle groups could not fit onto the protein gel with 3 technical replicates.

Western Blot Protocol

Homogenate samples of hooded seal *M. long* and *P. Major* (n=12; Table 3) were thawed on ice along with the molecular ladder (Spectra Multicolour Broad Range Protein Ladder, Cat. No: 26634, Thermo Fisher Scientific, Massachusetts, USA) and 4x Bolt™ LDS (Cat. No: B0007, Thermo Fisher Scientific, Massachusetts, USA) sample buffer was brought to room temperature. Using the BCA calculated protein concentrations, the amount of protein to add was calculated depending on the total protein needed (Appendix B).

300µl of total LDS + 2.5% ß-mercaptoethanol sample buffer was prepared. For each sample 10µl of the LDS sample buffer was added to a 1ml centrifuge tubes along with a 1/10 dilution homogenate sample and RIPA lysis buffer to make a total volume of 30µl in each tube and a desired concentration of (4µg/µl) (Table 3).

Table 3. Hooded seal skeletal muscle homogenate used within Western blot protocol*. Samples were loaded into the 15 well 4-12% Bis-Tris Western Blot gels.*

Pups	LDS sample buffer	Amount of Protein loaded (4µg/µl)	1/10 sample µl	Ripa µl
K321 M.long	10	4	3.7	16.3
K321 P. major	10	4	4.4	15.6
K8b21 M.long	10	4	4.6	15.4
K8b21 P.major	10	4	4.6	15.4
K10b21 M.long	10	4	3.8	16.2
K10b21 P.major	10	4	3.3	16.7
Adult				
K121 M.long	10	4	3.5	16.5
K121 P.major	10	4	2.9	17.1
K821 M.long	10	4	2.9	17.1
K821 P.major	10	4	2.5	17.5
K921 M.long	10	4	4.0	16.0
K921 P.major	10	4	3.7	16.3
Blank	10	0	0.0	20.0

Samples were then inserted into a heat block at 70°C for 10 minutes in order to denature the proteins to access the amino acid string, once completed samples were transferred immediately on ice. A 'Bolt Mini Gel Tank' (Cat. No: A25977, Thermo Fisher Scientific, Massachusetts, USA) was prepared by inserting two gels and filling each chamber with 400ml of 1x Bolt™ MES SDS Running buffer (Cat. No: B0002, Thermo Fisher Scientific, Massachusetts, USA) including 5ml of 5mM Sodium bisulphite. Samples were then loaded into the gels along with the molecular ladder and blank (Table 3, Fig.16). The gels then ran at 200V for ~22 mins at room temperature using a Powerpac™ Basic (Cat. No:1645050, BioRad, California, USA) as a power supply.

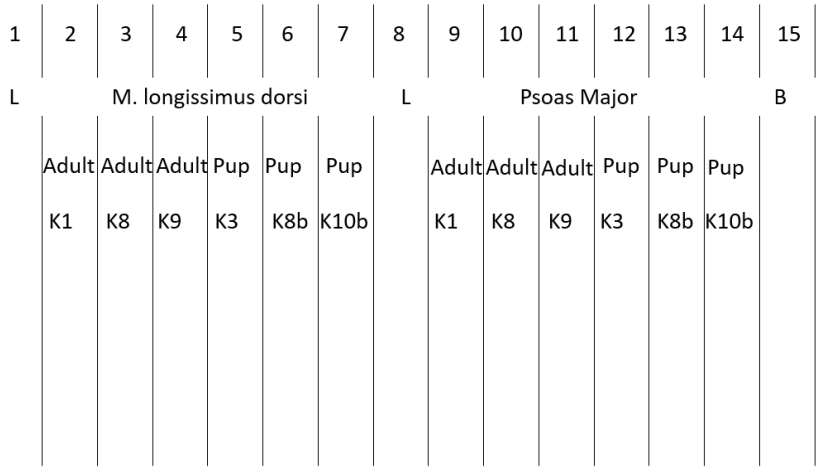

Figure 16. The layout of Hooded seal homogenate samples within 15 well Bis-Tris gels*. Molecular Ladder (L) loaded in wells 1 and 8. Muscle group M. Longissimus dorsi loaded in wells 2-7. Muscle group Psoas Major loaded in wells 9-14. Blank (B) loaded in well 15.*

Transfer and Incubation of Primary Antibody

Sponges, filter paper (Cat. No: 1703965, BioRad, California, USA) and 0.2µm Nitrocellulose membranes (Cat. No: 1620112, BioRad, California, USA) were cut to size to match the size of the Bis-Tris gels and soaked in 1x Bolt™ Transfer Buffer (Cat. No: BT0006, Thermo Scientific, Massachusetts, USA) +20% Methanol. Using the same Bolt mini gel tank, each gel and membrane was situated between sponge and filter papers and placed between two electrodes (Fig.17).

Figure 17. Orientation of Sponges, filter papers, the gel and membrane in a Western Blot transfer.

The tank was filled with 1x Transfer buffer was run at 10V for 1h at 4°C. Once completed the membranes were washed in Tris-buffered saline w/ Tween 20 solution (TBST, 15.4Mm Trizma HCL, 137mM NaCl, 0.1% (v/v) Tween 20, pH 7.6). Membranes were then stained in a protein staining solution (Ponceau S solution, 1.3mM Ponceau S, 5% (v/v) glacial acetic acid) for 2-3 minutes and rinsed with distilled water to reveal protein bands. The membranes were then inserted in between two acetate sheets and scanned at 300dpi to JPG file using a standard scanner (Epson Perfection V800, Epson, Nagano, Japan).

Ponceau S stains were removed using 0.1M of NaOH and rinsed using distilled water. Membranes were then incubated in 5% (w/v) milk in TBST for 1h at 4°C to block non-specific binding sites. The membranes were then incubated with 2 ml of 5% milk (skim milk powder, Cat. No:115363, MilliporeSigma, Massachusetts, USA) in TBST containing the primary antibody in a heat sealed bag and left on a rocker (IKA® Rocker 2D) overnight at 4°C.

Incubation of Secondary Antibody and Development

After the incubation of the primary antibody, membranes are washed in TBST solution 5x for 5 minutes. Once completed, membranes are incubated in 5ml of 5% milk in TBST containing the secondary antibody with a 1:10,000 dilution within a heat-sealed bag. The membranes were incubated for 1hr at room-temperature under dark conditions (wrapped in foil) and kept agitated on a rocker.

Membranes were then washed in TBST 5x for 5 minutes wrapped in foil and developed using Pierce™ ECL Western Blotting Substrate (Cat.No: 32132, Thermo Fisher Scientific, Massachusetts, USA).

Under red light, 2ml of ECL Western blot substrate was pipetted onto the membranes for 5 minutes. Membranes were then wrapped in seran wrap and placed face up into a development cassette. Single emulsion film (BIOMAX MR Film, Cat.No: 8701302, Carestream, New York, USA) was placed emulsion side down within the cassette and exposed for 10 seconds.

The emulsion film was then placed face up in developing solution (Carestream® Kodak® autoradiography GBX developer/replenisher, Cat.No: P7042, Sigma-Aldrich, Missouri, USA) for 3 minutes, washed in water for 10 seconds and then placed in fixing solution (Carestream ® autoradiography GBX fixer/replenisher, Cat.No: P7167, Sigma-Aldrich, Missouri, USA). The film was then washed under running water and scanned under the same conditions as the Ponceau staining.

Antibodies

Given my research aims, the antibodies used within this study were acquired to detect Sln, SERCA1 and SERCA2. Primary antibodies which bind to the target protein must also be compatible to the target species. Most primary antibodies have a tested reactivity with human, mouse and rat as these are considered model species and most of their genome has been sequenced. A high amino-acid alignment would indicate a high probability of reactivity and therefore binding of the target protein.

Secondary antibodies must be able to bind to the primary antibodies and this is dependent on the species the primary antibody was cultured in. Secondary antibodies are made by inoculating a host species, the most common being a goat, with immunoglobulins specific to

the host species of the primary antibody. Both Sln and SERCA2a antibodies were made using a rabbit as a host. This would mean that Sln and SERCA2a antibodies have antigen-binding sites specific to rabbits. SERCA1a however was created using mouse as a host species. Within this study separate secondary antibodies that have anti-rabbit binding sites and anti-mouse binding sites are essential.

Nitrocellulose membranes within the western blot protocol were incubated with SERCA1a (Cat. No ab233647, abcam, Cambridge, UK), SERCA2a (Cat. No ab150435, abcam, Cambridge, UK) and Sarcolipin (Cat. No 18395-1-AP, proteintech, Illinois, USA) primary antibodies (Table 4).

To detect the presence of SERCA1a primary antibodies, a goat anti-mouse secondary antibody was procured from abcam (Cat. No ab205719, Cambridge, UK). For detection of SERCA2a, sarcolipin and β-Actin primary antibodies a goat anti-rabbit secondary antibody was also procured by abcam (Cat. No ab205718, Cambridge, UK)(Table 4).

Table 4 Primary and Secondary western blot antibodies. *Ratios denote concentrations used in this study*

Primary Antibody	Concentration	Secondary Antibody	Concentration2
β-actin	1:250	Goat Anti-rabbit IgG	1:5000
β-actin	1:500	Goat Anti-rabbit IgG	1:2000
β-actin	1:500	Goat Anti-rabbit IgG	1:3000
β-actin	1:500	Goat Anti-rabbit IgG	1:5000
β-actin	1:750	Goat Anti-rabbit IgG	1:5000
SERCA2a	1:500	Goat Anti-rabbit IgG	1:3000
SERCA2a	1:750	Goat Anti-rabbit IgG	1:5000
SERCA2a	1:750	Goat Anti-rabbit IgG	1:7500
SERCA2a	1:750	Goat Anti-rabbit IgG	1:10000
SERCA2a	1:1000	Goat Anti-rabbit IgG	1:8000
Sarcolipin	1:500	Goat Anti-rabbit IgG	1:5000
Sarcolipin	1:500	Goat Anti-rabbit IgG	1:10000
Serca1a	1:500	Goat Anti-mouse IgG	1:2000
Serca1a	1:500	Goat Anti-mouse IgG	1:3000
Serca1a	1:500	Goat Anti-mouse IgG	1:10000
Serca1a	1:750	Goat Anti-mouse IgG	1:5000
Serca1a	1:1000	Goat Anti-mouse IgG	1:2000
Serca1a	1:1000	Goat Anti-mouse IgG	1:8000
Serca1a	1:1000	Goat Anti-mouse IgG	1:10000

Normalisation of Western Blots

Due to the protocol of Western blot production, many factors can affect western blot data, these include but are not restricted to imperfections in protein extraction and sample loading, unfavourable protein separation during gel electrophoresis and unequal transfers due to air bubbles (Ghosh et al., 2014). In order to reduce the effects of these extraneous variables a normalisation control is needed. There are two types of normalisation techniques commonly used; housekeeping protein normalisation and total protein normalisation (Thellin et al., 1999;Romero-Calvo et al., 2010).

Housekeeping protein normalisation

Housekeeping proteins are proteins which are expressed constitutively, and the presence is detected through the use of antibody binding, incubating alongside the target protein (Gilda et al., 2015) or probed after stripping a previously used blot (Sander et al., 2019). The most common housekeeping proteins are β-actin, glyceraldehyde 3-phosphate dehydrogenase (GAPDH), or α-tubulin. The abundance of these proteins on western blots can then be compared to the target protein acting as an internal standard. This form of normalisation is the most common but relies on working antibodies and knowledge of a protein that is stably expressed in your tissue type (Gilda et al., 2015). Housekeeping protein normalisation was originally adopted using β-actin (Cat. No SAB2108641, Sigma-Aldrich, Missouri, USA) as the house keeping protein as it was the most common technique and β-actin antibody was already on hand. However, incubating with β-actin antibody did not provide specific bands (Appendix A). Therefore, a switch to total protein normalisation was implemented.

Total protein normalisation

This form of normalisation takes into account the total protein loaded in each lane. All proteins present on the membrane are stained using a protein stain, the most common being Ponceau S. The stain can then be used the same way as the housekeeping proteins comparing the stain to the target protein (Romero-Calvo et al., 2010). This method removes the need for a primary housekeeping antibody, the uncertainty of specific binding to the target proteins and does not undergo the whole western blot protocol which increases time efficiency. This form of normalisation was utilised in this specific study.

Scanned images of the Ponceau S stained membranes and developed emulsion film were used in the total protein normalisation of the target proteins. Protein density was measured using ImageJ software (U. S. National Institutes of Health, Bethesda, Maryland, USA) in all lanes 2-14 (Fig.14) and protein density ratios between Ponceaus S stain and target protein bands were calculated (Appendix C).

Tissue respirometry

During the last week of November (24^{th}, 25^{th},26^{th}) and mid-December (14^{th}, 15^{th}, 16^{th}), the live seals (n=6) residing in the animal research facility at AMB were culled using the same procedure as adult seals caught and culled on board the RV Helmer Hanssen (NFSA permit FOTS 22751).

Once culled, a muscle biopsy from *M.long* (n=6) and *P. major* (n=3)(Table 1) was taken using a 6mm Biopsy punch (Cat.No:33-36, Miltex Inc, Pennsylvania, USA) and placed in a centrifuge tube filled with 2ml of ice cold biopsy preservation solution (BIOPS 2.77mM CaK_2EGTA, 7.23mM K_2EGTA, 5.77mM Na_2ATP, 6.56mM $MgCl_2 \cdot 6\ H_2O$, 20mM Taurine, 15mM Na_2Phosphocreatine, 20mM Imadazole, 0.5mM Dithiothreitol, 50Mm MES hydrate). Originally, muscle biopsies were to be taken only from *M. long* during November (n=3), proceeding with muscle biopsies from *P. major* during December (n=3). This was due to the tissue respirometer's capacity to only test one muscle tissue at a time and live muscle tissue was uncertain to survive within BIOPS solution for extended periods of time. However, during muscle biopsies of *P. major*, the muscle biopsies of *M. long* was included and was placed in BIOPS for roughly 1-2 hours during analysis of *P. major* muscle groups.

Samples were then dried with delicate task wipes and 50mg was cut and transferred to a weigh ship containing 500µl of BIOPS. Muscle samples were then cut into 1mm pieces and 50µl of 2.5% (v/v) Trypsin (Cat. No: 15090046, Thermo Fisher Scientific, Massachusetts, USA) was added in order to permeabilise the fibres. The samples incubated on ice for 20 mins and then washed two times with 2ml of BIOPS using a glass pipette. The samples were then transferred into a cold shredder tube, placed directly onto the lysis disc. 500µl of respiration medium known as MiR05 (0.5mM EGTA, 3mM $MgCl_2 \cdot 6\ H_2O$, 60mM Lactobionic acid, 20mM Taurine, 10mM KH_2PO_4, 20mM Hepes, 110mM D-sucrose, 1g/L BSA) was added to

achieve 10% homogenate. The shredder tube was inserted into the cooling block chilled to 4°C and shredded for 12 seconds at position 1(Fig.18).

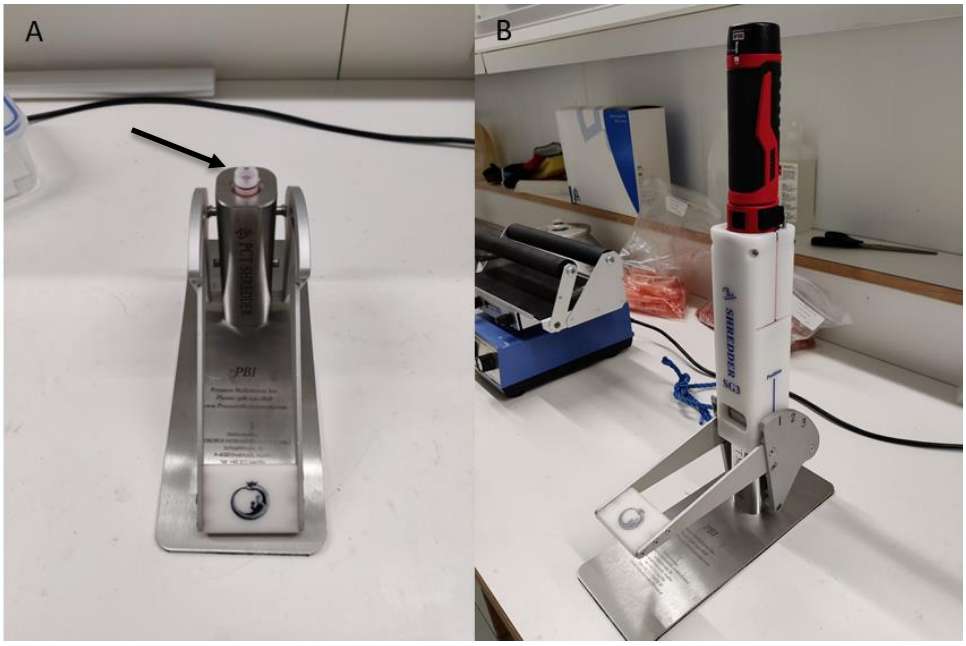

Figure 18. The shredder and cooling block provided by Oroboros instruments (Innsbruck, Austria). ***A****: Shredder tube (indicated with arrow) inserted into the cooling block.* ***B****: The shredder inserted on the cooling block, set at position 1.*

The homogenised samples were then transferred to 1.5ml Eppendorf tubes and centrifuged at 2000g for 1 minute at 4°C (Himac CT15RE centrifuge, Hitachi Koki Co., Ltd). The supernatant was then collected and 20µl was added to each oxygraphy chamber (Oroboros respirometers, Oroboros Instruments, Innsbruck, Austria).

Oroboros respirometers allow for the measurement of mitochondrial respiration, through detection of the rate of oxygen consumption, termed, oxygen flux per mass ($pmol \cdot s^{-1} \cdot mg^{-1}$).

In normal mitochondrial function, energy substrates are needed to allow for the production of $NADH_2$ and $FADH_2$. Within the Krebs cycle pyruvate, malate and glutamate are oxidised to form NADH which affects complex I activity, while succinate is oxidised by Complex II to form $FADH_2$. These energy substrates can be added to the oroboros chambers in a Substrate-Uncoupler-Inhibitor Titration (SUIT) protocol to specifically assess different states of mitochondrial function.

SUIT Protocol

Respirometric experiments were performed in 2.1ml glass chambers of 2 Oroboros Oxygraphs to give a total of 4 technical replicates. LEAK respiration was assessed in 10% skeletal muscle homogenate in Miro5 using 10mM Pyruvate, 0.5mM Malate, 10mM Glutamate and 10mM Succinate. These substrates activated Complex I and II however no coupled respiration is occurring due to the absence of ADP (LEAK state). After 5 minutes, 5mM of ADP was added to observe the transition from LEAK to oxidative phosphorylation of complex I and II (OXPHOS), the presence of ADP allowing for coupled respiration to occur. Cytochrome c (10µM) was added to check for mitochondrial membrane integrity: any increase in mitochondrial respiration above 10% would indicate presence of mitochondrial damage (Gnaiger, 2020). FCCP (, a potent uncoupler of oxidative phosphorylation was added (0.5µM) to uncouple the respiration and observe the max output of the electron transport chain. Finally, 10mM of Malonate was added to inhibit Complex II and assess max respiration of complex I (Fig.19).

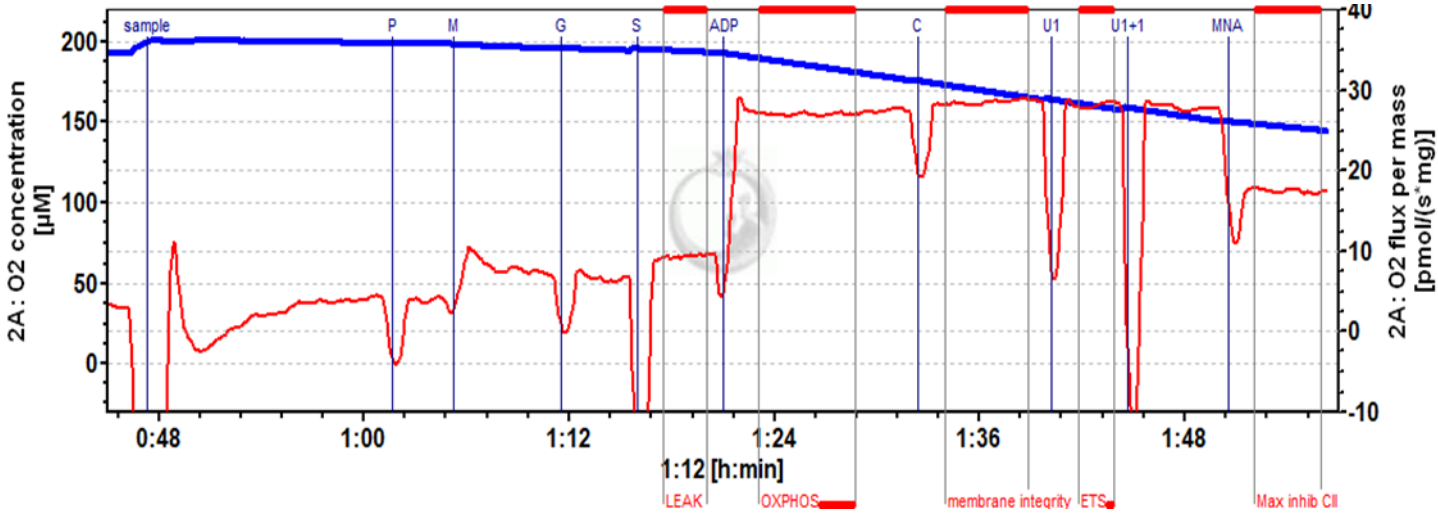

Figure 19 The software Datlab provides information on O_2 flux per mass and O_2 concentration. *Red line =O_2 flux per mass. Blue line= O_2 concentration Sample= insertion of hooded seal skeletal muscle. P=pyruvate, M=Malate, G= Glutamate, S=Succinate, ADP= adenosine diphosphate, C= Cytochrome c, U1= 1µl FCCP uncoupler U1+1= 1µl FCCP uncoupler for a total of 2µl. MNA= Malonate. Highlighted in red show mitochondrial respiration states, LEAK (uncoupled respiration in the absence of ADP for complex I and II). OXPHOS (oxidative phosphorylation), membrane integrity (an increase in O_2 flux by 10% would indicate damaged mitochondria. ETS (max capacity of the electron transport chain). Max inhib CII (max capacity of the electron transport chain inhibiting CII).*

Data analysis

Western Blot

Image analysis and protein normalisation of Ponceau stained membranes and developed films was done through ImageJ software (U. S. National Institutes of Health, Bethesda, Maryland, USA). (Appendix C)

Organisation of data was done using Excel (version 2203). Initial plotting of data was done by Graphpad Prism (Version 9.3.1, Graphpad Software, California, USA), a statistical analysis and visualization software, in order to assess for outliers within the data. Statistical analysis was done using the programming language R (Version 4.0.3, R Foundation for Statistical Computing, Vienna, Austria) and RStudio (Version 1.3.1093, RStudio PBC, Massachusetts, USA).

Analysis of protein bands between life stage and muscle groups were done using a two-way anova. Specific variability of means within groups and individuals was assessed using a Tukey honest significant test within R studio and Šídák's multiple comparisons test within Graphpad Prism.

Mitochondria Respiration

For online display and data analysis, the software DatLab (Oroboros Instruments, Innsbruck, Austria) was used. Means of each mitochondrial state was taken and organised in Excel (Version 2203).

All statistical analysis was done through the R programming language (Version 4.0.3) and RStudio (Version 1.3.1093).

Two flux control ratios (FCR) were calculated which were coupling control ratio (CCR; LEAK/OXPHOS) and P/E control ratios (OXPHOS/ETS) within RStudio by using mean values taken from DatLab.

One-way anova was used to assess the significant difference between individuals, as well as to assess the possible difference in the technical replications produced in the 4 different chambers of the Oroboros respirometers. FCR values were also compared to sea otter data collected by Wright et al., 2020 by a two sample T-test to determine the presence of

mitochondrial LEAK. Differences in sex between FCR was also determined by a two sample t-test.

In order to compare FCR values between muscle groups a Mann-Whitney U test was carried out due to the dataset being small and not conforming to a normal distribution.

To determine if seal body mass had an effect on the CCR and P/E ratios, Pearson correlation analysis was carried out.

Results

My first aim was to ask whether the seal expressed sarcolipin, SERCA1 and SERCA2. The first step was to establish if the DNA sequence coding for these proteins was present in a phocid seal. The second step was to determine whether the protein could be extracted from the hooded seal skeletal muscle and be quantified. The third step was to source antibodies for western blotting that were raised using peptides matching the protein sequences in seals and test them on hooded seal skeletal muscle.

Sln, SERCA1a and SERCA2a are highly conserved across mammals and found in phocid seals.

In silico analysis of DNA sequences from the Weddell seal reveals high conservation of sarcolipin, SERCA1 and SERCA2a across species. The translated DNA sequence acquired from Expasy included DNA which did not code for the Sln protein, in order to isolate the exons (protein coding sequence) specific for Sln, 56 amino acids pertaining to 168 DNA bases were removed from the beginning of the sequence in the DNA editing software ApE. Once removed, the Sln exon (96 base pairs) could be copied from the beginning of the sequence and blasted against the seal genome providing a match (Fig.20). The match indicates that the Sln DNA sequence is present within the Weddell seal genome. Both the human and Weddell seal Sln DNA sequence was translated into the amino acid sequence and compared using Clustal Omega and it was shown that humans Sln have a 94% protein alignment with Weddell seal Sln. When this amino acid sequence was compared to 10 other mammalian species, the similarity ranged between 80%-100% indicating a highly conserved protein (Table 5).

```
LepWed1.0 scaffold01852, whole genome shotgun sequence
Length=605896

 Score = 145 bits (78),  Expect = 4e-33
 Identities = 90/96 (94%), Gaps = 0/96 (0%)
 Strand=Plus/Plus

Query  1       ATGGGGATAAACACCCGGGAGCTGTTTCTCAACTTCACTATTGTCTTGATTACGGTTATT  60
               |||||||||  |||||||||||||||||||||||||||||||| |||| || || |||
Sbjct  358486  ATGGGGATATCCACCCGGGAGCTGTTTCTCAACTTCACTATTGTCCTGATCACCGTGATT  358545

Query  61      CTTATGTGGCTCCTTGTGAGGTCCTATCAGTACTGA  96
               ||||||||||||||||||||||||||||||||||||
Sbjct  358546  CTTATGTGGCTCCTTGTGAGGTCCTATCAGTACTGA  358581
```

Figure 20*. *High conservation between human and Weddell seal Sln. *Output from BLAST, query sequence is the predicted Weddell seal Sln DNA, the subject is the human Sln sequence.*

***Table 5 High conservation across mammalian species for Sln**. Table shows the percent identity matrix of the Sln amino acid sequence from 10 mammal species. Created using Clustal omega.*

	Mouse	Human	Dog	Weddel_Seal	Walrus	Grey_Seal	Ferret	Cow	Orca	Naked_Mole_Rat
1: Mouse	100.00	79.17	84.38	83.33	83.33	83.33	82.29	80.21	80.21	83.33
2: Human	79.17	100.00	94.79	93.75	93.75	93.75	92.71	84.38	84.38	84.38
3: Dog	84.38	94.79	100.00	98.96	98.96	98.96	97.92	86.46	86.46	86.46
4: Weddel_Seal	83.33	93.75	98.96	100.00	100.00	100.00	97.92	86.46	85.42	85.42
5: Walrus	83.33	93.75	98.96	100.00	100.00	100.00	97.92	86.46	85.42	85.42
6: Grey_Seal	83.33	93.75	98.96	100.00	100.00	100.00	97.92	86.46	85.42	85.42
7: Ferret	82.29	92.71	97.92	97.92	97.92	97.92	100.00	87.50	84.38	84.38
8: Cow	80.21	84.38	86.46	86.46	86.46	86.46	87.50	100.00	95.83	88.54
9: Orca	80.21	84.38	86.46	85.42	85.42	85.42	84.38	95.83	100.00	88.54
10: Naked_Mole_Rat	83.33	84.38	86.46	85.42	85.42	85.42	84.38	88.54	88.54	100.00

The steps above were repeated for SERCA1a and SERCA2a. SERCA1a and SERCA2a gave a protein alignment of 94.29% and 81.91% respectively when comparing to humans. When comparing to 10 other mammalian species protein alignment for SERCA1a was shown to be at its highest when compared to the grey seal (*Halichoerus grypus)* and walrus (*Odobenus rosmarus)*, 98% and 97% respectively (Table 6A). However, the SERCA2a amino acid sequence in the Weddell seal was shown to be less similar when compared to the grey seal and walrus, with a protein alignment of 82% for both species (Table 6B).

***Table 6. High conservation of SERCA1a and SERCA2a across mammals**. Percent identity matrix between 10 amino acid sequences of 10 mammal species. SERCA1a (**A**) and SERCA2a (**B**).*

Percent Identity Matrix - created by Clustal2.1

A

	Orca	Cow	Grey_Seal	Weddell Seal	Ferret	Dog	Walrus	Naked mole rat	Human	Mouse
1: Orca	100.00	96.57	93.14	93.71	94.29	96.00	94.29	92.53	94.86	93.71
2: Cow	96.57	100.00	94.86	95.43	94.86	96.57	94.86	93.68	95.43	95.43
3: Grey_Seal	93.14	94.86	100.00	97.71	94.86	96.57	96.00	92.53	94.29	93.71
4: Weddell_Seal	93.71	95.43	97.71	100.00	96.00	97.71	97.14	93.10	94.29	94.29
5: Ferret	94.29	94.86	94.86	96.00	100.00	98.29	97.71	93.10	96.00	96.00
6: Dog	96.00	96.57	96.57	97.71	98.29	100.00	98.29	93.10	96.57	95.43
7: Walrus	94.29	94.86	96.00	97.14	97.71	98.29	100.00	92.53	96.00	94.86
8: Naked_mole_rat	92.53	93.68	92.53	93.10	93.10	93.10	92.53	100.00	93.14	96.00
9: Human	94.86	95.43	94.29	94.29	96.00	96.57	96.00	93.14	100.00	96.59
10: Mouse	93.71	95.43	93.71	94.29	96.00	95.43	94.86	96.00	96.59	100.00

Percent Identity Matrix - created by Clustal2.1

B

	Weddell Seal	Cow	Human	Mouse	Dog	Walrus	Grey Seal	Orca	Naked mole rat	Ferret
1: Weddell_Seal	100.00	81.91	81.91	81.91	81.91	81.91	81.91	81.91	81.91	80.85
2: Cow	81.91	100.00	98.99	98.99	98.99	98.99	98.99	98.99	98.99	97.98
3: Human	81.91	98.99	100.00	100.00	100.00	100.00	100.00	100.00	100.00	98.99
4: Mouse	81.91	98.99	100.00	100.00	100.00	100.00	100.00	100.00	100.00	98.99
5: Dog	81.91	98.99	100.00	100.00	100.00	100.00	100.00	100.00	100.00	98.99
6: Walrus	81.91	98.99	100.00	100.00	100.00	100.00	100.00	100.00	100.00	98.99
7: Grey_seal	81.91	98.99	100.00	100.00	100.00	100.00	100.00	100.00	100.00	98.99
8: Orca	81.91	98.99	100.00	100.00	100.00	100.00	100.00	100.00	100.00	98.99
9: Naked_mole_rat	81.91	98.99	100.00	100.00	100.00	100.00	100.00	100.00	100.00	98.99
10: Ferret	80.85	97.98	98.99	98.99	98.99	98.99	98.99	98.99	98.99	100.00

BCA assay analysis showed a successful protein extraction

A successful protocol to extract and quantify protein from hooded seal skeletal muscle was established. During the testing phase, proteins were extracted using two main homogenisation techniques one utilising the TissueRuptor II and the other utilising the TissueLyser II. However, the tissue ruptor could only process one sample at a time and probes were used only once per sample to avoid cross contamination. This would increase sample processing time and was not deemed satisfactory for this study. Therefore, the method utilising the tissue lyser was preferred. This method of homogenisation had to be validated using a BCA assay to ensure a successful protein extraction to proceed with the western blot protocol.

Values produced by the BCA assay were plotted against the final BSA concentration shown in Table. 2. However, the absorbance given from the muscle homogenate samples was too high which gave a protein concentration outside of the working range of the BCA assay (Fig.21, red symbols). Therefore, the muscle samples could not be reliably compared to the standard curve. The solution to the problem was to dilute the original samples by a factor of 10 so that the absorbance fell within the working range (Fig.21, blue symbols). Once within the working range protein content could be calculated through the simple linear equation y=mx+c (Appendix B).

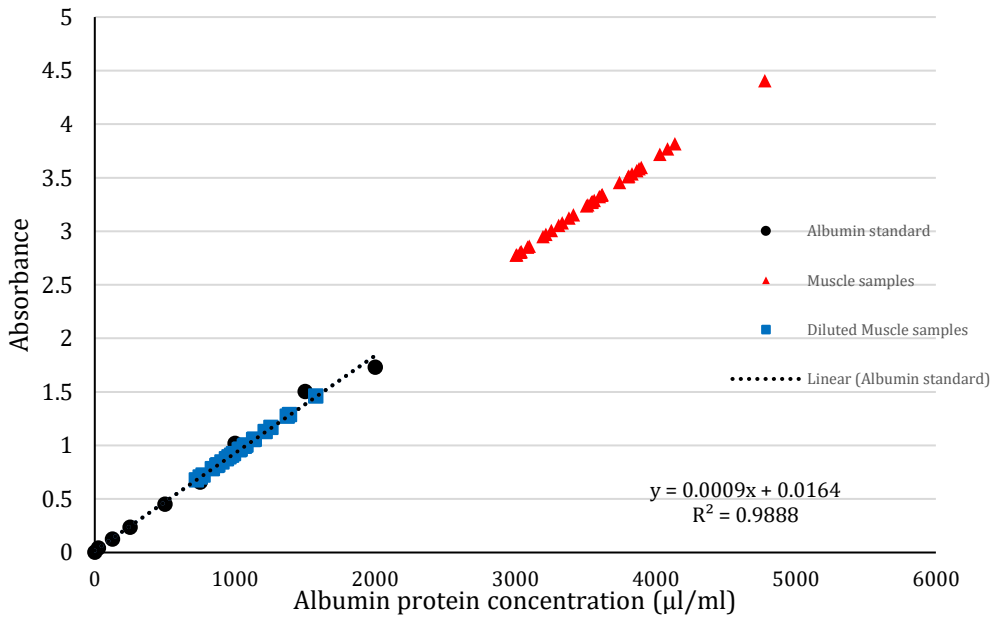

Figure 21. Standard curve to determine protein concentration of hooded seal skeletal muscle protein*. Black dots represent albumin (BSA) known protein concentration standards. Red triangles are undiluted protein extracts from hooded seal skeletal muscle which fall outside the range of the standard curves. The blue squares are 1/10 dilution of hooded seal muscle homogenate (blue) which fits within the standard curve. The absorbance of the diluted muscle homogenate can be accurately compared to the Albumin standards providing a reliable protein concentration.*

Sarcolipin antibody does not bind with the expected molecular weight in hooded seal skeletal muscle.

The Sln antibody (Cat. No: 18395-1-AP, proteintech, Illinois, USA) was raised using the human Sln with the entirety of the amino acid sequence. Which corresponds to 94% protein alignment in the Weddell seal (Table 5). Using protein extracted from hooded seal skeletal muscle the Sln primary antibody was tested. Membranes incubated with Sln primary antibody did not show bands at the expected weight of 10 kiloDaltons (kDa)(Fig.22). Instead, bands appeared at just under 120kDa. After multiple attempts trying to resolve this issue the specific bands of Sln could not be detected and therefore analysis of Sln could not continue.

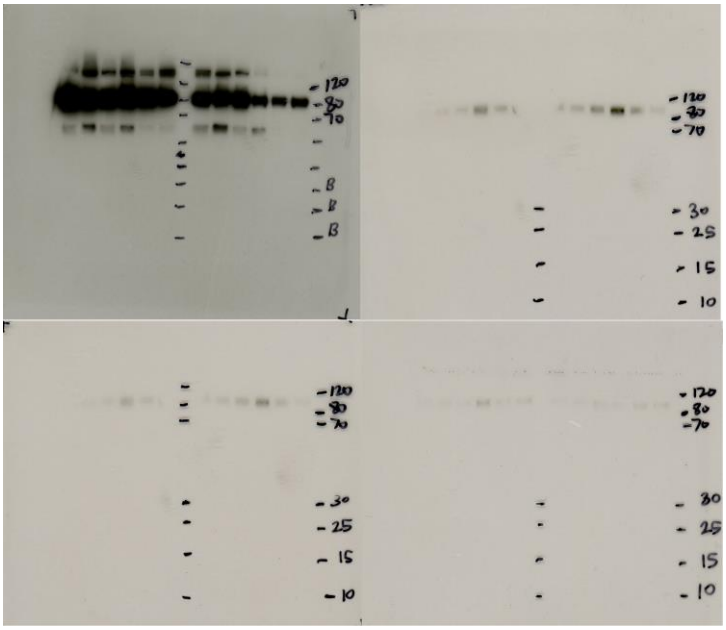

Figure 22. Sln western blots *Nitrocellulose membrane incubated with Sarcolipin antibody exposed on emulsion film. Numbers indicate protein weight in kiloDalton (kDa) No bands detected at 10kDa. Primary antibody concentration 1:500. Secondary antibody concentration 1:10,000.*

SERCA1a antibody does not bind to hooded seal skeletal muscle.

SERCA1a antibodies were procured from Abcam (Cat.no ab233647) and was created using Human SERCA1 ATPase with the amino acid sequence between 450-650.

Membranes incubated with SERCA1a antibody were developed and bands did not show at the expected weight of ~110kDa (Fig.23). After multiple attempts to resolve this issue, involving a range of primary and secondary antibody concentrations specific bands for SERCA1a did not appear. The goat anti-mouse secondary antibody was shown to exhibit non-specific binding when membranes were only incubated with this antibody (Fig.24). The analysis of SERCA1a could not continue.

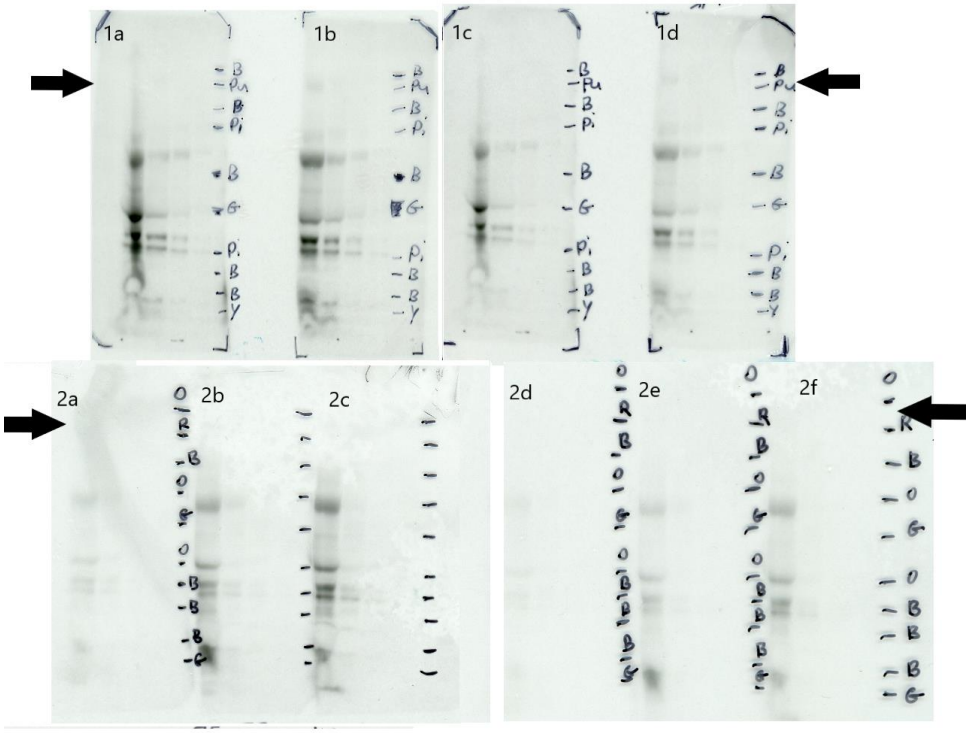

Figure 23. Western blots showed no specific bands for SERCA1a*. Black arrows indicate the position of expected bands for SERCA1a at ~110kDa. Bands shown appear between 25 and 75kDa.* ***1a*** *and* ***1c*** *incubated with 1:1000 primary, 1:10,000 secondary antibody.* ***1b*** *and* ***1d*** *incubated with 1:500, 1:10,000.* ***2a*** *and* ***2d*** *incubated with 1:1000, 1:8000.* ***2b*** *and* ***2e*** *incubated with 1:750, 1:5000.* ***2c*** *and* ***2f*** *incubated with 1:500, 1:3000.*

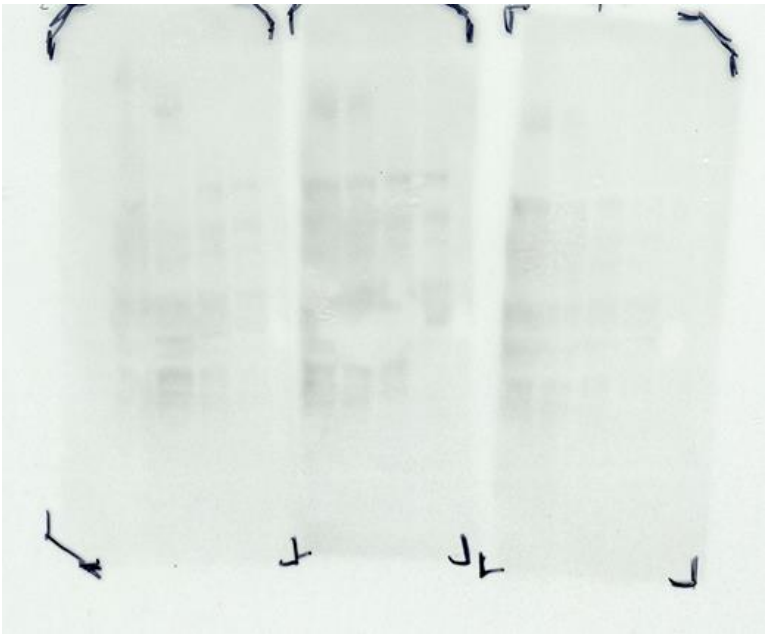

Figure 24. Secondary antibody control incubation shows non-specific binding*. Membranes were not incubated with SERCA1a primary antibody, however the emulsion film still provided binds. Indicating non-specific binding.*

SERCA2a antibody binds to hooded seal skeletal muscle with the expected molecular weight

SERCA2a antibodies were also procured from Abcam (Cat.no ab3625) and created using the human SERCA2 ATPase with the amino acid sequence between 250-550 which corresponded to 82% in the Weddell seal. Originally gels were loaded with 40µg/µl of protein, however the bands produced were highly oversaturated, therefore less protein was required to produce quantifiable bands. The amount of protein loaded was lowered to 20µg/µl, however this still provided bands that were high in saturation and unable to quantify (Fig.25). Using the 1/10 diluted samples utilised in the BCA assay, a final concentration of 4µg/µl was established as the best course of action. Bands appeared at the expected weight of ~115kDa (Fig.26). This indicates that SERCA2a is present within the skeletal muscle of hooded seals.

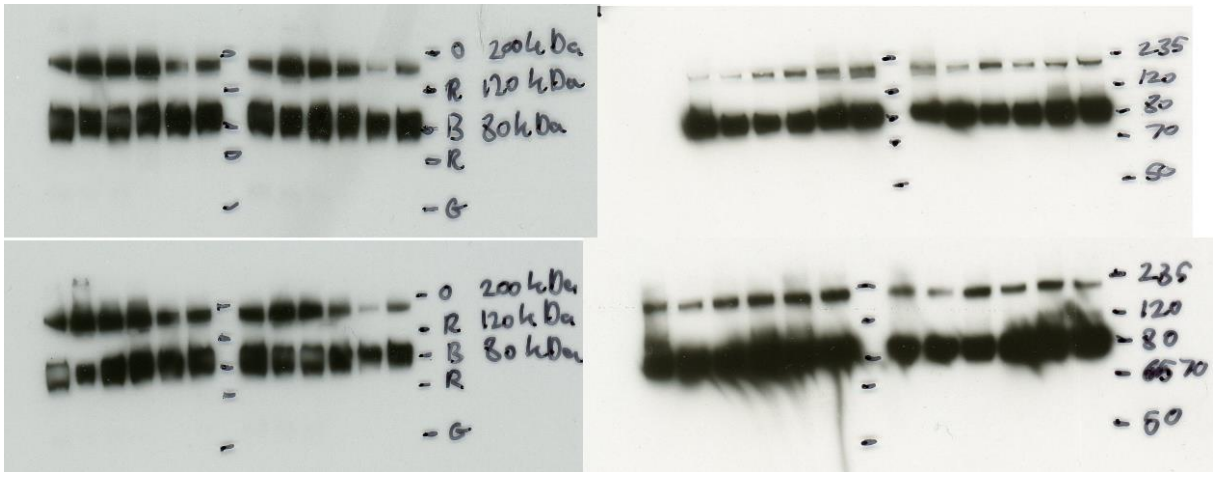

Figure 25. Oversaturated western blots of SERCA2a. *Protein concetration of 20µg/µl loaded into gels resulted in oversaturated bands when incubated with SERCA2a. Concentrations of primary and secondary for all 4 blots were 1:750 and 1:10,000 respectively*

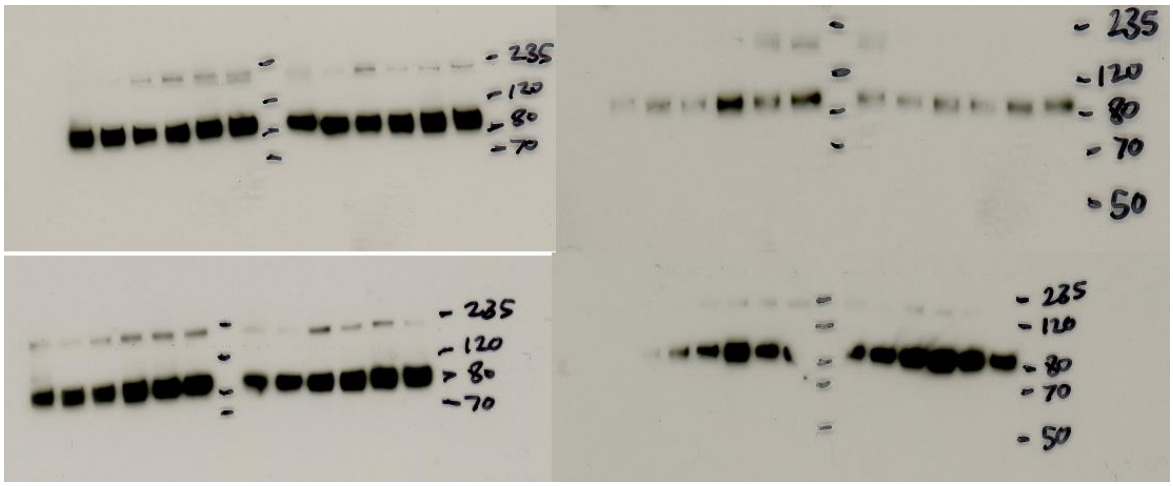

Figure 26. Western blot of SERCA2a showed specific bands (~115kDa)*. Western blot emulsion film was exposed (10 seconds) to nitrocellulose membrane with 1:750 SERCA2a primary antibody and 1:10,000 secondary antibody. Protein per lane = 4µg/µl*

It was then possible to continue with aims II and III and establish whether the amount of SERCA2a protein decreases with age and is dependent on the muscle group.

Using the method of total protein normalization, the density of bands from 4 Ponceau stained (PS) membranes and 4 emulsion film blots (EFB) were produced using scanned images analysed using ImageJ software. Density ratios (EFB/PS) were calculated within Excel (Table 7). The ratios were then plotted using Graphpad prism to assess for any outliers in the data (Fig.27). Outliers could be the result of factors mentioned in the chapter "Normalisation of Western Blots". Within blot 3, an outlier was present showing a density ratio of 9.21 (Fig.27;Table 7) this was omitted from the dataset as it would increase the variability of the results.

Table 7 Density ratios of SERCA2a normalised against Ponceau S stained membranes. *Four blots were produced using hooded seal skeletal muscle homogenate incubated with SERCA2a antibody. Density ratios shown in blots 1-4 were calculated using density of SERCA2a bands/density of Ponceaus S stained bands . M.long= M.longissimus dorsi, P.major= Psoas major. Density was provided through ImageJ. NA values indicate no density values due to failed transfer*

ID	Life Stage	Muscle	Blot 1	Blot 2	Blot 3	Blot 4
K1-21	Adult	M.long	1.306	2.606	3.555	3.407
K8-21	Adult	M.long	0.825	2.853	3.352	3.182
K9-21	Adult	M.long	0.363	1.976	2.794	2.533
K3-21	Pup	M.long	0.957	4.358	3.526	4.281
K8b-21	Pup	M.long	0.608	3.699	5.713	2.320
K10b-21	Pup	M.long	0.850	NA	9.211	2.619
K1-21	Adult	P.major	1.663	NA	3.050	2.942
K8-21	Adult	P.major	0.922	2.405	2.558	3.327
K9-21	Adult	P.major	1.551	2.405	3.416	2.791
K3-21	Pup	P.major	0.401	2.202	4.044	3.274
K8b-21	Pup	P.major	0.655	1.181	5.189	3.875
K10b-21	Pup	P.major	0.218	0.132	4.550	2.978

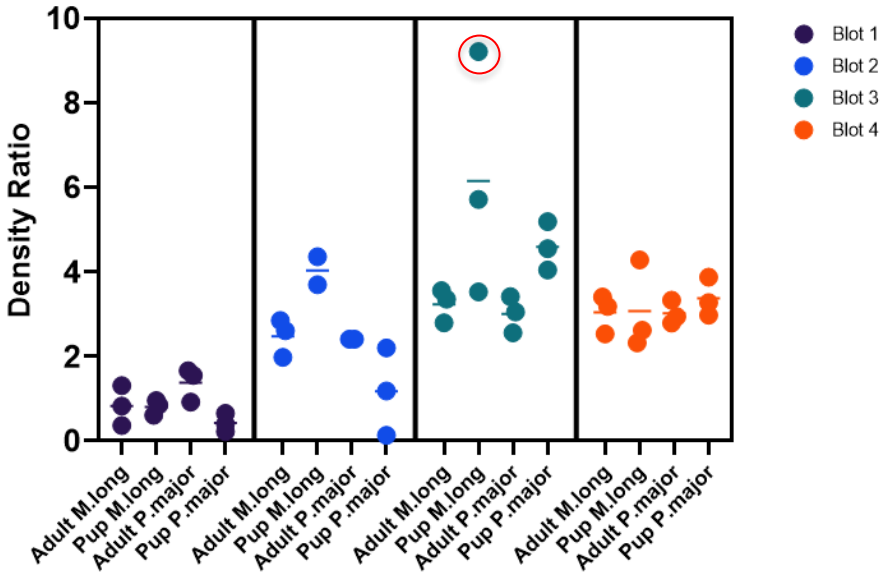

Figure 27 Density ratios of SERCA2a normalised against Ponceau S stained membranes. *Four blots were produced using hooded seal skeletal muscle homogenate. X axis shows hooded seals, separated into adult and pup life stages as well as different muscle types. M.long= M. longissimus dorsi, P.major= Psoas major. Red outlined data point is to be omitted.*

SERCA2a protein expression is highest in hooded seal pups when compared to adult seals but only in *M.longissimus dorsi*.

Once the outlier data was omitted, mean values were calculated for each life stage and muscle group. Within muscle *M.long*, pups showed a noticeably high expression of SERCA2a (Density Ratio= 3.53±0.61) compared to all other life stage and muscle groups (Fig.28).

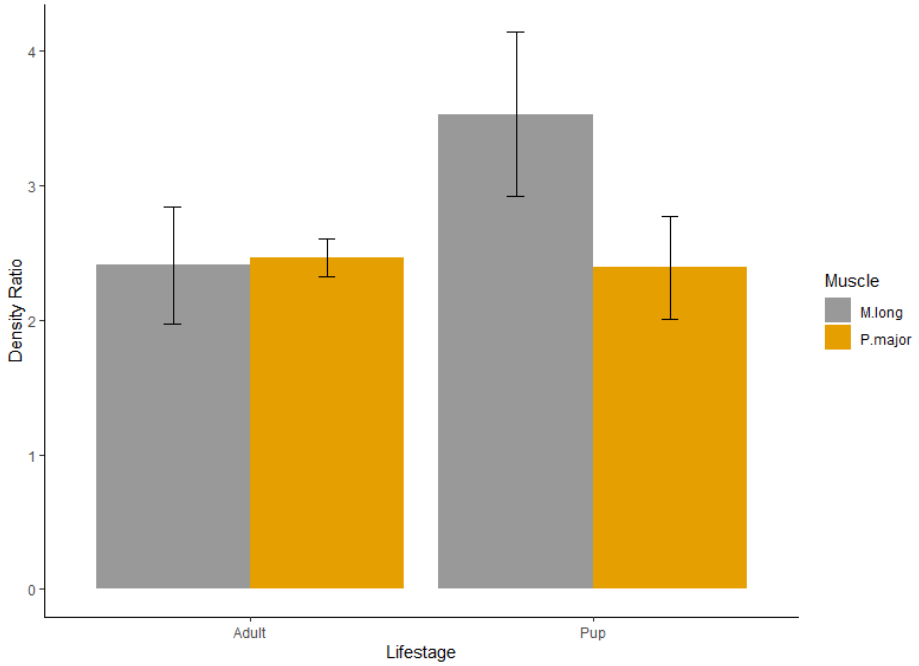

Figure 28 Mean SERCA2a/Ponceau S density ratios in Adults and Pups. *Grey bars indicate muscle M. longissimus dorsi, orange bars indicate muscle Psoas major. Error bars show ±1sd.*

Statistical analysis showed that there was no significant difference between life stages or muscle groups (p=0.067 and p=0.06 respectively). However, an interaction effect between life stage and muscle group was present (p=0.042) indicating that the combined effect of life stage and muscle group affects the expression of SERCA2a, probably indicating the significance of SERCA2a in pups but only in the *M. long* muscle group. To find the specific interaction, a Tukey honest significant difference post hoc test was applied; this indicated a significant difference of SERCA2a expression between life stages within the muscle *M.long* (P adj=0.049) and a significant difference between muscle within the pup life stage (P adj= 0.046). However, the Tukey post hoc test calculated adjusted p values, in order to obtain absolute p-values a Šídák's multiple comparisons test was done within Graphpad prism which showed pups having a significant effect of SERCA2a expression between muscle groups

(P=0.023) and *M.long* having a significant effect of SERCA2a expression between life stages (P=0.025). Therefore, hooded seal pups exhibit a higher expression of SERCA2a in the muscle *M.long* only (Fig.29)

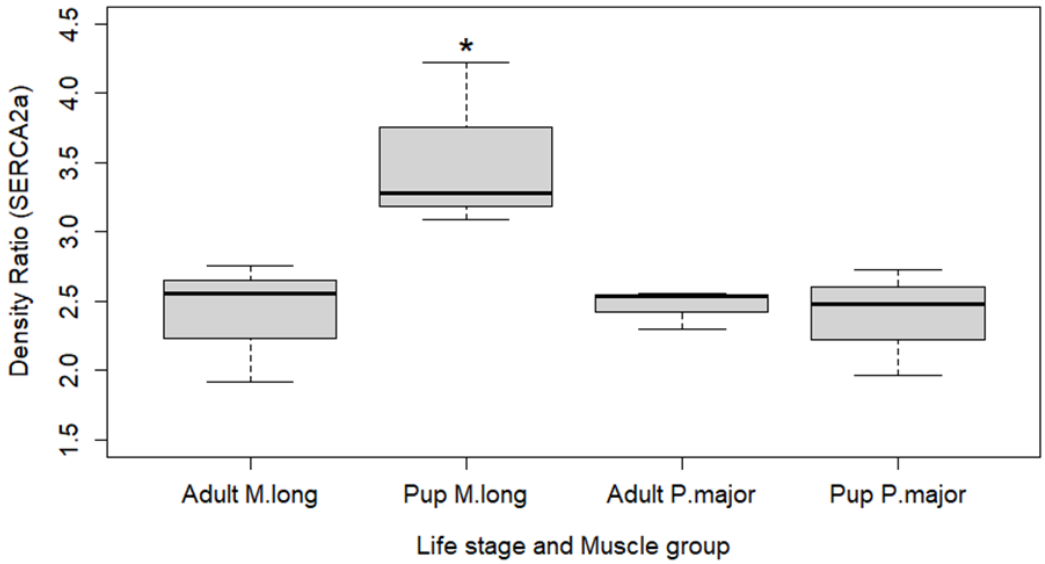

Figure 29 Hooded seal pups exhibit a higher SERCA2a expression within muscle M. longissimus dorsi. *Boxplot showing median values of density ratios (SERCA2a/Ponceau S) between hooded seals of different life stages and different muscle groups. M.long= M. longissimus dorsi, P.major= Psoas major. "*" shows a significance of p<0.05.*

Mitochondrial Respiration

The final aim (IV) of my thesis was to establish whether there is an increased mitochondrial proton leak (LEAK) present within hooded seals, which could generate heat. Individuals used within the mitochondrial respirometry were juvenile hooded seals around the same age (7-8 months) and so age was not considered as a factor and the principal comparisons were done between muscle groups *M. long* and *P. major*. Secondary to these comparisons, body mass and sex were assessed to check whether they affected the results shown within these muscle groups.

Data from the Oroboros respirometers provided 4 technical replicates from 4 respiration chambers for each juvenile hooded seal. Variability may have presented itself between the 4 respiration chambers which may affect the validity of the data. Therefore, a one-way anova was used to assess this variability, which showed a p-value of 0.94, indicating there was no significant difference in the variability between the 4 chambers. During the SUIT protocol Cytochrome c was added to assess the integrity of the mitochondrial membrane. As mentioned earlier, an increase in 10% of mitochondrial respiration would indicate that the mitochondria are compromised which would result in invalid results. However mitochondrial respiration within this study did not increase above the 10% threshold, indicating healthy mitochondria and therefore valid results. (Appendix D).

CCR (LEAK/OXPHOS) and the P/E ratios (OXPHOS/ETS) were calculated for all individuals and muscle groups used in the respirometry experiment, both these ratios are termed flux control ratios (FCR). CCR indicate how much LEAK constitutes in relation to OXPHOS capacity. A higher CCR indicates a higher level of mitochondrial LEAK.

P/E ratios indicate the limits of oxidative phosphorylation within the electron transport system as well as the extent of how tightly coupled the production of ATP is to the ETS. A higher P/E ratio indicates that respiration is tightly coupled and LEAK is not associated with thermogenesis.

When visualizing individual data, K13-21, *M.long* data was omitted as mitochondria did not respond to the injection of ADP, giving an unreliable CCR values (Fig.30).

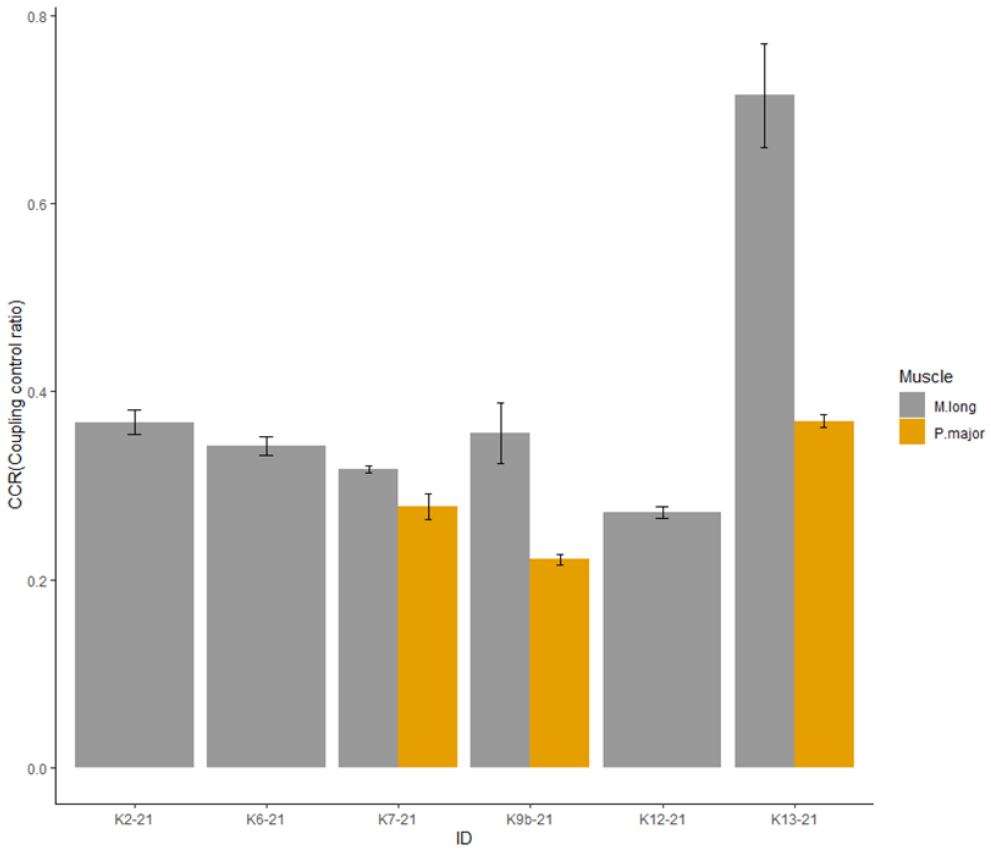

Figure 30 Individual data for Coupling control ratio (LEAK/OXPHOS) shows K13-21 has unreliable results*. Grey bars represent values for M.long and yellow bars indicate P.major. Plot shows mean values with 1 s.d.*

FCR ratios were not significantly different between individuals.

Both *M.long* and *P.major* were collated and analysis between individuals was carried out. This was due to the lack of statistical power to determine an interaction of FCR values between individuals in separate muscle groups. FCR values were expected to be similar between individuals due to them being similar in age and size. Although CCR values showed high variability between individuals K12-21 showed the lowest CCR (0.27±0.006) and K2-21 showing the highest CCR (0.37±0.01). A One-way anova provided a p value of 0.84 indicating CCR did not differ significantly between individuals. P/E ratios was observed to be less variable between individuals and a one-way anova confirmed this observation with a p-value of 0.9 indicating that P/E ratios did not differ significantly between individuals (Fig.31; Fig.32). Both FCR ratios, CCR and P/E ratios are statistically similar between all individuals, indicating that the extent of the mitochondrial LEAK and coupled respiration was consistent between individuals.

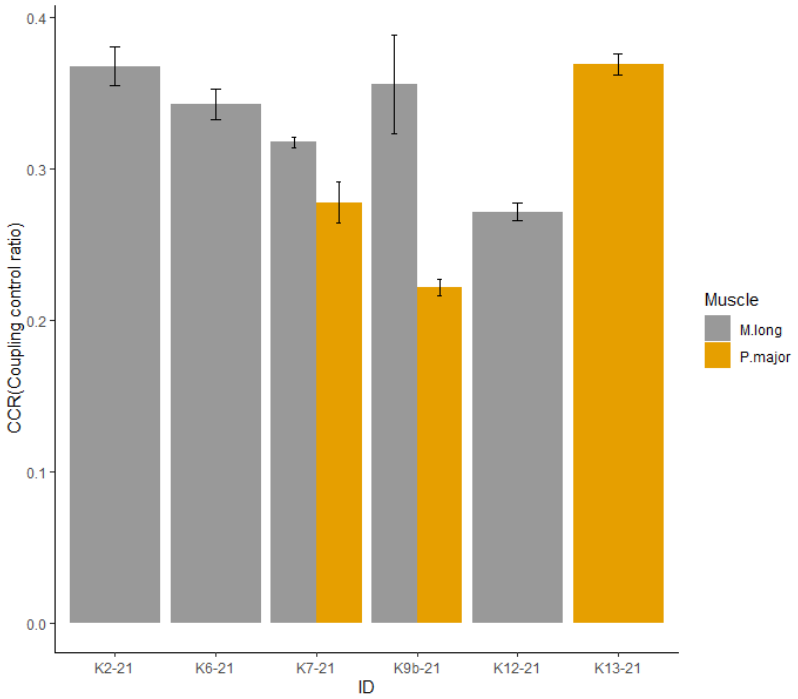

Figure 31 CCR coupling control ratio (LEAK/OXPHOS) between all individuals. *Grey bars indicate muscle group M. longisimuss dorsi (M.long), orange bars indicate Psoas major muscle group (P.major). Error bars indicate ±1sd.*

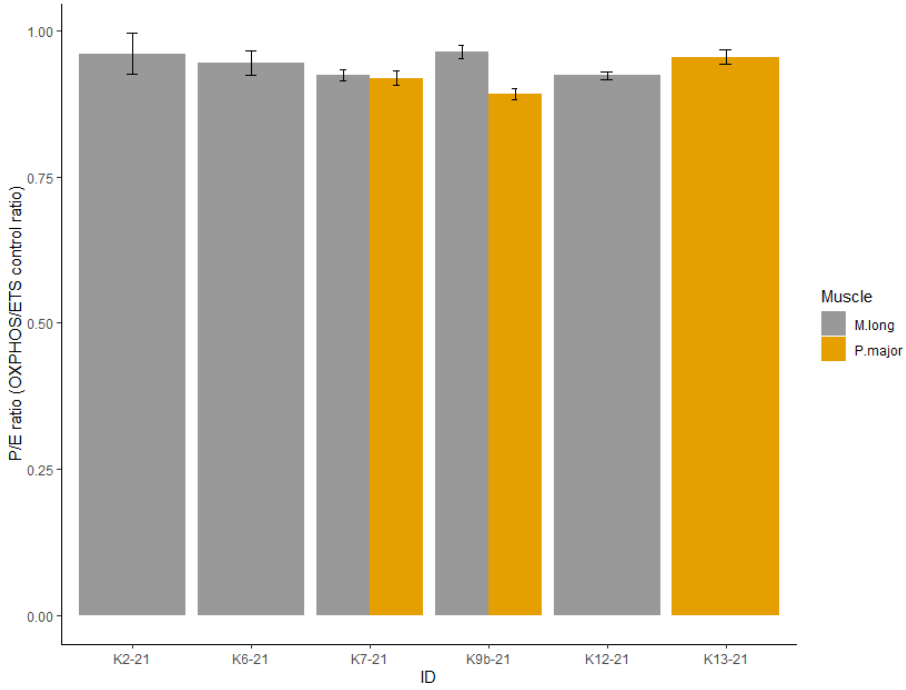

Figure 32 P/E ratios between individual hooded seals. *Grey bar= muscle group, M. longissimus dorsi. Orange bars= Muscle group Psoas major. Error bars indicate ±1sd*

Juvenile hooded seals show a high level of mitochondrial LEAK, however respiration is considered to be tightly coupled.

M. long exhibited a coupling control ratio (0.33±0.04) compared to *P.major* (0.28±0.06) averaged across all individuals, excluding K-13 (Fig.33). Both muscle groups show a high level of mitochondrial LEAK, indicating relatively large amounts of H^+ ions are flowing through the inner mitochondrial membrane. Although CCR of *M. long* was higher compared to *P. major*, the difference between muscle groups was not significant (p=0.79). P/E ratio of *M.long* and *P.major* were high 0.94±0.02 and 0.92±0.03 respectively, indicating that phosphorylation capacity is close to the maximum capacity of oxidative respiration and that the production of ATP using the proton gradient is tightly coupled under carbohydrate oxidation (Fig.33). Between muscle groups however, the difference was also deemed insignificant (p=0.25).

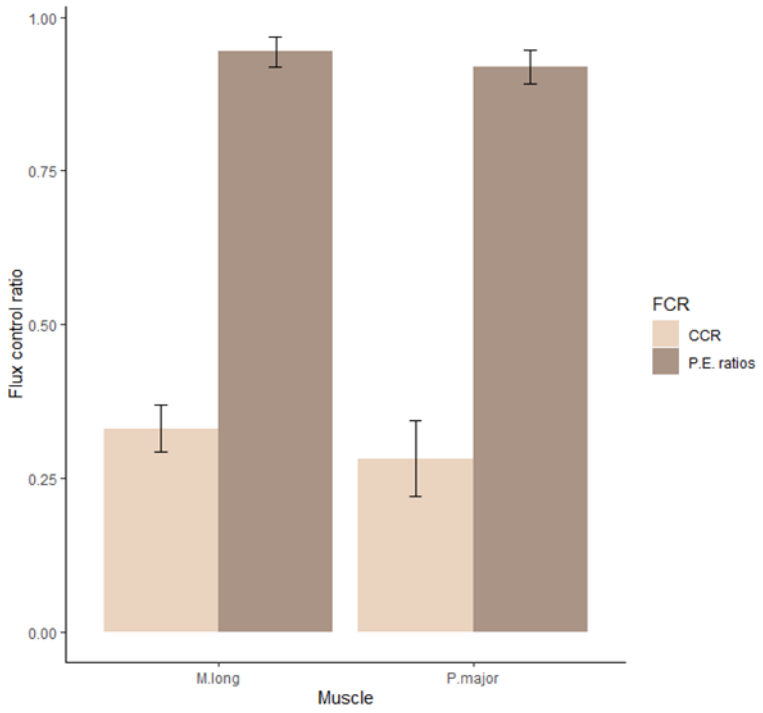

Figure 33 Mean Flux control values between muscle groups*. CCR= coupling control ratio (LEAK/OXPHOS). P.E. ratios= OXPHOS/ETS. Error bars show ± 1sd*

An increase in body mass reduces coupled respiration in the muscle *P.major.*

The relationship between body mass and FCR and its significance were determined as body mass may have affected the results seen between *M. long* and *P.* major (Fig.33). Body mass showed a negative relationship with FCR values suggesting that an increase in weight decreases CCR and P/E ratios (Fig.34). Pearson correlation indicated it was not a determinate factor with regards to CCR and P/E ratios. However within muscle *P.major*, the P/E ratio shows a total linear negative relationship with body mass which was shown to be significant (Table 8) (Fig.34D). This indicates that as body mass increases, respiration becomes more uncoupled in the muscle *P.major*.

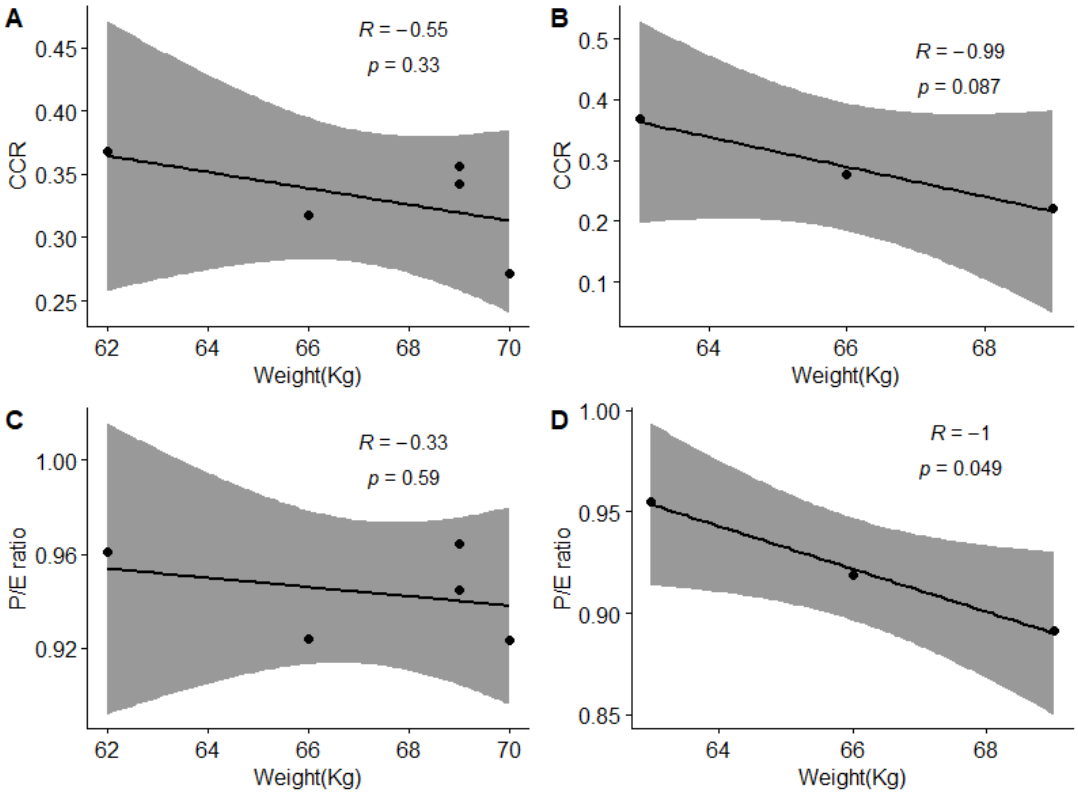

***Figure 34 Pearson correlation of Flux control ratios against Weight (Kg)**. **A**= CCR (coupling control ratio, LEAK/OXPHOS) of muscle M. longissimus dorsi (M.long) against. **B**= CCR of muscle Psoas major (P.major). C= P/E ratio (LEAK/ETS) of M.long. D=P/E ratio of P.major. Grey area denotes confidence interval of 95%.*

Table 8 Pearson correlation of Flux control ratios (FCR) and weight*. CCR (coupling control ratio LEAK/OXPHOS), P/E ratio (OXPHOS/ETS).*

Muscle group	**FCR**	**FCR~Body mass r value**	**P value**
M.long	CCR	-0.55	0.32
P.major	CCR	-0.99	0.09
M.long	P/E ratio	-0.33	0.59
P.major	P/E ratio	-1	0.049

Males have a more coupled respiration compared to females within muscle *M. long.*

Sex may also have been a factor which affected the results between *M. long* and *P. major* as the distribution of males and females was shown to be unequal in both muscle groups. Unfortunately, the influence of sex on CCR and P/E ratios within the muscle *P. major* could not be investigated due to the lack of data. However, within *M. long*, males (n=3) were shown to have a higher P/E ratio indicating a significantly more coupled respiration (p=0.025) compared to females (n=2). This significance may have inflated the values of the P/E ratios in *M. long*, as more males are present in the dataset (Fig.35B). However, sex was shown not to be a factor in determining CCR within *M. long* (P=0.053), indicating that mitochondrial LEAK did not differ between males and females (Fig.35A).

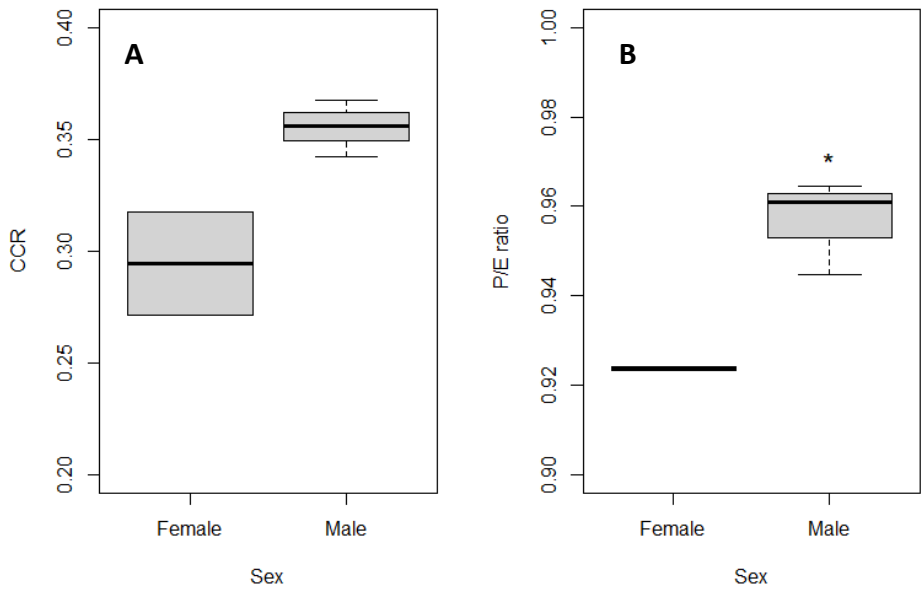

Figure 35. Boxplots of flux control ratio with regards to sex*. A= CCR (coupling control ratio, LEAK/OXPHOS). B= P/E ratio (OXPHOS/ETS). Data derived from muscle group M. longissimus dorsi only. "*" indicates a significance p<0.05.*

Mitochondrial LEAK in hooded seals is elevated compared to other species

In order to realise if the mitochondrial LEAK present in the hooded seal is considered high the CCR was compared to different species. When comparing CCR values of hooded seals to CCR values found for sea otters in the paper written by Wright et al., (2021); otter CCR values (0.41±0.05) were higher compared to hooded seal CCR (0.34±0.04) (Fig.36). The overlap of CCR values seem to indicate similarity of LEAK between the two species however when applying a two sample T-test these values were significantly different from each other (p=0.004). Compared with the reported CCR of the northern elephant seal (0.13±0.03; *Mirounga angustirostris*)(Wright et al., 2020), hooded seal CCR was observed to be significantly higher, however the statistical significance could not be calculated as only the average values and its standard deviation was reported. Hooded seal CCR was also observed to be higher compared to CCR reported in humans (0.2;n=1) (Porter et al., 2015) but the statistical significance could not be calculated due to the lack of data.

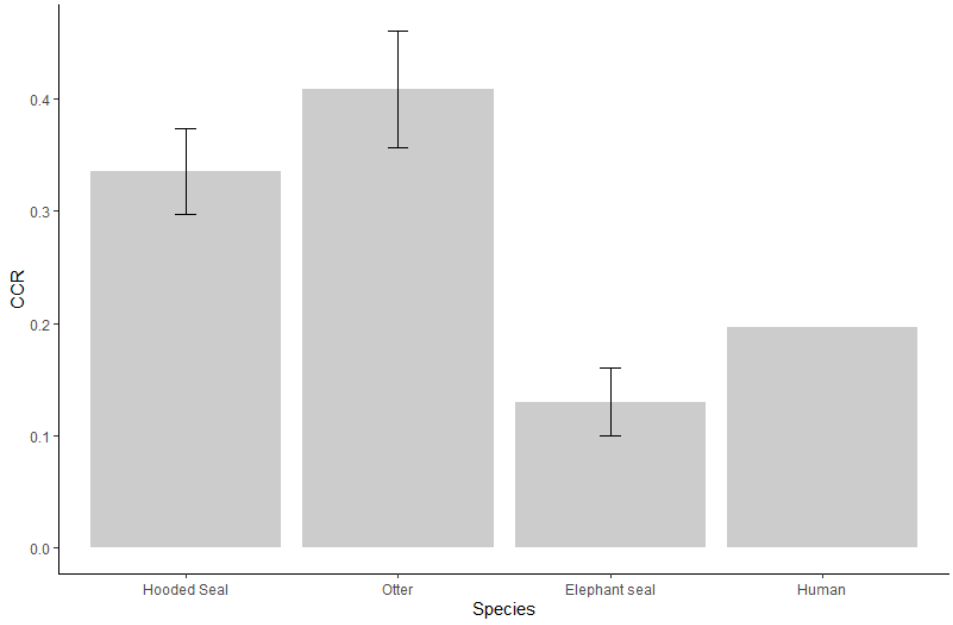

Figure 36. CCR (coupling control ratio) between hooded seal, sea otter, northern elephant seal and human. *Error bars indicate ±1sd. Hooded seal data used was from muscle group M. longissimus dorsi only. Otter data was derived from Wright et al.,2020. CCR values for elephant seal and human were calculated from an induced LEAK from complex 1 only, whereas CCR from hooded seal and otters were calculated from an induced LEAK from complex I and II.*

Discussion

Due to the disadvantageous effects of long-term shivering on the muscle, non-shivering thermogenesis has evolved to maintain thermal balance (Aydin et al., 2008;Periasamy et al., 2017). The use of skeletal muscle non-shivering thermogenesis has been adopted by fish species such as the Opah (*Lampris guttatus*) which exhibits cranial endothermy in order to protect the central nervous system through the use of ATP hydrolysis in SERCA pumps. (Runcie et al., 2009). This mechanism would allow the Opah to expand its vertical niche in the water column allowing it to withstand a rapid decrease in temperature when diving below the thermocline (Polovina et al., 2008). The stable temperatures produced by the cranial endothermy and the protection it provides to the central nervous system may allow it to maintain visual acuity when capturing prey in deeper, colder waters (Block, 1987). In other species of fish such as the swordfish (*Xiphias gladius*), and the fish family *Scombridae* a modified skeletal tissue is present in the cranial region and is termed, the heater organ, express high levels of mitochondria as well as high levels of SERCA due to the increased surface area of the SR (Carey, 1982;Block, 1986;Block, 1994). The presence of muscle NST in fish species has led to the hypothesis that this mechanism of thermogenesis has been around since the divergence of fish and mammals and that it is a predecessor of the mechanism found in BAT. The absence of BAT in fish species has reinforced this hypothesis (Rowland et al., 2015;Nowack et al., 2017;Periasamy et al., 2017). The importance of skeletal muscle based NST due to the absence of BAT has been highlighted in more recent phylogenetic groups such as birds and mammals. BAT found in the likes of harp seals is not present in avian species (Freeman, 1971;Johnston, 1971;Saarela et al., 1991) and so in cold acclimated ducklings which lack BAT, there seems to be an increase in oxygen consumption and SERCA activity within skeletal muscle, leading to the conclusion that skeletal muscle is a site for NST when BAT is not present (Duchamp and Barre, 1993;Dumonteil et al., 1993). Within mammals, cold acclimated mice have been shown to exhibit skeletal muscle NST with the help of a SERCA regulator, sarcolipin (Sln), which when bound to SERCA, uncouples the transport of Ca^{2+} and ATP hydrolysis allowing this form of NST to produce heat and effectively compensate for the loss of BAT function (Fig.10)(Bal et al., 2012;Bal et al., 2016).

Currently, literature has expressed that NST has not been found in the hooded seal species despite them inhabiting a cold and wet habitat due to pups being born with a significant blubber layer (Blix and Steen, 1979;Blix, 2005;Pearson et al., 2011). However, the focus of NST within seals has been mainly on the mechanism found in BAT. This focus is presumably due to the presence of this specialised fatty tissue within other arctic and non-arctic seal species, e.g. the harp seal and northern fur seals (Blix and Steen, 1979;Blix et al., 1979b); as well as the notion that the evolutionary development of BAT gave a selective advantage in the early evolution of the mammalian group (Cannon and Nedergaard, 2004;Rowland et al., 2015).

Questions arose between my supervisors and I as to why BAT was not expressed in hooded seals despite experiencing the same habitat conditions as harp seals which do express BAT (Blix and Steen, 1979). Therefore, my attention was soon shifted to the skeletal muscle as a potential source of NST which included the Sln-SERCA NST mechanism found in mice (Bal et al., 2012;Bal et al., 2016). However, skeletal muscle is the largest organ in the body with regards to homeotherms (Zurlo et al., 1990;Janssen et al., 2000) and distribution of NST may vary between skeletal muscle groups and muscle fibre types. Since different muscle fibres have different types of metabolism (Schiaffino and Reggiani, 2011), the ability of generating heat through NST may vary according to fibre type and their "preferred" metabolic pathway. Dependency on NST within the skeletal muscle may also diminish as hooded seals age, as is the case with BAT within harp seals as well as other mammal species (Pearson et al., 2014;Symonds et al., 2015). The extent of NST within skeletal muscle of hooded seals may not be limited to the Sln-SERCA NST mechanism. For instance, within the mitochondria of skeletal muscle, a mitochondrial LEAK may be present, where the protons essentially leak through the inner mitochondrial membrane. The energy derived from the electrochemical proton gradient is then released as heat as is the case for the marine mammal, the sea otter (Wright et al., 2021).

This line of thinking led to the hypotheses and goals outlined in the introduction: That hooded seals may resort to skeletal muscle-based, non-shivering thermogenesis mechanisms, and that those mechanisms are most likely to be present in the neonatal and juvenile life stages due to their increased surface area and exposure to the cold environment compared to adult life stages. Specifically, I set out to test:

I. Whether hooded seals expresses sarcolipin and SERCA in skeletal muscle.

II. If the amount of sarcolipin or SERCA protein differ between muscle groups.

III. Whether either the amount of sarcolipin or SERCA protein decreases with age as other thermoregulatory mechanisms develop.

IV. Whether an increased mitochondrial proton leak (LEAK) is present within hooded seal skeletal muscle which could generate heat.

In silico detection of Sln and SERCA gene expression within hooded seal skeletal muscle

Hooded seals have the potential to house a Sln-SERCA interaction within the skeletal muscle.

According to the DNA comparison and amino acid sequence alignment, the protein Sln is present within the Weddell seal and is highly conserved between other species of the seal line *Pinnepedia* tested within this study, these being the walrus and grey seal (Table 5). These findings confirm the evolutionary conservation of Sln discussed in Rowland et al., (2015) and suggests that hooded seals would also have an Sln gene, which may also be 100% identical to that of the Weddell seal, grey seal and walrus. The 100% amino acid sequence alignment for Sln within *pinnepedia* adds weight to the notion that the Weddell seal genome can be used as a proxy for other seal species.

Protein alignment of SERCA1a and SERCA2a although not identical are above 90% and 80% respectively across 10 mammal species (Table 6). Specifically, for SERCA1a the alignment is at its highest between species within the suborder *Pinnepedia* and suggesting a high conservation within *Pinnipeds*. SERCA2a protein alignment does not vary considerably between species even within the *Pinnepedia* suborder. Although the protein alignment of SERCA is in general less compared to that of Sln this may be related to the size of the actual proteins themselves. Sln is a comparably smaller protein (31 aa) than that of SERCA1a (994aa) and SERCA2a (997aa), and so Sln may have a higher probability of remaining unchanged between species. However, despite both SERCA1a and SERCA2a being considerably bigger in size a high protein alignment is still evident. SERCA's main function within the skeletal muscle is to re-uptake Ca^{2+} from the cytosol into the SR, thereby

controlling the termination of a muscle contraction. Therefore, it is not surprising that all mammals should possess the genetic coding needed to produce these proteins. The fact that Sln and SERCA are present within seal species provides the notion that Sln and SERCA can also be found within the hooded seal species, thereby implying that they may also operate a Sln-SERCA NST mechanism. This gave the confidence to proceed with antibody detection of the target proteins through Western Blotting.

Protein normalisation of Western blots

Originally the protein normalisation of western blots was to be done using the housekeeping protein, β-actin. However, this soon proved to be difficult as the β-actin antibodies did not bind as expected onto the nitrocellulose membrane. In the past decade, it has been found that β-actin is not a reliable protein for normalisation of western blots, as it fails to distinguish between actin levels at high protein concentration of the target sample; this pattern also occurs during long incubations of 1hr or more (Dittmer and Dittmer, 2006). When trying to find solutions to the housekeeping normalisation another method presented itself, this being total protein normalisation (Romero-Calvo et al., 2010) as described in the Methods section.

Total protein normalisation eradicated the need for a housekeeping protein and much to my elation did not need to provide specific protein bands in a developed image. Instead, nitrocellulose membranes could be stained using Ponceaus S solution which binds to the positively charged amino acids of proteins due to the stains negative charge (Sander et al., 2019). This method is more favourable due to the process being reversible with a simple wash of distilled water, compared to housekeeping normalisation that required the nitrocellulose membrane to be stripped and incubated again which could result in some of the protein being lost. The use of Ponceau S as a method for western blot normalisation is also preferred by research journals; the Journal of Biological Chemistry and the American Journal of Physiology due to it not effecting further procedures on nitrocellulose membranes (Fosang and Colbran, 2015;Brooks and Lindsey, 2018)

In situ detection of Sln and SERCA in the skeletal muscle of hooded seals.

Sarcolipin

Although data points to the notion that Sln is highly conserved and is identical within some seal species, Sln could not be detected within the skeletal muscle of hooded seals. This would point to the conclusion that the protein Sln and hence the Sln-SERCA NST mechanism is not expressed within hooded seals. However, the failed detection of Sln may not be due to the simple absence of this protein. Researchers have highlighted that the role of Sln is more dominant and is more expressed in larger mammals such as rabbit, dog and humans (Odermatt et al., 1997;Rowland et al., 2015), therefore hooded seals which are also considered large mammals, should have expressed Sln within the skeletal muscle. Undetected bands may have been the result of the antibody used; to maximise reactivity of the target species, previous studies have used primary antibodies for Sln which had been custom made (Bal et al., 2012;Bombardier et al., 2013;Fajardo et al., 2013). Within this study Sln primary antibody was acquired through commercial means and hooded seal was not cited as reactive species. The high protein alignment of Sln was thought to offset this uncertainty, however there may have been a mismatch between the hooded seal Sln and the anti-Sln primary antibody resulting in a failed detection. The molecular weight of Sln is also very small (10kDa) and the electrophoresis gels may have lost the protein during the running process. Reducing the gel concentration could allow for the retention of smaller molecular weight protein however this was outside the achievable aims for this study.

Bands did appear at ~115kDa, roughly the same weight as the SERCA protein (Fig.22). This may be due to the specific binding that occurs between SERCA and Sln (Fig.11)(Asahi et al., 2003;Asahi et al., 2004). Sln may have bound to SERCA during the stages of protein extraction, providing the bands seen in Fig.22. This suggests that the Sln primary antibody may have succeeded in detecting Sln but was not at the expected weight of 10kDa. However, the denaturation step would have been expected to denature any complexes.

SERCA1

Similar to the results of Sln, no bands occurred at the expected weight for SERCA1 (~110kDa) (Fig.23). The bands that did occur, were not associated with SERCA1a. Secondary antibody of SERCA1a was shown to exhibit unspecific binding due to these bands occurring again when membranes were only incubated with secondary antibody (Fig.24). Although secondary antibody, was shown to exhibit non-specific binding, results suggest that SERCA1 is not present within hooded seal *M.longissimus dorsi* and *Psoas major* skeletal muscle groups. This may be due to SERCA1 being exclusively expressed in certain muscle fibre types, these being the fast twitch fibre type (MacLennan et al., 1985;Brandl et al., 1987;Periasamy and Kalyanasundaram, 2007) and that the skeletal muscles used in this study are known to be the slow oxidative type (George et al., 1971;Blix et al., 1979a;Kanatous et al., 2002).

In situ SERCA2 expression is highest within pups but only within *M.longissimus dorsi*

Unlike Sln and SERCA1a, SERCA2a could be successfully detected using the western blot protocol. The level of SERCA2a within the skeletal muscle of hooded seals was relatively high considering membranes loaded with just 4µg/µl of protein produced a blot which gave a high saturation of bands at the expected weight (~115kDa; Fig.26). This indicates a high concentration of SERCA2a within the skeletal muscle and an increased ability to recycle Ca^{2+}.

This high expression of SERCA2a within *M. long* and *P.major* are indicative of muscle groups involved in increased activity such as locomotion (Kubo et al., 2003). Although SERCA2a is expressed in cardiac and skeletal muscle, they are exclusively expressed in the slow twitch muscle fiber type of skeletal muscle (MacLennan et al., 1985;Zarain-Herzberg et al., 1990;Periasamy and Kalyanasundaram, 2007). The absence of SERCA1a and a high expression of SERCA2a speculates that *M. long* and *P. major* are in fact slow-twitch oxidative fibers which confirm findings by Kanatous et al. (2002).

SERCA2a was found to be expressed across both muscle groups in pups and adults. However, a significantly higher expression of SERCA2a was detected within *M. long* skeletal muscle at the pup life stage. This higher expression of SERCA2a may equate to a higher concentration of SERCA2a within the *M. long* muscle resulting in a higher rate of ATP hydrolysis

(Dumonteil et al., 1993). Seal neonates in general have a higher metabolic rate compared to juveniles and adults (Lavigne et al., 1986;Burns, 1999;Donohue et al., 2000). The elevated metabolic rate is usually linked to the growth of the pup (Brody, 1945) but the metabolic demands of such high concentrations of SERCA2a within *M. long* may also contribute to this. The increased metabolic demands brought about by high SERCA2a concentrations seems counterintuitive when pups need to conserve energy during fasting (Castellini and Rea, 1992), a possible reason for this contradiction is that *M. long* may be a site for thermogenesis due to the pups need to thermoregulate.

M. long is the largest muscle in the dorsal region running along the length of the spine. Due to its size and location, the high levels of SERCA2a equating to a high rate of ATP hydrolysis within *M. long* may point to a major site for thermogenesis. However, Sln is yet to be found within the skeletal muscle and therefore thermogenesis from the *M. long* within pups may be linked to shivering capacity instead.

Skeletal muscle mitochondrial respiration

Hooded seals exhibit a high coupling control ratio

Three mitochondrial stages were measured with the Oroboros-O2k: LEAK (respiration compensating for H^+ ion leak), OXPHOS (oxidative phosphorylation) and ETS (max capacity of the electron transport system). Values obtained were converted into flux control ratios (FCR) which were CCR (LEAK/OXPHOS) and PER (OXPHOS/ETS). The importance of this is to be able to normalize to a specific state obtaining a theoretical range between 0 and 1 (Gnaiger, 2020). CCR indicate the percentage of mitochondrial leak (LEAK) present in the mitochondria with regards to oxidative phosphorylation (OXPHOS). The closer the CCR is to 1 the higher the percentage of LEAK. P/E ratios indicate the limits of oxidative phosphorylation within the electron transport system as well as the extent of how tightly coupled the production of ATP is to the ETS. A higher PER indicates that respiration is tightly coupled and LEAK is not associated with thermogenesis

This study shows that LEAK respiratory capacity constitutes up to 33% of OXPHOS capacity within *M.long* and 28% in *P. major*. Comparing to data from Wright et al., (2020) which showed an increased mitochondrial LEAK in sea otter mitochondria, these values were statistically different compared to the LEAK of hooded seal indicating that they do not display

the same level of LEAK that sea otters do. When comparing to other seal species, CCR values within this study was observed to be significantly higher compared to northern elephant seals (Wright et al., 2020) and humans (Porter et al., 2015) suggesting that LEAK within hooded seals is still considered to be elevated (Fig.36). Despite this, it must be noted that LEAK state values obtained for the northern elephant seals and humans were developed under a different SUIT protocol. CCR values from northern elephant seal and humans also only included complex I, instead of both complexes I and II which were calculated in this study. In addition, the northern elephant seal SUIT protocol involved the addition of substrate Oligomycin A after addition of ADP (Wright et al., 2020). Oligomycin A inhibits the function of ATP synthase by blocking the proton channel (Lardy et al., 1958;Racker, 1963) but does not affect non-phosphorylating or uncoupled respiration, i.e. LEAK respiration (Huijing and Slater, 1961). Assessing LEAK state using the SUIT protocol involving oligomycin compared to the SUIT protocol within this study can yield significantly different results, something that Wright et al., (2020) addressed within their own paper. Therefore, effective comparisons with differing SUIT protocols cannot be made.

Similarities in OXPHOS and ETS capacity

Although the CCR values indicate a high LEAK which suggests the presence of uncoupled respiration in hooded seal juveniles, P/E ratios must also be considered to understand the relationship between OXPHOS and ETS and provide information on the coupled respiration of the skeletal mitochondria. Within this study a P/E ratio of 0.94 in *M. long* and 0.92 in *P. major* are close to one which indicates that OXPHOS capacity and ETS capacity are similar. This suggests that even under normal mitochondrial function, the rate of ATP production is not limited by the transfer of electrons across the phosphorylation system (complex I-IV) and indicates that respiration within the skeletal muscle is coupled. These PER ratios also indicate that both *M.long* and *P.major* are type 1 slow oxidative fibres as these muscle rely heavily on oxidative phosphorylation to produce ATP which support the interpretation of the results in the in situ protein detection of SERCA1a and SERCA2a (C. Ciccone, pers comm, June 2022)

These results bring a level of ambiguity as CCR values indicate a high LEAK suggesting uncoupled respiration is present in the skeletal muscle of hooded seals, however PER provide information which points to respiration being highly coupled. Due to the similarities of the OXPHOS capacity and ETS capacity, ATP synthase in this case is presumably running at max

capacity. The phosphorylation system (complexes I-IV) pumping protons into the intermembrane space do so at a faster rate than the max capacity of ATP synthase resulting in a back pressure leading to LEAK through the inner mitochondrial membrane itself.

The LEAK present in this study, still provides hooded seals with heat but may not pertain to a thermoregulatory mechanism due to the highly coupled respiration. Instead, the heat produced from LEAK may only contribute to the normal whole body endothermy.

Factors affecting Flux control ratios

Hooded seals used within this experiment were captured within the two-week research cruise onboard the RV Helmer Hanssen at roughly one week old and were maintained in captivity at the research facility at the Department of Arctic and Marine Biology (AMB) for 8-9 months for other research purposes. Before the application (FOTS ID 22751) that allowed for the captivity and research expired, the seals were culled between months November-December 2021. Juveniles hooded seals were considered to be the same age and therefore age/life-stage was not considered as a factor that could introduce variability within the data compared to the samples procured for western blot analysis which

However, body mass and Sex were included within the data analysis to address the possible extraneous effects of these variables on flux control ratios as the main objective was to find the presence of LEAK within the mitochondria of *M. long* and *P. major* and compare these values. Body mass had a negative relationship with FCR however these relationships were shown to be insignificant, except for PER within *P. major* ($p=0.049$; Fig.35). This contradicted the sea otter findings from Wright et al., (2021) where respiration ratios were shown not to be correlated with body mass. However, due to the small sample size it is hard to speculate the importance of body mass on mitochondrial processes, more data is needed. Increasing sample size could for instance eradicate the negative relationship seen within the data which follows the pattern displayed in Wright et al., (2021) or confirm the significance in the relationship seen in Fig.35;D.

P/E ratios within *M. long* were significantly different between sexes where females exhibited a lower P/E ratio compared to males. This indicates that females have a more uncoupled respiration (although small) within the *M. long* muscle group. In general hooded seals are sexually dimorphic with males having the characteristic “hood” as well as being much larger

than females, with adult males weighing an average of 300kg and females weighing an average of 200kg but in the early life stages morphology between males and females does not vary maintaining their "blueblack" pelage for up to two years (Lavigne and Kovacs, 1988). However research has shown that sexual dimorphism does occur in the early life stages of seals at the microbial level, before being morphologically distinguishable (Stoffel et al., 2020). This early sexual dimorphism may also occur at the mitochondrial level which could explain the lower PER in females within the muscle *M.long*.

LEAK is linked to Reactive oxygen species (ROS) production

Hooded seals are breath hold divers. When hooded seals attempt a dive, they undergo a dive response which results in bradycardia leading to a reduced cardiac output and peripheral vasoconstriction (Scholander, 1940). During dives, hooded seals must rely on their inherent oxygen stores, such as increased myoglobin, hematocrit and blood volumes in order to navigate an oxygen deficient environment (Scholander, 1940;Butler and Jones, 1997;Ramirez et al., 2007). Although seals are specialist divers which have a multitude of adaptations that increase the O_2 storing capabilities; diving still provides the chance of developing hypoxia, particularly with regards to skeletal muscle, when it must rely only on the O_2 stores within the myoglobin due to seals being essentially reduced to a "brain, heart and lung machine" (Scholander, 1940).

ROS production within all tissues is already apparent under normal metabolic conditions where roughly 0.1% of the oxygen consumed is ultimately transformed into ROS (Fridovich, 2004). Usually, ROS remains in check through the use of antioxidants/ROS scavengers which compete with the production of ROS resulting in a steady state equilibrium between production and decomposition (Bergamini et al., 2004). During hypoxic conditions however, the rate of production of ROS may increase and overwhelm the mechanisms of ROS decomposition resulting in oxidative stress (Zenteno-Savín et al., 2002;Halliwell and Gutteridge, 2015).

The rate of ROS production usually increases with maturation (Nohl and Hegner, 1978). Within hooded seals, an increase of ROS production does not equate to an increase in oxidative stress, this was due to an increase in ROS scavengers (Vázquez-Medina et al., 2011). It has also been shown that LEAK has the potential to decrease production of ROS by affecting the protonmotive force within the mitochondria as there is a strong link between ROS production

and proton gradient (Brand, 2000;Cadenas, 2018). The high LEAK shown within this study may help to reduce the production of ROS alongside its decomposition using antioxidants/ROS scavengers. This high LEAK may also be inherent within hooded seals as it was shown to be present in juveniles where ROS production remains relatively low compared to adults and defence against oxidative stress is not needed (Vázquez-Medina et al., 2011). This is due to the diving behaviour of juveniles being not as extreme compared to adults (Folkow et al., 2010) and the chances of developing oxidative stress is smaller.

Conclusion

Due to the absence of BAT in hooded seals, I hypothesised that other forms of NST, specifically in the form of a Sln-SERCA interaction and mitochondrial LEAK, are present in their skeletal muscle. This was investigated by in silico detection of Sln, SERCA1a and SERCA2a genes and in situ detection using western blot techniques; mitochondrial LEAK was assessed using tissue respirometry. This could not determine whether the NST mechanism exhibited between Sln and SERCA is present in the skeletal muscle of hooded seals because Sln could not be detected in the muscle groups *M. long* and *P. major* using western blotting techniques. However, SERCA2a expression was high in both skeletal muscles. The presence of SERCA2a and absence of SERCA1a in both muscle groups suggested that *M. long* and *P. major* are type 1 slow oxidative muscles which was confirmed in the tissue respirometry as both muscle groups relied heavily on oxidative phosphorylation. Pups showed a higher expression of SERCA2a but only in the muscle group *M. long*, indicating that SERCA2a protein diminishes with age. Lastly a high mitochondrial LEAK is present within the skeletal muscle of juvenile hooded seals, however mitochondrial respiration was shown to be highly coupled suggesting that the heat provided by the LEAK was not part of a thermoregulatory mechanism. Instead, I propose that the high LEAK could be linked to an inherent system which reduces the increased production of harmful reactive oxygen species.

DNA comparisons of Sln, SERCA1a and SERCA2a between mammals used the Weddell seal genome as a proxy for the hooded seal. Although Sln was shown to be identical within phocid species future research could focus on the establishment of the hooded seal genome to provide a definitive comparison. More information of the hooded seal Sln amino acid sequence could provide more robust antibodies in the detection of Sln using western blot techniques. Finally,

only a certain number of muscle groups were selected due to limited capacity of time as well as the limited capacity of the tissue respirometers. The presence of skeletal muscle NST may occur in other muscle groups which were not tested in this study. The continuation and expansion of hooded seal skeletal muscle research with regards to mitochondrial respiration and western blot techniques will provide more data and bolster the results shown within this study.

Appendix

Appendix A

Testing of the Western blot protocol

Testing of the Western blot Protocol was extensive and against all hope, irrevocably trial and error where only one variable can be changed per experiment in order to know its effects.

The first western blot attempts were with homogenate samples which also included PMSF (Phenylmethylsulfonyl fluoride, Cat.No: 36978, Thermo Fisher Scientific, Massachusetts, USA) a type of protease inhibitor which is soluble in isopropyl alcohol. These samples were homogenised using a 'TissueRuptor' developed by Qiagen. However, the use of the TissueRuptor was deemed inefficient as probes needed to be changed for each sample to negate cross contamination and only one sample could be processed at a time. Western Blots using the homogenates prepared by the TissueRuptor and PMSF were incubated with 1:500 β-Actin primary and 1:2000 Secondary Goat Anti-rabbit. Unfortunately, this experiment failed.

The next set of Western Blots removed the use of the TissueRuptor, still incorporated the PMSF and β-Actin as my primary antibody. BCA analysis for these sets of homogenates were skipped and instead 2, 5, 10, 20 and 30µl of undiluted protein was used. If the Western blots were a success, the BCA analysis could be done after and the "best-looking" band could indicate how much protein to load. This also failed. PMSF was removed from the subsequent experiments and provided a much better pipetting experience and allowed for an 'as expected' run through the gel. The use of PMSF and the introduction of isopropyl alcohol reduced the density of the samples and pipetting into the wells proved rather difficult as the samples tended to float rather than sink. This affected the run of the gel and resulted in a failed experiment.

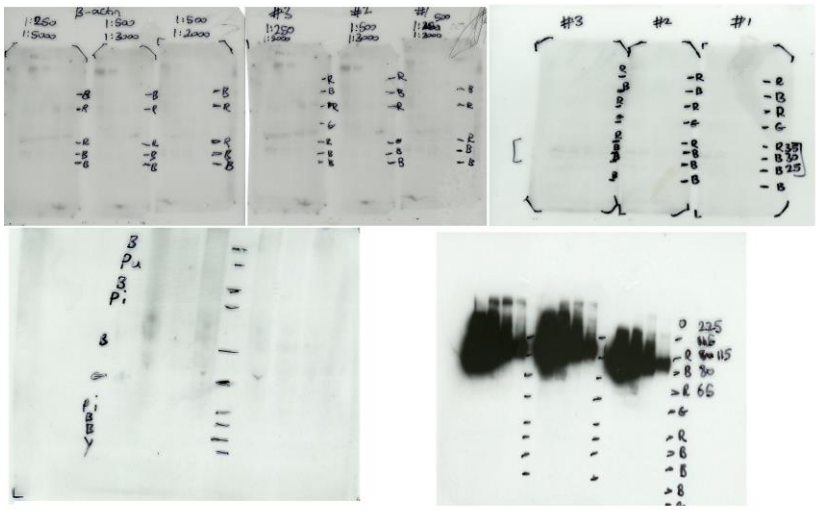

Appendix A;Fig.1. Multiple Western Blots incubated with β-actin. All blots shown did not detect the presence of β-actin.

The next step in testing was to find the appropriate concentration levels for the primary and secondary antibodies as well as introduce the SERCA1a antibodies. 2,5,10 and 20µl of undiluted protein was used. The subsequent membrane produced was cut into 3 pieces so that different concentrations could be tested. Membrane #1 was incubated with 1:500 Primary and 1:10,000 secondary. Membrane #2 was incubated with 1:1000 primary and 1:2000 secondary. Membrane #3 was incubated with 1:1000 primary and 1:10000 secondary. This test however did not seem to be successful as bands shown in the exposure film were not specific. To test the specificity of the secondary antibody, membranes were stripped and incubated with secondary antibody only at 1:2000 concentration. The results concluded that the secondary antibody did not have specificity as bands appeared without the presence of a primary antibody. However, when membranes were stripped again, incubating with a 1:5000 and 1:10,000 secondary antibodies only, no bands occurred. Therefore, these concentrations will be used for the next round of tests to account for non-specific binding.

SERCA1a and SERCA2a antibodies were included in this round of experiment testing. 2,5,10 and 20µl of undiluted protein homogenate was used. 2 membranes (A, B) were produced and cut into 3 pieces. Membrane A was incubated with different concentrations of SERCA1a antibody; 1A (1:500), 2A (1:750) and 3A (1:1000). Membrane B was incubated with SERCA2a antibodies under the same concentrations as membrane A. The secondary antibody concentrations for both membrane A and B were identical, 1:3000, 1:5000 and 1:10,000. This test concluded that SERCA1a antibodies was not giving specific bands and therefore could not be used in this study. SERCA2a however worked as expected and gave bands at the

expected molecular weight (115 kDa). The membrane B was then stripped and incubated with the β-actin housekeeping antibody however bands did not signify the presence of β-actin and were extremely saturated. Therefore the β-Actin primary antibodies was removed from the protocol as a house keeping protein as this protein did not give bands at an expected weight of (42 kDa) instead normalisation of protein bands included the use Ponceau staining (Romero-Calvo et al., 2010).

This round of testing included the use of SERCA2a antibody. Freshly made homogenate of the muscle samples was used and a BCA analysis (Appendix B) was carried out. Primary and secondary antibody concentrations were 1:750 and 1:5000 respectively. However the bands given off in this experiment were highly saturated and could not be used for quantification. These membranes were stripped and incubated with a lower concentration of secondary, 1:7500 and 1:10,000 but the same result occured.

Due to the high saturation of bands, 20µg/µl of protein was loaded instead, essentially reducing the protein content in the wells by 50%. Primary antibody concentration remained the same however secondary concentration was now 1:10,000. The gels were run for substantially longer, nearly running the 10kDa marker off the gel, to allow for a better seperation of bands. The transfer of one gel was not successful and the bands produced by both membranes within this experiment were still highly saturated. The membrane with the successful transfer was then stripped and inoculated with 1:500 Sln primary antibody and 1:10,000 secondary for the potential detection of Sln however no band was revealed at the 10kDa potentially due to the long run of the gel.

The next course of action included the 1/10 diluted homogenate which was created during the BCA analysis, the use of this homogenate essentially gave a loading concentration of 4µg/µl. This low concentration of loading protein can potentially help with the separation of proteins and allow for better detection of SERCA2a and potentially other isoforms present in the skeletal muscle. This course was also done with Sln primary antibody under the same pretext.

Appendix B

***Appendix B Table 1 Skeletal muscle homogenate used in the BCA Assay analysis**. Using the simple linear equation y=mx+c protein concentration was calculated from absorbance (Abs). Protein concentration was given the final unit of µg/µl.*

UNKNOWN	Abs	Protein concentration (µg/ml)	µl used in assay	µl total sample	dilution factor	Total protein content of sample (µg)	[µg/µl]
K121 M.long	1.06	1136.80	25	1000	10	11368.00	11.37
K121 P.major	1.27	1371.67	25	1000	10	13716.69	13.72
K321 M.long	1.00	1077.10	25	1000	10	10770.97	10.77
K321 P. major	0.85	906.14	25	1000	10	9061.39	9.06
K421 M.long	0.91	974.16	25	1000	10	9741.61	9.74
K421 P.major	0.88	938.99	25	1000	10	9389.87	9.39
K821 M.long	1.29	1387.58	25	1000	10	13875.84	13.88
K821 P.major	1.46	1574.23	25	1000	10	15742.33	15.74
K8b21 M.long	0.81	870.29	25	1000	10	8702.90	8.70
K8b21 P.major	0.82	875.66	25	1000	10	8756.61	8.76
K921 M.long	0.92	989.10	25	1000	10	9890.97	9.89
K921 P.major	1.00	1070.06	25	1000	10	10700.63	10.70
K1021 M.long	0.97	1036.77	25	1000	10	10367.70	10.37
K1021 P.major	1.05	1132.90	25	1000	10	11328.98	11.33
K10b21 M.long	0.99	1064.88	25	1000	10	10648.75	10.65
K10b21 P.major	1.13	1214.71	25	1000	10	12147.07	12.15
K1121 M.long	1.17	1255.68	25	1000	10	12556.79	12.56
K1121 P.major	0.89	957.44	25	1000	10	9574.40	9.57
H421 M.long	0.78	837.61	25	1000	10	8376.08	8.38
H421 P.major	0.72	771.90	25	1000	10	7719.04	7.72
H1b21 M.long	0.68	722.96	25	1000	10	7229.61	7.23
H1b21 P.major	0.96	1028.52	25	1000	10	10285.24	10.29
K8b21 M.long	0.70	751.14	25	1000	10	7511.40	7.51

Appendix C

ImageJ Total protein normalisation

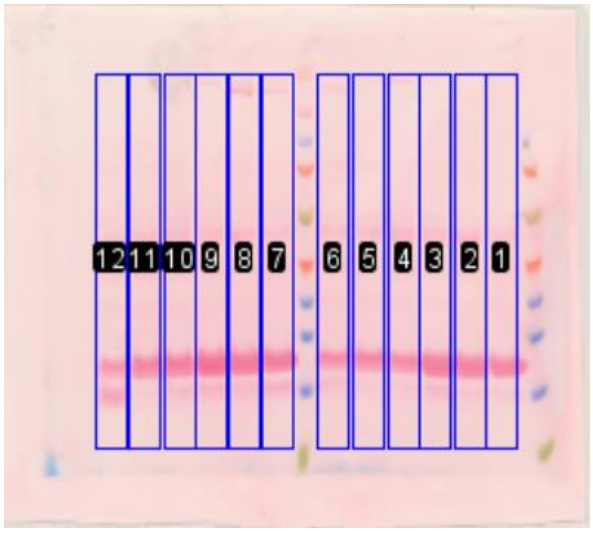

***Appendix C Fig.1 12 lanes selected of Ponceau S stained membranes for Total protein normalisation.** Produced within ImageJ software.*

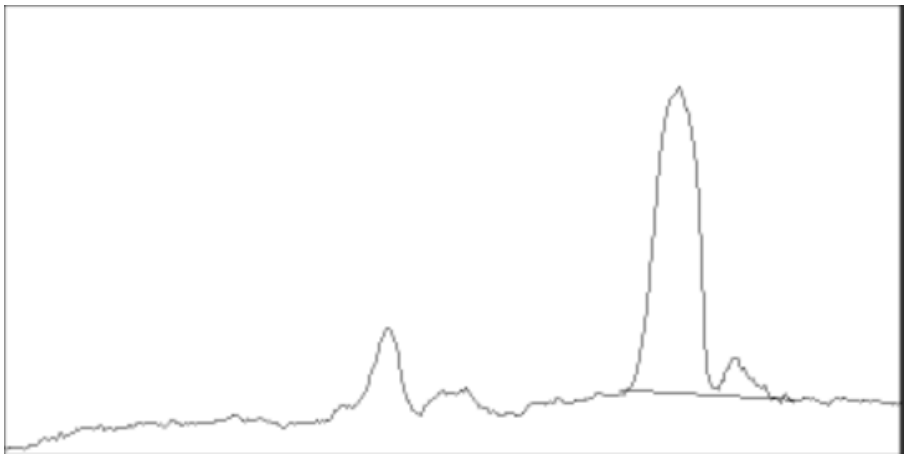

Appendix C Fig.2. Density curve of a single selected lane of a Ponceau S stained membrane. *The area of the highest peak, which was the most consistent in all 12 lanes were highlighted and used within the total protein normalisation.*

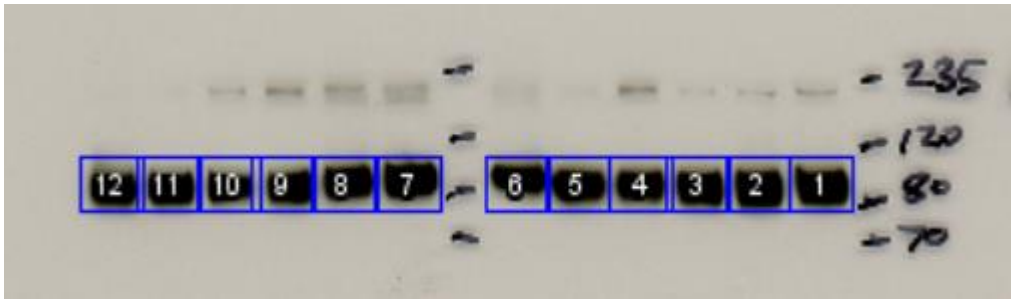

Appendix C Fig.3. 12 bands showing SERCA2a expression. *Bands were highlighted using ImageJ software.*

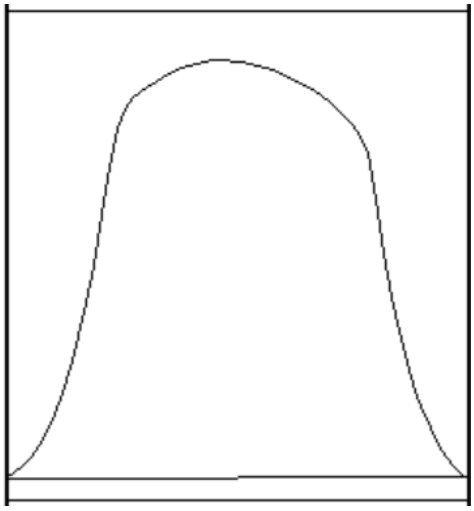

Appendix C Fig.4 Density curve of a single SERCA2a band. *Background was dismissed and the area of the curve was calculated within ImageJ software. Comparison of SERCA2a density curves and Ponceaus S stained density curves provided density ratios used within this study.*

Appendix D

Appendix D Table 1. Mitochondrial membranes are intact in all sampled juvenile hooded seals. *Percent change mitochondrial respiration did exceed the 10% threshold when adding cytochrome c.*

ID	Muscle	Percent_change	sd
K12-21	M.long	8.174721	0.9330370
K13-21	M.long	5.386321	1.2797239
K2-21	M.long	4.658037	0.9452268
K6-21	M.long	5.876826	0.8355404
K7-21	M.long	4.954723	0.4931318
K9b-21	M.long	2.729002	0.9547872
K13-21	P.major	4.901943	0.7753188
K7-21	P.major	4.979695	1.3324889
K9b-21	P.major	3.205756	0.9333781

Appendix E

R code for western blot data

```
Ws=read.csv("Westernserca.csv", header= TRUE, sep = ",", dec=".")
head(Ws)
par(mfrow=c(1,1))
boxplot(Ratio~Life.stage*Muscle, data= Ws)# outlier present in Pup. m.long 9.21
###outlier removed
Ws <- Ws[-c(13),]
rownames(Ws) <- c(1:45)
Ws
Wsagg <- aggregate(Ws$Ratio, list(Ws$Life.stage, Ws$Muscle), FUN=mean)
Wsagg

Wsaggsd <- aggregate(Ws$Ratio, list(Ws$Life.stage, Ws$Muscle), FUN=sd)
Wsaggsd
Wsx <- factor(Wsagg$Group.1, levels = c("Adult","Pup"))
##General plot
Wsplot <- ggplot(data=Wsagg, aes(Wsx, x, fill=Group.2, group=Group.2))+
  geom_col(position = "dodge") +
  labs(fill= "Muscle")+
  geom_errorbar(aes(ymax=x+Wsaggsd$x, ymin=x-Wsaggsd$x), width=.1, position = position_dodge(width = .9
)) +
  theme_classic() + ylab("Arbitrary Units") + xlab("Lifestage") +
  scale_fill_manual(values=c(cbPalette))
Wsplot
###
Wsblot <- aggregate(Ws$Ratio, list(Ws$Blot, Ws$Life.stage, Ws$Muscle),FUN=mean)
Wsblotsd <- aggregate(Ws$Ratio, list(Ws$Blot, Ws$Life.stage, Ws$Muscle),FUN=sd)
Wsblot
Wsbx <- factor(Wsblot$Group.1, levels= c("1.1", "1.2","2.1","2.2"))
Wsbx

Wsbplot <- ggplot(data=Wsblot, aes(Wsbx, x, fill=Group.2, group=Group.2))+
  geom_col(position = "dodge") +
  labs(fill= "Treatment")+
  geom_errorbar(aes(ymax=x+Wsblotsd$x, ymin=x-Wsblotsd$x), width=.1, position = position_dodge(width =
.9)) +
  theme_classic() + ylab("Arbitrary Units") + xlab("Blot") +
  facet_wrap(~factor(Group.3, levels = unique(Group.3)))
Wsbplot
###Must average technical replicates
Wsagg1 <- aggregate(Ws$Ratio, list(Ws$ID, Ws$Life.stage, Ws$Muscle), FUN=mean)
Wsagg1
library(tidyverse)
```

```
Wsagg1 <- Wsagg1%>%rename(ID =Group.1, Life.stage=Group.2, Muscle= Group.3, Ratio=x)
Wsagg1
aggm <- aggregate(Wsagg1$Ratio, list(Wsagg1$Life.stage, Wsagg1$Muscle), FUN=mean)
aggm
sdagg1 <- aggregate(Wsagg1$Ratio, list(Wsagg1$Life.stage, Wsagg1$Muscle), FUN=sd)
sdagg1
##plot with averaged technical replicates
agg1plot <- ggplot(data=aggm, aes(Wsx, x, fill=Group.2, group=Group.2))+
  geom_col(position = "dodge") +
  labs(fill= "Muscle")+
  geom_errorbar(aes(ymax=x+sdagg1$x, ymin=x-sdagg1$x), width=.1, position = position_dodge(width = .9))
 +
  theme_classic() + ylab("Density Ratio") + xlab("Lifestage") +
  scale_fill_manual(values=c(cbPalette))
agg1plot
##### Data analysis
Wsagg1
Wsagg1$Life.stage <- as.factor(Wsagg1$Life.stage)
Wsagg1$Muscle <- as.factor(Wsagg1$Muscle)
boxplot(Ratio~Life.stage*Muscle, data=Wsagg1, ylim=c(1.5,4.5), xlab = "Life stage and Muscle group", yl
ab="Density Ratio (SERCA2a)",
        names=c("Adult M.long", "Pup M.long", "Adult P.major", "Pup P.major"), par(cex.lab=1.2), par(ce
x.axis=1.2))
text(2,4.3,cex=2,expression(paste("*")))

anovaws <- aov(Ratio~Life.stage*Muscle, data=Wsagg1)
summary(anovaws)
TukeyHSD(anovaws)
DunnettTest(x=Wsagg1$Ratio, Wsagg1$Life.stage*Muscle)
#Anova shows there was no significance between life stage when muscle group was collated
#Anova shows there was no significance between muscle group when life stage was collated.
#Anova shows a significance in ratios when Life stage and muscle group is taken into account.
####What are my analysis questions?
#is there a difference between muscle?
# Is there a difference between life stage?

#separating muscle group
M.longWs <- subset(Wsagg1,Muscle=="M.long")
M.longWs
var.test(Ratio~Life.stage, data=M.longWs)# P>0.05 variance is equal
t.test(M.longWs$Ratio~M.longWs$Life.stage, mu=0, alt="two.sided", conf=0.95, var.eq=TRUE, paired=F) ##
P=0.061
##SERCA expression is not significantly different with regards to Life stage in Mlong
Wsagg1
install.packages("writexl")
library("writexl")
write_xlsx(Wsagg1,"C:\\Users\\matth\\OneDrive\\My Documents\\R\\Serca data.xlsx")
```

Appendix F

R code for mitochondrial data

```
library(tidyr)
Dt=read.csv("LEAKOXPH.csv", header= TRUE, sep = ",", dec=".")
head(Dt)
#Means of LEAK and OXPHOS BETWEEN MUSCLE GROUPS.
lo=aggregate(Dt$Mean, list(Dt$Treatment, Dt$Muscle), FUN=mean)
lo
sb=factor(lo$Group.1, levels = c("LEAK","OXPHOS"))
sb
sd2=aggregate(Dt$Mean, list(Dt$Treatment, Dt$Muscle), FUN=sd)
sd2
library(ggplot2)
ggplot(data=lo, aes(sb, x, fill=Group.2, group=Group.2))+
  geom_col(position = "dodge") +
  labs(fill= "Muscle")+
```

```
  geom_errorbar(aes(ymax=x+sd2$x, ymin=x-sd2$x), width=.1, position = position_dodge(width = .9)) +
  theme_classic() + ylab("Oxygen consumption (pmol/s*mg)") + xlab("Mitochondrial phase") +
  scale_fill_manual(values=c(cbPalette))

#Means of treatment between seals
lo2=aggregate(Dt$Mean, list(Dt$ID, Dt$Treatment, Dt$Muscle), FUN=mean)
lo2
lo2$bar <- paste(lo2$Group.2,lo2$Group.3)
lo2
sb1=factor(lo2$Group.1, levels = c("K2-21","K6-21","K7-21","K9b-21","K12-21","K13-21"))
sb1
sb2=factor(lo2$Group.3, levels= c("M.long", "P.major"))
sb2
sd1=aggregate(Dt$Mean, list(Dt$ID, Dt$Treatment, Dt$Muscle), FUN=sd)
sd1
ggplot(data=lo2, aes(sb1, x, fill=Group.2, group=Group.2))+
  geom_col(position = "dodge") +
  labs(fill= "Treatment")+
  geom_errorbar(aes(ymax=x+sd1$x, ymin=x-sd1$x), width=.1, position = position_dodge(width = .9)) +
  theme_classic() + ylab("Oxygen consumption (pmol/s*mg)") + xlab("ID") +
  facet_wrap(~factor(Group.3, levels = unique(Group.3)))


P <- ggplot(data=lo2, aes(sb1, x, fill=bar, group=bar))+
  geom_col(position = "dodge") +
  labs(fill= "Mitochondrial phase in muscle")+
  geom_errorbar(aes(ymax=x+sd1$x, ymin=x-sd1$x), width=.1, position = position_dodge(width = .9)) +
  theme_classic() + ylab("Oxygen consumption (pmol/s*mg)") + xlab("ID")
P
#changing colour of bars
install.packages("RColorBrewer")
library("RColorBrewer")
cbbPalette <- c("#000000", "#E69F00", "#56B4E9", "#009E73", "#F0E442", "#0072B2", "#D55E00", "#CC79A7")
P + scale_fill_manual(values = cbbPalette)
cbPalette <- c("#999999", "#E69F00", "#56B4E9", "#009E73", "#F0E442", "#0072B2", "#D55E00", "#CC79A7")
P + scale_fill_manual(values = cbPalette)

install.packages("wesanderson")
library(wesanderson)
P+scale_fill_manual(values=wes_palette(n=4, name="FantasticFox1"))
?wes_palette

Hood <- read.csv("Oroboros data.csv", header= TRUE, sep = ",", dec=".")
#Finding Ratios leak and oxphos of muscle groups
lo

ccrM <- 7.301317/20.981400
ccrp <- 6.364891/23.157818
Muscle_Group <- c("M.long", "P.major")
r <- data.frame(Muscle_Group, CCR=c(ccrM,ccrp))
r
#Finding ratios between Oxphos and ets of musclegroups
H=aggregate(Hood$Mean, list(Hood$Treatment, Hood$Muscle), FUN=mean)
H
FCRm <- 20.981400/22.300930
FCRp <- 23.157818/25.291727
r <- data.frame(Muscle_Group, CCR=c(ccrM,ccrp), FCR=c(FCRm,FCRp))
r
#Finding ratios between Oxphos and ETS of individuals
FCR0<- subset(Hood, Treatment=="OXPHOS")
FCRE <- subset(Hood, Treatment=="ETS")
RDATA <- data.frame(FCR0,FCRE)
FCRi <- data.frame(RDATA$Mean/RDATA$Mean.1)

#Finding ratios between Leak and Oxphos of individuals
L <- subset(Hood, Treatment=="LEAK")
RDATA <- data.frame(FCR0,FCRE,L)
CCRi <- data.frame(RDATA$Mean.2/RDATA$Mean)


#renaming columns/datasets
```

```
library(tidyverse)
CCRi <- CCRi%>%rename(CCR =RDATA.Mean.2.RDATA.Mean )
FCRi <- FCRi%>%rename(FCR =RDATA.Mean.RDATA.Mean.1 )
RDATA <- RDATA%>%rename(OXPHOS = Treatment, Oxmean = Mean, ETS= Treatment.1, ETSmean= Mean.1,LEAK= Trea
tment.2, LEAKmean= Mean.2)

#deleting columns
RDATA <- subset(RDATA, select= -c(Chamber.1,ID.1,Muscle.1, Chamber.2,ID.2, Muscle.2))

Alld <- data.frame(RDATA,FCRi,CCRi)
head(Alld)


#### removing K13 M.long from data due to faulty ADP.
rownames(Alld)
rownames(Alld) <- c(1:34)
Alld
Alld1 <- Alld[-c(13,14,15),]
Alld1
rownames(Alld1) <- c(1:31)

#####adding sex column
Alld1["Sex"] <- NA

Alld1[c(1:8, 24:31),12]= "Male"
Alld1[c(9:23),12]= "Female"
####Adding weight
Alld1["Weight"] <- NA
Alld1[1:4,13]= 62
Alld1[5:8,13]=69
Alld1[9:12,13]= 70
Alld1[13:15,13]=63
Alld1[16:23,13]=66
Alld1[24:31,13]=69
########
FCRA <- aggregate(Alld1$FCR, list(Alld1$ID, Alld1$Muscle, Alld1$Sex, Alld1$Weight), FUN=mean)
head(FCRA)
FCRA<- FCRA%>%rename(ID =Group.1, Muscle=Group.2, FCR=x, Sex=Group.3, Weight=Group.4)
head(FCRA)
class(FCRA$Sex)
FCRA$Sex <- as.factor(FCRA$Sex)
FCRA1 <- subset(FCRA, Muscle=="M.long")
head(FCRA1)
FCRA2 <- subset(FCRA, Muscle=="P.major")
head(FCRA2)
CCRA <- aggregate(Alld1$CCR, list(Alld1$ID, Alld1$Muscle, Alld1$Sex, Alld1$Weight), FUN=mean)
CCRA<- CCRA%>%rename(ID =Group.1, Muscle=Group.2, CCR=x, Sex=Group.3, Weight=Group.4)
head(CCRA)
class(CCRA$Sex)
CCRA$Sex <- as.factor(CCRA$Sex)
CCRA1 <- subset(CCRA, Muscle=="M.long")
head(CCRA1)
CCRA2 <- subset(CCRA,Muscle=="P.major")
CCRA2
#############################################################################
#Data analysis between muscle groups, Anova and two key test.
anova <- aov(CCR~Muscle, data=CCRA)
summary(anova)
TukeyHSD(anova)#Significant difference of CCR between muscle groups


anova1 <- aov (FCR~Muscle, data=FCRA)
summary(anova1)
TukeyHSD(anova1)# Significant difference between RCR between muscle groups.

#Data analysis of individuals.
anovai <- aov(FCR~ID, data=FCRA)
summary(anovai)#FCR shows no significant difference between individuals
TukeyHSD(anovai)
anovaii <- aov(CCR~ID, data=CCRA)
summary(anovaii)
```

```r
TukeyHSD(anovaii)
##separating muscle
FCRAM <- subset(Alld1, Muscle=="M.long")
FCRAM
FCRAP <- subset(Alld1,Muscle=="P.major")
FCRAP

#Anova FCR between individuals M.long
anovaFCRA1 <- aov(FCR~ID,data= FCRA1)
summary(anovaFCRA1)## Sample size too small
TukeyHSD(anovaFCRA1)
# dunnet test
install.packages("DescTools")
library(DescTools)
?DunnettTest
FCRAM$ID <- as.factor(FCRAM$ID)

DunnettTest(x=FCRA1$FCR, g=FCRA1$ID)

#Anova ccr between individuals M.long, check chambers too.
anovaccra1 <- aov(CCR~ID, data= CCRA1)
summary(anovaccra1)
TukeyHSD(anovaccram)
######CCR anova between individuals including all muscle groups
anovaccra2 <- aov(CCR~ID, data=CCRA)
summary(anovaccra2)
TukeyHSD(anovaccra2)
anovaccra3 <- aov(CCR~ID*Muscle, data=CCRA)
summary(anovaccra3)
#########

anovafcr <- aov(FCR~ID, data=FCRA)
summary(anovafcr)
##Anova of p/e ratio between individuals
#dunnet test
DunnettTest(x=FCRAM$CCR, g=FCRAM$ID)
##chambers
anovach <- aov(CCR~Chamber, data=FCRAM)##no difference between chambers in CCR P=0.94
summary(anovach)
TukeyHSD(anovach)
##what about absolut values?
anovaox <- aov(Oxmean~Chamber, data=FCRAM)
summary(anovaox)
TukeyHSD(anovaox)
summary(aov(FCR~Chamber, data=FCRAM))## no difference between chambers in FCR P=0.56


#~~~checking chambers within expermiments
CK2 <- subset(Alld1, ID=="K2-21")
CK2
CK2A <- aov(CCR~Chamber, data= CK2)
summary(CK2A)
TukeyHSD(CK2A)
#Anova between individuals P.major
anovaFCRAP <- aov(FCR~ID, data=FCRAP)
summary(anovaFCRAP)
TukeyHSD(anovaFCRAP)
anovaccrap <- aov(CCR~ID, data=FCRAP)
summary(anovaccrap)
TukeyHSD(anovaccrap)

##############################################################################################
#### Plot of FCR between individuals inc. Muscle group- K13 ADP was not fresh.
head(FCRA)
R1 <- factor(FCRA$ID, levels = c("K2-21","K6-21","K7-21","K9b-21","K12-21","K13-21"))
sdR=aggregate(Alld1$FCR, list(Alld1$ID, Alld1$Muscle), FUN=sd)
sdR
PFCR<- ggplot(data=FCRA, aes(R1, FCR, fill=Muscle, group=Muscle))+
  geom_col(position = "dodge") +
  labs(colour= "Treatment")+
  geom_errorbar(aes(ymax=FCR+sdR$x, ymin=FCR-sdR$x), width=.1, position = position_dodge(width = .9)) +
```

```
  theme_classic() + ylab("P/E ratio (OXPHOS/ETS control ratio)") + xlab("ID") + scale_fill_manual(value
s=cbPalette)
PFCR
##Plot of ccr between individuals inc. muscle groups
head(CCRA)
C1 <- factor(CCRA$ID, levels = c("K2-21","K6-21","K7-21","K9b-21","K12-21","K13-21"))
sdc <- aggregate(Alld1$CCR, list(Alld1$ID, Alld1$Muscle), FUN=sd)
sdc
PCCR <- ggplot(data=CCRA, aes(C1, CCR, fill=Muscle, group=Muscle))+
  geom_col(position = "dodge") +
  labs(colour= "Treatment")+
  geom_errorbar(aes(ymax=CCR+sdc$x, ymin=CCR-sdc$x), width=.1, position = position_dodge(width = .9)) +
  theme_classic() + ylab("CCR(Coupling control ratio)") + xlab("ID") + scale_fill_manual(values=cbPalet
te)
PCCR
######Merging SD AND MEAN VALUES OF P/E RATIO AND CCR
FCRA <- data.frame(FCRA, sdR$x)
FCRA
FCRA <- FCRA%>%rename(sd =sdR.x)
FCRA
CCRA <- data.frame(CCRA, sdc$x)
CCRA
CCRA <- CCRA%>%rename(sd =sdc.x)
CCRA
#Mean leak of all individuals
mean(Alld1$Oxmean)
# Plot of Leak oxphos and ets.Means
LOEM=read.csv("leakoxphets.csv", header= TRUE, sep = ",", dec=".")
head(LOEM)
agg <- aggregate(LOEM$Mean, list(LOEM$Treatment, LOEM$Muscle),FUN=mean)
agg
agg <- agg[-c(3,4,8,9),]
agg
agg <- agg%>%rename(Treatment =Group.1, Muscle=Group.2, Mean=x )
agg
sdagg <- aggregate(LOEM$Mean, list(LOEM$Treatment, LOEM$Muscle),FUN=sd)
sdagg
sdagg <- sdagg[-c(3,4,8,9),]
sdagg
x <- factor(agg$Treatment,levels = c("LEAK","OXPHOS","ETS") )
x
aggplot <-ggplot(data=agg, aes(x, Mean, fill=Muscle, group=Muscle))+
  geom_col(position = "dodge") +
  labs(fill= "Muscle")+
  geom_errorbar(aes(ymax=Mean+sdagg$x, ymin=Mean-sdagg$x), width=.1, position = position_dodge(width =
.9)) +
  theme_classic() + ylab("Oxygen consumption (pmol/s*mg)") + xlab("Mitochondrial phase") +
  scale_fill_manual(values=c(cbPalette))
aggplot
aggall <- data.frame(agg, sdagg$x)
aggall <- aggall%>%rename(SD =sdagg.x )
aggall
###Mean fcr and RCR OF MUSCLE GROUPS
meanfcr <- aggregate(Alld1$FCR, list(Alld1$Muscle), FUN=mean)
meanfcr
meanfcr <- meanfcr%>%rename(Muscle =Group.1, "P/E ratio"=x )
meanfcr
meanccr <- aggregate(Alld1$CCR, list(Alld1$Muscle), FUN=mean)
meanccr
meanccr <- meanccr%>%rename(Muscle =Group.1, CCR=x )
meanccr
ratiosm <- data.frame(meanfcr, meanccr$CCR)
ratiosm
rsd <- aggregate(Alld1$FCR, list(Alld1$Muscle), FUN=sd)
rsd
rsd1 <- aggregate(Alld1$CCR, list(Alld1$Muscle), FUN=sd)
rsd1

ratiosm <- data.frame(meanfcr, meanccr$CCR,rsd$x, rsd1$x)
ratiosm
ratiosm <- ratiosm%>%rename(CCR =meanccr.CCR, P.E.ratio.sd=rsd.x, CCR.sd=rsd1.x )
```

```
ratiosm
ratios=read.csv("ratios.csv", header= TRUE, sep = ",", dec=".")
ratios
plotx <- factor(gsub("\\s*", "", ratios$Muscle), levels= c("M.long","P.major" ) )
plotx
plotr <- ggplot(data=ratios, aes(plotx,Values  , fill=Ratios, group=Ratios))+
  geom_col(position = "dodge") +
  labs(fill= "FCR")+
  geom_errorbar(aes(ymax=Values+Sd, ymin=Values-Sd), width=.1, position = position_dodge(width = .9)) +
  theme_classic() + ylab("Flux control ratio") + xlab("Muscle") +
  scale_fill_manual(values=wes_palette(n=2, name="IsleofDogs2"))
?wes_palette
plotr
levels(as.factor(ratios$Muscle))

#####Linear regression models???
class(Alld1$Sex)
Alld1$Sex <- as.factor(Alld1$Sex)
##CCR~muscle
Alld1$Muscle <- as.factor(Alld1$Muscle)
Muslm <- lm(CCR~Muscle, data=Alld1)
plot(Muslm)
summary(Muslm)
##CCR~Weight M.long
plot(CCR~Weight, data=CCRA1)
abline(lm(CCR~Weight, data=CCRA1))
abline(0,1,col="red")
plot(lm(CCR~Weight, data=CCRA1),which=1)
CCRlm <- lm(CCR~Weight, data=CCRA1)
hist(resid(CCRlm))
summary(CCRlm)
#use pearson to look at weight
install.packages("ggpubr")
library(ggpubr)
#~~~~~~~~~~~~~~~~~~~~~CCR M.long
ggscatter(CCRA1, x="Weight", y="CCR",
          add="reg.line", conf.int=TRUE,
          cor.coef= TRUE,cor.method = "pearson",
          xlab= "Weight(Kg)", ylab= "CCR")

###testing normality
shapiro.test(CCRA1$CCR) #P=0.77
ggqqplot(CCRA1$CCR, ylab="CCR") #visual inspection of normality
shapiro.test(CCRA1$Weight)#P=0.045
ggqqplot(CCRA1$Weight,ylab= "Weight")
##Pearson correlation test
PECCR <-  cor.test(CCRA1$Weight, CCRA1$CCR,
                   method="pearson")
PECCR #Weight is not correlated to CCR in M.long
#~~~~~~~~~~~~~~~~~~~~~CCR P. major
ggscatter(CCRA2, x="Weight", y="CCR",
          add="reg.line", conf.int=TRUE,
          cor.coef= TRUE,cor.method = "pearson",
          xlab= "Weight(Kg)", ylab= "CCR")
###testing normality
shapiro.test(CCRA2$CCR) #P=0.74
ggqqplot(CCRA2$CCR, ylab="CCR") #visual inspection of normality
shapiro.test(CCRA2$Weight)#P=1
ggqqplot(CCRA2$Weight,ylab= "Weight")
PECCR2 <-  cor.test(CCRA2$Weight, CCRA2$CCR,
                    method="pearson")
PECCR2#Weight not significant in P.major P=0.09
#~~~~~~~~~~~~~~~~~~~~FCR M.long
ggscatter(FCRA1, x="Weight", y="FCR",
          add="reg.line", conf.int=TRUE,
          cor.coef= TRUE,cor.method = "pearson",
          xlab= "Weight(Kg)", ylab= "FCR")
shapiro.test(FCRA1$FCR) #P=0.3
ggqqplot(FCRA1$FCR, ylab="FCR") #visual inspection of normality
shapiro.test(FCRA1$Weight)#P=0.045
ggqqplot(FCRA1$Weight,ylab= "Weight")
```

```r
PFCCR <-  cor.test(FCRA1$Weight, FCRA1$FCR,
                   method="pearson")
PFCCR #Weight is not correlated to CCR in M.long P=0.74
#~~~~~~~~~~~~~~~~~~~~~~~~~~~~ FCR P.major
ggscatter(FCRA2, x="Weight", y="FCR",
          add="reg.line", conf.int=TRUE,
          cor.coef= TRUE,cor.method = "pearson",
          xlab= "Weight(Kg)", ylab= "FCR")
shapiro.test(FCRA2$FCR) #P=0.85
ggqqplot(FCRA2$FCR, ylab="FCR") #visual inspection of normality
shapiro.test(FCRA2$Weight)#P=1
ggqqplot(FCRA2$Weight,ylab= "Weight")
PFCCR2 <-  cor.test(FCRA2$Weight, FCRA2$FCR,
                    method="pearson")
PFCCR2#Weight may affect FCR in P.major
#######


###################is sex affecting results
#M.long CCR~sex
ggscatter(CCRA1, x= "Sex", y="CCR")
boxplot(CCR~Sex, data=CCRA1, ylim= c(0.2,0.4))#need to plot y axis starting at zero
summary(aov(CCR~Sex, data=CCRA1))# P=0.06
DunnettTest(x=CCRA1$CCR, g=CCRA1$Sex)
var.test(CCR~Sex, data=CCRA1) #P> 0.05 variance is equal
t.test(CCRA1$CCR~CCRA1$Sex, mu=0, alt="two.sided", conf=0.95, var.eq=TRUE, paired=F)
#P.major CCR lack of data

##M.long P/E ratio
ggscatter(FCRA1, x="Sex", y="FCR")
boxplot(FCR~Sex, data=FCRA1, ylim= c(0.9,1.0), ylab= "P/E ratio")
var.test(FCR~Sex, data=FCRA1) #P>0.05 variance is equal
t.test(FCRA1$FCR~FCRA1$Sex, mu=0, alt="two.sided", conf=0.95, var.eq=TRUE, paired=F)
summary(aov(FCR~Sex, data=FCRA1))
FCRA1
par(mfrow=c(1,2))
boxplot(CCR~Sex, data=CCRA1, ylim= c(0.2,0.4))
boxplot(FCR~Sex, data=FCRA1, ylim= c(0.9,1.0),ylab="P/E ratio")
text(x=2,y=max(FCRA1$FCR[FCRA1$Sex=="Male"]),"*",pos=3,cex=1.5)
aggregate(FCRA1$FCR, list(FCRA1$Sex), FUN=mean)
aggregate(FCRA1$FCR, list(FCRA1$Sex), FUN=sd)
#~~seperating sex in CCR
CCRmale <- subset(CCRA1, Sex=="Male")
CCRmale
CCRfem <- subset(CCRA1, Sex=="Female")
CCRfem
qqnorm(CCRmale$CCR)
qqline(CCRmale$CCR, col="red")
qqnorm(CCRfem$CCR)
qqline(CCRfem$CCR, col="red")#data not normally distributed
######## seperating sex in FCR
FCRmale <- subset(FCRA1, Sex=="Male")
FCRmale
FCRfem <- subset(FCRA1, Sex=="Female")
FCRfem
qqnorm(FCRmale$FCR)
qqline(FCRmale$FCR, col="red")
qqnorm(FCRfem$FCR)
qqline(FCRfem$FCR, col="red")
##Man whitney U test CCR~Sex
Whitsex <- wilcox.test(CCR~Sex, data=CCRA1, exact=TRUE)
Whitsex

############################################################################## Man whitney U tests
####~CCR~muscle
shapiro.test(CCRA$CCR) #data is not normally distributed can't trust anova
Whitmuscle <- wilcox.test(CCR~Muscle, data=CCRA)
Whitmuscle

#####FCR~muscle
shapiro.test(FCRA$FCR) # data is not normally distributed can't trust anova.
```

```
Whitfcr <- wilcox.test(FCR~Muscle, data=FCRA)
Whitfcr
##############CCR by species otter, seal and Elephant seal in M.long
Species <- NA
CCRCOMP <- data.frame(CCRA1,Species)
CCRCOMP
rownames(CCRCOMP) <- c(1:6)
CCRCOMP
CCRCOMP[1:6, 6]= "Hooded Seal"
CCRCOMP
CCRCOMP <- subset(CCRCOMP, select=-c(Muscle))
CCRCOMP
otter <- read.csv("Sea otter.csv", header= TRUE, sep = ",", dec=".")
head(otter)
otter <- subset(otter, select=-c(Muscle))
COMP <- rbind(CCRCOMP,otter)
COMP
comp1 <- aggregate(COMP$CCR, list(COMP$Species), FUN=mean)
comp1
###Adding CCR for elephant seal
comp1[nrow(comp1) + 1,] = c("Elephant seal", 0.13)
comp1
###adding human CCR
comp1[nrow(comp1) + 1,] = c("Human", 0.196)
comp1
comp1$x <- as.numeric(comp1$x)
comp1sd <- aggregate(COMP$CCR, list(COMP$Species), FUN=sd)
comp1sd
###adding elephant seal SD
comp1sd[nrow(comp1sd) + 1,] = c("Elephant seal",0.03)
comp1sd
##adding human SD which is NA
comp1sd[nrow(comp1sd) + 1,] = c("Human",NA)
comp1sd
comp1sd$x <- as.numeric(comp1sd$x)
compx <- factor(comp1$Group.1, levels = c("Hooded Seal","Otter","Elephant seal", "Human"))
compx
complt <- ggplot(data=comp1, aes(compx, x))+
  geom_col(fill= "#CCCCCC") +
  geom_errorbar(aes(ymax=x+comp1sd$x, ymin=x-comp1sd$x), width=.1, position = position_dodge(width = .9
)) +
  theme_classic() + ylab("CCR") + xlab("Species")+ scale_fill_manual(values= cbPalette)
complt
companova <- aov(CCR~Species, data=COMP)
summary(companova)
whitcomp <- wilcox.test(CCR~Species, data=COMP)
whitcomp
shapiro.test(COMP$CCR)
var.test(CCR~Species, data=COMP)###P>0.05 Variance is equal
t.test(COMP$CCR~COMP$Species, mu=0, alt="two.sided", conf=0.95, var.eq=TRUE, paired=F) #####is signific
antly different

#~~~~~~~~~~~~~~~~~~~~~CCR M.long
p1 <- ggscatter(CCRA1, x="Weight", y="CCR",
          add="reg.line", conf.int=TRUE,
          cor.coef= TRUE, cor.method = "pearson",
          xlab= "Weight(Kg)", ylab= "CCR", cor.coeff.args = list(label.x = 67, label.y=0.45, label.sep
= "\n"))
p1
#~~~~~~~~~~~~~~~~~~~~~CCR P. major
p2 <- ggscatter(CCRA2, x="Weight", y="CCR",
          add="reg.line", conf.int=TRUE,
          cor.coef= TRUE,cor.method = "pearson",
          xlab= "Weight(Kg)", ylab= "CCR",cor.coeff.args = list(label.x = 67, label.y=0.45, label.sep =
 "\n"))
p2
#~~~~~~~~~~~~~~~~~~FCR M.long
p3 <- ggscatter(FCRA1, x="Weight", y="FCR",
          add="reg.line", conf.int=TRUE,
          cor.coef= TRUE,cor.method = "pearson",
          xlab= "Weight(Kg)", ylab= "P/E ratio",cor.coeff.args = list(label.x = 67, label.y=1, label.se
```

```
p = "\n"))
p3
#~~~~~~~~~~~~~~~~~~~~~~~~~~~~ FCR P.major
p4 <- ggscatter(FCRA2, x="Weight", y="FCR",
          add="reg.line", conf.int=TRUE,
          cor.coef= TRUE,cor.method = "pearson",
          xlab= "Weight(Kg)", ylab= "P/E ratio",cor.coeff.args = list(label.x = 67, label.y=0.98, label
.sep = "\n"))
p4
ggarrange(p1,p2,p3,p4,
          labels= c("A","B","C", "D"),
          ncol=2, nrow=2)
RStudio.Version()
##########
```

Works cited

ALLEN, D. G., LAMB, G. D. & WESTERBLAD, H. 2008. Impaired calcium release during fatigue. *Journal of applied physiology,* 104**,** 296-305.

AQUILA, H., LINK, T. A. & KLINGENBERG, M. 1985. The uncoupling protein from brown fat mitochondria is related to the mitochondrial ADP/ATP carrier. Analysis of sequence homologies and of folding of the protein in the membrane. *The EMBO journal,* 4**,** 2369-2376.

ASAHI, M., OTSU, K., NAKAYAMA, H., HIKOSO, S., TAKEDA, T., GRAMOLINI, A. O., TRIVIERI, M. G., OUDIT, G. Y., MORITA, T. & KUSAKARI, Y. 2004. Cardiac-specific overexpression of sarcolipin inhibits sarco (endo) plasmic reticulum Ca2+ ATPase (SERCA2a) activity and impairs cardiac function in mice. *Proceedings of the National Academy of Sciences,* 101**,** 9199-9204.

ASAHI, M., SUGITA, Y., KURZYDLOWSKI, K., DE LEON, S., TADA, M., TOYOSHIMA, C. & MACLENNAN, D. H. 2003. Sarcolipin regulates sarco (endo) plasmic reticulum Ca2+-ATPase (SERCA) by binding to transmembrane helices alone or in association with phospholamban. *Proceedings of the National Academy of Sciences,* 100**,** 5040-5045.

AYDIN, J., SHABALINA, I. G., PLACE, N., REIKEN, S., ZHANG, S.-J., BELLINGER, A. M., NEDERGAARD, J., CANNON, B., MARKS, A. R., BRUTON, J. D. & WESTERBLAD, H. 2008. Nonshivering thermogenesis protects against defective calcium handling in muscle. *The FASEB Journal,* 22**,** 3919-3924.

BAL, N. C., MAURYA, S. K., SINGH, S., WEHRENS, X. H. & PERIASAMY, M. 2016. Increased reliance on muscle-based thermogenesis upon acute minimization of brown adipose tissue function. *Journal of Biological Chemistry,* 291**,** 17247-17257.

BAL, N. C., MAURYA, S. K., SOPARIWALA, D. H., SAHOO, S. K., GUPTA, S. C., SHAIKH, S. A., PANT, M., ROWLAND, L. A., BOMBARDIER, E. & GOONASEKERA, S. A. 2012. Sarcolipin is a newly identified regulator of muscle-based thermogenesis in mammals. *Nature medicine,* 18**,** 1575-1579.

BARANY, M. 1967. ATPase activity of myosin correlated with speed of muscle shortening. *The Journal of general physiology,* 50**,** 197-218.

BARRE, H. & NEDERGAARD, J. 1987. Cold-induced changes in Ca2+ transport in duckling skeletal muscle mitochondria. *American Journal of Physiology-Regulatory, Integrative and Comparative Physiology,* 252**,** R1046-R1054.

BARTHOLOMEW, G. A. & WILKE, F. 1956. Body temperature in the northern fur seal, Callorhinus ursinus. *Journal of Mammalogy,* 37**,** 327-337.

BERGAMINI, C. M., GAMBETTI, S., DONDI, A. & CERVELLATI, C. 2004. Oxygen, reactive oxygen species and tissue damage. *Current pharmaceutical design,* 10**,** 1611-1626.

BERMAN, A. 2003. Effects of body surface area estimates on predicted energy requirements and heat stress. *Journal of Dairy Science,* 86**,** 3605-3610.

BHUPATHY, P., BABU, G. J. & PERIASAMY, M. 2007. Sarcolipin and phospholamban as regulators of cardiac sarcoplasmic reticulum Ca2+ ATPase. *Journal of molecular and cellular cardiology,* 42**,** 903-911.

BLIX, A. S. 2005. *Arctic animals and their adaptations to life on the edge*, Tapir Academic Press.

BLIX, A. S., FOLKOW, L. P. & NORDØY, E. S. 2013. Changing the Look on Seals from Pole to Pole with Satellite Technology. *Adaptation and Evolution in Marine Environments, Volume 2.* Springer.
BLIX, A. S., GRAV, H. J. & RONALD, K. 1979a. Some aspects of temperature regulation in newborn harp seal pups. *American Journal of Physiology-Regulatory, Integrative and Comparative Physiology,* 236**,** R188-R197.
BLIX, A. S., MILLER, L. K., KEYES, M. C., GRAV, H. J. & ELSNER, R. 1979b. Newborn northern fur seals (Callorhinus ursinus)--do they suffer from cold? *American Journal of Physiology-Regulatory, Integrative and Comparative Physiology,* 236**,** R322-R327.
BLIX, A. S. & STEEN, J. B. 1979. Temperature regulation in newborn polar homeotherms. *Physiological Reviews,* 59**,** 285-304.
BLIX, A. S., WALLØE, L., MESSELT, E. B. & FOLKOW, L. P. 2010. Selective brain cooling and its vascular basis in diving seals. *Journal of Experimental Biology,* 213**,** 2610-2616.
BLOCK, B. 1987. Strategies for regulating brain and eye temperatures: a thermogenic tissue in fish. *Comparative Physiology: Life in the Water and on Land (ed. P. Dejours, L. Bolis, CR Taylor and ER Weibel)***,** 401-420.
BLOCK, B. A. 1986. Structure of the brain and eye heater tissue in marlins, sailfish, and spearfishes. *Journal of Morphology,* 190**,** 169-189.
BLOCK, B. A. 1994. Thermogenesis in muscle. *Annual review of physiology,* 56**,** 535-577.
BOBE, R., BREDOUX, R., CORVAZIER, E., LACABARATZ-PORRET, C., MARTIN, V., KOVACS, T. & ENOUF, J. 2005. How many Ca2+ ATPase isoforms are expressed in a cell type? A growing family of membrane proteins illustrated by studies in platelets. *Platelets,* 16**,** 133-150.
BOMBARDIER, E., SMITH, I. C., VIGNA, C., FAJARDO, V. A. & TUPLING, A. R. 2013. Ablation of sarcolipin decreases the energy requirements for Ca2+ transport by sarco (endo) plasmic reticulum Ca2+-ATPases in resting skeletal muscle. *FEBS letters,* 587**,** 1687-1692.
BOWEN, W., BONESS, D. J. & OFTEDAL, O. T. 1987. Mass transfer from mother to pup and subsequent mass loss by the weaned pup in the hooded seal, Cystophora cristata. *Canadian Journal of Zoology,* 65**,** 1-8.
BOWEN, W. D., OFTEDAL, O. T. & BONESS, D. J. 1985. Birth to weaning in 4 days: remarkable growth in the hooded seal, Cystophora cristata. *Canadian Journal of Zoology,* 63**,** 2841-2846.
BRAND, M. 2000. Uncoupling to survive? The role of mitochondrial inefficiency in ageing. *Experimental gerontology,* 35**,** 811-820.
BRANDL, C., DELEON, S., MARTIN, D. & MACLENNAN, D. 1987. Adult forms of the Ca2+ ATPase of sarcoplasmic reticulum. Expression in developing skeletal muscle. *Journal of Biological Chemistry,* 262**,** 3768-3774.
BRANDL, C. J., GREEN, N. M., KORCZAK, B. & MACLENNAN, D. H. 1986. Two Ca2+ ATPase genes: Homologies and mechanistic implications of deduced amino acid sequences. *Cell,* 44**,** 597-607.
BRODY, S. 1945. Bioenergetics and growth; with special reference to the efficiency complex in domestic animals.
BROOKS, H. L. & LINDSEY, M. L. 2018. Guidelines for authors and reviewers on antibody use in physiology studies. *American Journal of Physiology-Heart and Circulatory Physiology,* 314**,** H724-H732.

BRÜCK, K. & WÜNNENBERG, B. Influence of ambient temperature in the process of replacement of nonshivering by shivering thermogenesis during postnatal development. Federation proceedings, 1966. 1332-1337.
BURNS, J., LESTYK, K., FOLKOW, L., HAMMILL, M. & BLIX, A. 2007. Size and distribution of oxygen stores in harp and hooded seals from birth to maturity. *Journal of Comparative Physiology B,* 177**,** 687-700.
BURNS, J. M. 1999. The development of diving behavior in juvenile Weddell seals: pushing physiological limits in order to survive. *Canadian Journal of Zoology,* 77**,** 737-747.
BURNS, J. M., SKOMP, N., BISHOP, N., LESTYK, K. & HAMMILL, M. 2010. Development of aerobic and anaerobic metabolism in cardiac and skeletal muscles from harp and hooded seals. *J Exp Biol,* 213**,** 740-8.
BUSIELLO, R. A., SAVARESE, S. & LOMBARDI, A. 2015. Mitochondrial uncoupling proteins and energy metabolism. *Frontiers in physiology,* 6**,** 36.
BUTLER, P. J. & JONES, D. R. 1997. Physiology of diving of birds and mammals. *Physiological reviews,* 77**,** 837-899.
CADENAS, S. 2018. Mitochondrial uncoupling, ROS generation and cardioprotection. *Biochimica et Biophysica Acta (BBA) - Bioenergetics,* 1859**,** 940-950.
CANNON, B. & NEDERGAARD, J. 2004. Brown adipose tissue: function and physiological significance. *Physiological reviews*.
CANNON, B. & VOGEL, G. 1977. The mitochondrial ATPase of brown adipose tissue Purification and comparison with the mitochondrial ATPase from beef heart. *Febs Letters,* 76**,** 284-289.
CAREY, F. G. 1982. A brain heater in the swordfish. *Science,* 216**,** 1327-1329.
CASTEILLA, L., CHAMPIGNY, O., BOUILLAUD, F., ROBELIN, J. & RICQUIER, D. 1989. Sequential changes in the expression of mitochondrial protein mRNA during the development of brown adipose tissue in bovine and ovine species. Sudden occurrence of uncoupling protein mRNA during embryogenesis and its disappearance after birth. *Biochemical Journal,* 257**,** 665-671.
CASTELLINI, M. & REA, L. 1992. The biochemistry of natural fasting at its limits. *Experientia,* 48**,** 575-582.
CHINNERY, P. F. & SCHON, E. A. 2003. Mitochondria. *Journal of Neurology, Neurosurgery & Psychiatry,* 74**,** 1188-1199.
CINTI, S. 2001. The adipose organ: morphological perspectives of adipose tissues. *Proceedings of the Nutrition Society,* 60**,** 319-328.
COLTMAN, D., STENSON, G., HAMMILL, M., HAUG, T., DAVIS, C. & FULTON, T. 2007. Panmictic population structure in the hooded seal (Cystophora cristata). *Molecular Ecology,* 16**,** 1639-1648.
CUNNINGHAM, F., ALLEN, J. E., ALLEN, J., ALVAREZ-JARRETA, J., AMODE, M R., ARMEAN, IRINA M., AUSTINE-ORIMOLOYE, O., AZOV, ANDREY G., BARNES, I., BENNETT, R., BERRY, A., BHAI, J., BIGNELL, A., BILLIS, K., BODDU, S., BROOKS, L., CHARKHCHI, M., CUMMINS, C., DA RIN FIORETTO, L., DAVIDSON, C., DODIYA, K., DONALDSON, S., EL HOUDAIGUI, B., EL NABOULSI, T., FATIMA, R., GIRON, C. G., GENEZ, T., MARTINEZ, JOSE G., GUIJARRO-CLARKE, C., GYMER, A., HARDY, M., HOLLIS, Z., HOURLIER, T., HUNT, T., JUETTEMANN, T., KAIKALA, V., KAY, M., LAVIDAS, I., LE, T., LEMOS, D., MARUGÁN, J. C., MOHANAN, S., MUSHTAQ, A., NAVEN, M., OGEH, DENYE N., PARKER, A., PARTON, A., PERRY, M., PILIŽOTA, I., PROSOVETSKAIA, I., SAKTHIVEL, MANOJ P.,

SALAM, AHAMED IMRAN A., SCHMITT, BIANCA M., SCHUILENBURG, H., SHEPPARD, D., PÉREZ-SILVA, JOSÉ G., STARK, W., STEED, E., SUTINEN, K., SUKUMARAN, R., SUMATHIPALA, D., SUNER, M.-M., SZPAK, M., THORMANN, A., TRICOMI, F. F., URBINA-GÓMEZ, D., VEIDENBERG, A., WALSH, THOMAS A., WALTS, B., WILLHOFT, N., WINTERBOTTOM, A., WASS, E., CHAKIACHVILI, M., FLINT, B., FRANKISH, A., GIORGETTI, S., HAGGERTY, L., HUNT, SARAH E., IISLEY, GARTH R., LOVELAND, JANE E., MARTIN, FERGAL J., MOORE, B., MUDGE, JONATHAN M., MUFFATO, M., PERRY, E., RUFFIER, M., TATE, J., THYBERT, D., TREVANION, STEPHEN J., DYER, S., HARRISON, PETER W., HOWE, KEVIN L., YATES, ANDREW D., ZERBINO, DANIEL R. & FLICEK, P. 2021. Ensembl 2022. *Nucleic Acids Research,* 50**,** D988-D995.

DALLY, S., BREDOUX, R., CORVAZIER, E., ANDERSEN, J. P., CLAUSEN, J. D., DODE, L., FANCHAOUY, M., GELEBART, P., MONCEAU, V. & DEL MONTE, F. 2006. Ca2+-ATPases in non-failing and failing heart: evidence for a novel cardiac sarco/endoplasmic reticulum Ca2+-ATPase 2 isoform (SERCA2c). *Biochemical Journal,* 395**,** 249-258.

DAVIS, M. W. & JORGENSEN, E. M. 2022. ApE, A Plasmid Editor: A Freely Available DNA Manipulation and Visualization Program. *Frontiers in Bioinformatics,* 2.

DAVIS, R. W. 2019. Metabolism and thermoregulation. *Marine mammals.* Springer.

DITTMER, A. & DITTMER, J. 2006. β - Actin is not a reliable loading control in Western blot analysis. *Electrophoresis,* 27**,** 2844-2845.

DONOHUE, M., COSTA, D., GOEBEL, M. & BAKER, J. 2000. The ontogeny of metabolic rate and thermoregulatory capabilities of northern fur seal, Callorhinus ursinus, pups in air and water. *Journal of Experimental Biology,* 203**,** 1003-1016.

DUCHAMP, C. & BARRE, H. 1993. Skeletal muscle as the major site of nonshivering thermogenesis in cold-acclimated ducklings. *American Journal of Physiology-Regulatory, Integrative and Comparative Physiology,* 265**,** R1076-R1083.

DUMONTEIL, E., BARRE, H. & MEISSNER, G. 1993. Sarcoplasmic reticulum Ca (2+)-ATPase and ryanodine receptor in cold-acclimated ducklings and thermogenesis. *American Journal of Physiology-Cell Physiology,* 265**,** C507-C513.

DURON, B. 1973. Postural and ventilatory functions of intercostal muscles. *Acta Neurobiol Exp,* 33**,** 355-380.

EBASHI, S. & ENDO, M. 1968. Calcium and muscle contraction. *Progress in biophysics and molecular biology,* 18**,** 123-183.

FAJARDO, V. A., BOMBARDIER, E., VIGNA, C., DEVJI, T., BLOEMBERG, D., GAMU, D., GRAMOLINI, A. O., QUADRILATERO, J. & TUPLING, A. R. 2013. Co-expression of SERCA isoforms, phospholamban and sarcolipin in human skeletal muscle fibers. *PLoS One,* 8**,** e84304.

FOLKOW, L. & BLIX, A. 1995. Distribution and diving behaviour of hooded seals. *Developments in Marine Biology,* 4**,** 193-202.

FOLKOW, L., BLIX, A. & EIDE, T. 1988. Anatomical and functional aspects of the nasal mucosal and ophthalmic retia of phocid seals. *Journal of Zoology,* 216**,** 417-436.

FOLKOW, L. P. 1992. Adrenergic vasomotor responses in nasal mucosa of hooded seals. *American Journal of Physiology-Regulatory, Integrative and Comparative Physiology,* 263**,** R1291-R1297.

FOLKOW, L. P. & BLIX, A. S. 1987. Nasal heat and water exchange in gray seals. *American Journal of Physiology-Regulatory, Integrative and Comparative Physiology,* 253**,** R883-R889.
FOLKOW, L. P., MÅRTENSSON, P.-E. & BLIX, A. S. 1996. Annual distribution of hooded seals (Cystophora cristata) in the Greenland and Norwegian Seas. *Polar Biology,* 16**,** 179-189.
FOLKOW, L. P., NORDØY, E. S. & BLIX, A. S. 2010. Remarkable development of diving performance and migrations of hooded seals (Cystophora cristata) during their first year of life. *Polar biology,* 33**,** 433-441.
FOSANG, A. J. & COLBRAN, R. J. 2015. Transparency is the key to quality. *Journal of Biological Chemistry,* 290**,** 29692-29694.
FREEMAN, B. 1971. Non-shivering thermogenesis in birds. *Non-shivering thermogenesis***,** 83-96.
FRIDOVICH, I. 2004. Mitochondria: are they the seat of senescence? *Aging cell,* 3**,** 13-16.
GASTEIGER, E., HOOGLAND, C., GATTIKER, A., WILKINS, M. R., APPEL, R. D. & BAIROCH, A. 2005. Protein identification and analysis tools on the ExPASy server. *The proteomics protocols handbook***,** 571-607.
GEMMELL, R., BELL, A. & ALEXANDER, G. 1972. Morphology of adipose cells in lambs at birth and during subsequent transition of brown to white adipose tissue in cold and in warm conditions. *American Journal of Anatomy,* 133**,** 143-163.
GEORGE, J., VALLYATHAN, N. & RONALD, K. 1971. The harp seal, Pagophilus groenlandicus (Erxleben, 1777). VII. A histophysiological study of certain skeletal muscles. *Canadian Journal of Zoology,* 49**,** 25-30.
GHOSH, R., GILDA, J. E. & GOMES, A. V. 2014. The necessity of and strategies for improving confidence in the accuracy of western blots. *Expert review of proteomics,* 11**,** 549-560.
GILDA, J. E., GHOSH, R., CHEAH, J. X., WEST, T. M., BODINE, S. C. & GOMES, A. V. 2015. Western blotting inaccuracies with unverified antibodies: need for a Western blotting minimal reporting standard (WBMRS). *PloS one,* 10**,** e0135392.
GJERTSEN, K. E., HORNELAND, P. A. & SKULSTAD, E. M. 2019. *Tema: Hooded seals* [Online]. Havforskningsinstituttet. Available: https://www.hi.no/en/hi/temasider/species/hooded-seals [Accessed 04/06 2022].
GNAIGER, E. 2020. Mitochondrial pathways and respiratory control: an introduction to OXPHOS analysis. *Bioenergetics Communications,* 2020**,** 2-2.
GRAV, H., BLIX, A. & PÅSCHE, A. 1974. How do seal pups survive birth in arctic winter? *Acta Physiologica Scandinavica,* 92**,** 427-429.
GRAV, H. & BLIX, A. S. 1979. A source of nonshivering thermogenesis in fur seal skeletal muscle. *Science,* 204**,** 87-89.
GRAV, H. J. & BLIX, A. S. 1976. Brown adipose tissue—a factor in the survival of harp seal pups. *Canadian journal of physiology and pharmacology,* 54**,** 409-412.
GUINET, C., DOMENICI, P., DE STEPHANIS, R., BARRETT-LENNARD, L., FORD, J. & VERBORGH, P. 2007. Killer whale predation on bluefin tuna: exploring the hypothesis of the endurance-exhaustion technique. *Marine Ecology Progress Series,* 347**,** 111-119.
GUTH, L. & SAMAHA, F. J. 1969. Qualitative differences between actomyosin ATPase of slow and fast mammalian muscle. *Experimental neurology,* 25**,** 138-152.
HALLIWELL, B. & GUTTERIDGE, J. M. 2015. *Free radicals in biology and medicine,* Oxford university press, USA.

HAMMILL, M. O. & STENSON, G. B. 2006. *Abundance of Northwest Atlantic harp seals (1960-2005),* Citeseer.
HAN, J., GAYAN-RAMIREZ, G., DEKHUIJZEN, R. & DECRAMER, M. 1993. Respiratory function of the rib cage muscles. *European Respiratory Journal,* 6**,** 722-728.
HANSEN, S. & LAVIGNE, D. M. 1997. Ontogeny of the thermal limits in the harbor seal (Phoca vitulina). *Physiological zoology,* 70**,** 85-92.
HAUG, T., NILSSEN, K. T. & LINDBLOM, L. 2004. Feeding habits of harp and hooded seals in drift ice waters along the east coast of Greenland in summer and winter. *Polar research,* 23**,** 35-42.
HILL, A. 1922. The mechanism of muscular contraction. *Physiological Reviews,* 2**,** 310-341.
HILL, R. W., WYSE, G. A. & ANDERSON, M. 2017. *Animal Physiology*, Oxford University Press.
HOHTOLA, E. Shivering thermogenesis in birds and mammals. Life in the cold: evolution, mechanisms, adaptation, and application. 12th International Hibernation Symposium, 2004. Citeseer, 241-252.
HOWELL, A. B. 1929. Contribution to the comparative anatomy of the eared and earless seals (genera Zalophus and Phoca). *Proceedings of the United States National Museum*.
HUIJING, F. & SLATER, E. 1961. The use of oligomycin as an inhibitor of oxidative phosphorylation. *The Journal of Biochemistry,* 49**,** 493-501.
HULL, D. 1966. The structure and function of brown adipose tissue. *British Medical Bulletin,* 22**,** 92-96.
HUXLEY, A. 1974. Muscular contraction. *The Journal of physiology,* 243**,** 1.
ICES 2019. ICES/NAFO/NAMMCO WORKING GROUP ON HARP AND HOODED SEALS

(WGHARP) *ICES Scientific Reports.*
INNES, S., WORTHY, G., LAVIGNE, D. & RONALD, K. 1990. Surface areas of phocid seals. *Canadian journal of zoology,* 68**,** 2531-2538.
IRVING, L. 1973. Aquatic mammals. *Comparative physiology of thermoregulation.* Elsevier.
IRVING, L. & HART, J. 1957. The metabolism and insulation of seals as bare-skinned mammals in cold water. *Canadian Journal of Zoology,* 35**,** 497-511.
JACKSON, D. C. & SCHMIDT-NIELSEN, K. 1964. Countercurrent heat exchange in the respiratory passages. *Proceedings of the National Academy of Sciences of the United States of America,* 51**,** 1192.
JANSSEN, I., HEYMSFIELD, S. B., WANG, Z. & ROSS, R. 2000. Skeletal muscle mass and distribution in 468 men and women aged 18–88 yr. *Journal of applied physiology*.
JOHNSEN, H. K., BLIX, A. S., JORGENSEN, L. & MERCER, J. B. 1985. Vascular basis for regulation of nasal heat exchange in reindeer. *American Journal of Physiology-Regulatory, Integrative and Comparative Physiology,* 249**,** R617-R623.
JOHNSON, R. E. 1968. Temperature regulation in the white-tailed ptarmigan Lagopus leucurus.
JOHNSTON, D. W. 1971. The absence of brown adipose tissue in birds. *Comparative Biochemistry and Physiology***,** 1107-1108.
KANATOUS, S. B., DAVIS, R. W., WATSON, R., POLASEK, L., WILLIAMS, T. M. & MATHIEU-COSTELLO, O. 2002. Aerobic capacities in the skeletal muscles of Weddell seals: key to longer dive durations? *Journal of Experimental Biology,* 205**,** 3601-3608.

KAPEL, F. O. 2000. Feeding habits of harp and hooded seals in Greenland waters. *NAMMCO Sci. Publ,* 2**,** 50-64.
KORSHUNOV, S. S., SKULACHEV, V. P. & STARKOV, A. A. 1997. High protonic potential actuates a mechanism of production of reactive oxygen species in mitochondria. *FEBS letters,* 416**,** 15-18.
KOVACS, K. M. 2009. Hooded seal: Cystophora cristata. *Encyclopedia of marine mammals.* Elsevier.
KUBO, H., LIBONATI, J. R., KENDRICK, Z. V., PAOLONE, A., GAUGHAN, J. P. & HOUSER, S. R. 2003. Differential effects of exercise training on skeletal muscle SERCA gene expression. *Medicine and science in sports and exercise,* 35**,** 27-31.
KVADSHEIM, P. & FOLKOW, L. 1997. Blubber and flipper heat transfer in harp seals. *Acta Physiologica Scandinavica,* 161**,** 385-395.
KVADSHEIM, P. H. & AARSETH, J. J. 2002. Thermal function of phocid seal fur. *Marine Mammal Science,* 18**,** 952-962.
KVADSHEIM, P. H., FOLKOW, L. P. & BLIX, A. S. 2005. Inhibition of shivering in hypothermic seals during diving. *American Journal of Physiology-Regulatory, Integrative and Comparative Physiology,* 289**,** R326-R331.
LABE, Z. 2022. *Arctic Temperatures* [Online]. Available: https://sites.uci.edu/zlabe/arctic-temperatures/ [Accessed June 2022].
LAPIERRE, J. L., SCHREER, J. F., BURNS, J. M. & HAMMILL, M. O. 2004. Developmental changes in cardiorespiratory patterns associated with terrestrial apnoeas in harbour seal pups. *Journal of experimental biology,* 207**,** 3891-3898.
LARDY, H. A., JOHNSON, D. & MCMURRAY, W. 1958. Antibiotics as tools for metabolic studies. I. A survey of toxic antibiotics in respiratory, phosphorylative and glycolytic systems. *Archives of biochemistry and biophysics,* 78**,** 587-597.
LARSSON, L., EDSTROM, L., LINDEGREN, B., GORZA, L. & SCHIAFFINO, S. 1991. MHC composition and enzyme-histochemical and physiological properties of a novel fast-twitch motor unit type. *American Journal of Physiology-Cell Physiology,* 261**,** C93-C101.
LAVIGNE, D. & KOVACS, K. 1988. Harps and Hoods, Ice-breeding Seals ofthe Northwest Atlantic. Universit y of Wate rloo Press, Wa terloo, Ontario.
LAVIGNE, D. M., INNES, S., WORTHY, G. A. J., KOVACS, K. M., SCHMITZ, O. J. & HICKIE, J. P. 1986. Metabolic rates of seals and whales. *Canadian Journal of Zoology,* 64**,** 279-284.
LAVOISIER, A. & LAPLACE, P. 1783. Mémoire de la Chaleur. *Académie Royale des Sciences*.
LAVOISIER, A. L. 1862. *Oeuvres de Lavoisier: Mémoire de chimie et de physique*, Ministre de L'instruction Publique et des Cultes.
LYDERSEN, C., KOVACS, K. & HAMMILL, M. 1997. Energetics during nursing and early postweaning fasting in hooded seal (Cystophora cristata) pups from the Gulf of St Lawrence, Canada. *Journal of Comparative Physiology B,* 167**,** 81-88.
MACLENNAN, D. H. 1974. Isolation of proteins of the sarcoplasmic reticulum. *Methods in Enzymology.* Academic Press.
MACLENNAN, D. H., BRANDL, C. J., KORCZAK, B. & GREEN, N. M. 1985. Amino-acid sequence of a Ca2++ Mg2+-dependent ATPase from rabbit muscle sarcoplasmic reticulum, deduced from its complementary DNA sequence. *Nature,* 316**,** 696-700.

MACLENNAN, D. H., RICE, W. J. & GREEN, N. M. 1997. The mechanism of Ca2+ transport by sarco (endo) plasmic reticulum Ca2+-ATPases. *Journal of Biological Chemistry*, 272**,** 28815-28818.
MALL, S., BROADBRIDGE, R., HARRISON, S. L., GORE, M. G., LEE, A. G. & EAST, J. M. 2006. The Presence of Sarcolipin Results in Increased Heat Production by Ca2+-ATPase*. *Journal of Biological Chemistry*, 281**,** 36597-36602.
MEEH, K. V. 1879. Ober flahenmessungen des mensch-lichen kopers. *Zeitschrift fur biologie*, 15**,** S. 425-S. 458.
MITCHELL, J. W. & MYERS, G. E. 1968. An analytical model of the counter-current heat exchange phenomena. *Biophysical journal*, 8**,** 897-911.
MITCHELL, P. 1961. Coupling of phosphorylation to electron and hydrogen transfer by a chemi-osmotic type of mechanism. *Nature*, 191**,** 144-148.
NÆRINGS- OG FISKERIDEPARTEMENTET. 2022. *Forskrift om utøvelse av selfangst* [Online]. LOVDATA. Available: https://lovdata.no/dokument/LTI/forskrift/2022-04-28-763 [Accessed].
NATIONAL LIBRARY OF MEDICINE (US) 2004. LepWed 1.0. National Center for Biotechnology.
NEDERGAARD, J. & CANNON, B. 1992. The uncoupling protein thermogenin and mitochondrial thermogenesis. *New comprehensive biochemistry*. Elsevier.
NEEDHAM, D. M. 1926. Red and white muscle. *Physiological Reviews*, 6**,** 1-27.
NOHL, H. & HEGNER, D. 1978. Do mitochondria produce oxygen radicals in vivo? *European journal of biochemistry*, 82**,** 563-567.
NOWACK, J., GIROUD, S., ARNOLD, W. & RUF, T. 2017. Muscle non-shivering thermogenesis and its role in the evolution of endothermy. *Frontiers in Physiology*, 8**,** 889.
NOWACK, J., VETTER, S. G., STALDER, G., PAINER, J., KRAL, M., SMITH, S., LE, M. H., JURCEVIC, P., BIEBER, C. & ARNOLD, W. 2019. Muscle nonshivering thermogenesis in a feral mammal. *Scientific reports*, 9**,** 1-10.
ODERMATT, A., KURZYDLOWSKI, K. & MACLENNAN, D. H. 1996. The Vmax of the Ca2+-ATPase of Cardiac Sarcoplasmic Reticulum (SERCA2a) Is Not Altered by Ca2+/Calmodulin-dependent Phosphorylation or by Interaction with Phospholamban*. *Journal of Biological Chemistry*, 271**,** 14206-14213.
ODERMATT, A., TASCHNER, P. E., SCHERER, S. W., BEATTY, B., KHANNA, V. K., CORNBLATH, D. R., CHAUDHRY, V., YEE, W.-C., SCHRANK, B. & KARPATI, G. 1997. Characterization of the gene encoding human sarcolipin (SLN), a proteolipid associated with SERCA1: absence of structural mutations in five patients with Brody disease. *Genomics*, 45**,** 541-553.
OFTEDAL, O. T. Milk composition, milk yield and energy output at peak lactation: a comparative review. Symposia of the Zoological Society of London, 1984. 33-85.
OFTEDAL, O. T., BONESS, D. J. & BOWEN, W. D. 1988. The composition of hooded seal (Cystophora cristata) milk: an adaptation for postnatal fattening. *Canadian Journal of Zoology*, 66**,** 318-322.
OLIVER, K., SEDDON, A. & TRASK, R. S. 2016. Morphing in nature and beyond: a review of natural and synthetic shape-changing materials and mechanisms. *Journal of Materials Science*, 51**,** 10663-10689.
OSIEWACZ, H. D. & SCHECKHUBER, C. Q. 2006. Impact of ROS on ageing of two fungal model systems: Saccharomyces cerevisiae and Podospora anserina. *Free radical research*, 40**,** 1350-1358.

PEARSON, L. E., HAMMILL, M. O. & BURNS, J. M. 2011. Brown adipose tissue and non‐shivering thermogenesis aid harp seals (Pagophilus groenlandicus) but not hooded seals (Cystophora cristata) or Weddell seals (Leptonychotes weddelli) at birth.
PEARSON, L. E., LIWANAG, H. E., HAMMILL, M. O. & BURNS, J. M. 2014. Shifts in thermoregulatory strategy during ontogeny in harp seals (Pagophilus groenlandicus). *Journal of Thermal Biology,* 44**,** 93-102.
PERIASAMY, M., HERRERA, J. L. & REIS, F. C. 2017. Skeletal muscle thermogenesis and its role in whole body energy metabolism. *Diabetes & metabolism journal,* 41**,** 327.
PERIASAMY, M. & KALYANASUNDARAM, A. 2007. SERCA pump isoforms: their role in calcium transport and disease. *Muscle & Nerve: Official Journal of the American Association of Electrodiagnostic Medicine,* 35**,** 430-442.
POLOVINA, J. J., HAWN, D. & ABECASSIS, M. 2008. Vertical movement and habitat of opah (Lampris guttatus) in the central North Pacific recorded with pop-up archival tags. *Marine Biology,* 153**,** 257-267.
PORTER, C., REIDY, P. T., BHATTARAI, N., SIDOSSIS, L. S. & RASMUSSEN, B. B. 2015. Resistance exercise training alters mitochondrial function in human skeletal muscle. *Medicine and science in sports and exercise,* 47**,** 1922.
RACKER, E. 1963. A mitochondrial factor conferring oligomycin sensitivity on soluble mitochondrial ATPase. *Biochemical and Biophysical Research Communications,* 10**,** 435-439.
RAMIREZ, J.-M., FOLKOW, L. P. & BLIX, A. S. 2007. Hypoxia tolerance in mammals and birds: from the wilderness to the clinic. *Annual review of physiology,* 69**,** 113-143.
RASMUSSEN, B. 1960. On the hooded seal stock in the North Atlantic Ocean. *Fisken Havet,* 1**,** 1-23.
ROLFE, D. & BRAND, M. D. 1996. Contribution of mitochondrial proton leak to skeletal muscle respiration and to standard metabolic rate. *American Journal of Physiology-Cell Physiology,* 271**,** C1380-C1389.
ROMERO-CALVO, I., OCÓN, B., MARTÍNEZ-MOYA, P., SUÁREZ, M. D., ZARZUELO, A., MARTÍNEZ-AUGUSTIN, O. & DE MEDINA, F. S. 2010. Reversible Ponceau staining as a loading control alternative to actin in Western blots. *Analytical Biochemistry,* 401**,** 318-320.
ROWLAND, L. A., BAL, N. C. & PERIASAMY, M. 2015. The role of skeletal-muscle-based thermogenic mechanisms in vertebrate endothermy. *Biol Rev Camb Philos Soc,* 90**,** 1279-97.
RUNCIE, R. M., DEWAR, H., HAWN, D. R., FRANK, L. R. & DICKSON, K. A. 2009. Evidence for cranial endothermy in the opah (Lampris guttatus). *Journal of Experimental Biology,* 212**,** 461-470.
SAARELA, S., KEITH, J. S., HOHTOLA, E. & TRAYHURN, P. 1991. Is the "mammalian" brown fat-specific mitochondrial uncoupling protein present in adipose tissues of birds? *Comparative Biochemistry and Physiology Part B: Comparative Biochemistry,* 100**,** 45-49.
SAHOO, S. K., SHAIKH, S. A., SOPARIWALA, D. H., BAL, N. C. & PERIASAMY, M. 2013. Sarcolipin protein interaction with sarco (endo) plasmic reticulum Ca2+ ATPase (SERCA) is distinct from phospholamban protein, and only sarcolipin can promote uncoupling of the SERCA pump. *Journal of Biological Chemistry,* 288**,** 6881-6889.
SANDELL, M. 1990. The evolution of seasonal delayed implantation. *The Quarterly Review of Biology,* 65**,** 23-42.

SANDER, H., WALLACE, S., PLOUSE, R., TIWARI, S. & GOMES, A. V. 2019. Ponceau S waste: Ponceau S staining for total protein normalization. *Analytical Biochemistry,* 575**,** 44-53.
SCHIAFFINO, S. & REGGIANI, C. 2011. Fiber types in mammalian skeletal muscles. *Physiological reviews,* 91**,** 1447-1531.
SCHMIDT-NIELSEN, K. 1997. *Animal physiology: adaptation and environment,* Cambridge university press.
SCHOLANDER, P., HOCK, R., WALTERS, V., JOHNSON, F. & IRVING, L. 1950. Heat regulation in some arctic and tropical mammals and birds. *The Biological Bulletin,* 99**,** 237-258.
SCHOLANDER, P. F. 1940. *Experimental investigations on the respiratory function in diving mammals and birds*, I kommisjon hos Jacob Dybwad.
SCHOLANDER, P. F. 1957. The wonderful net. *Scientific American,* 196**,** 96-110.
SCHOLANDER, P. F. & SCHEVILL, W. E. 1955. Counter-current vascular heat exchange in the fins of whales. *Journal of Applied Physiology,* 8**,** 279-282.
SCHOTS, P. C., BUE, M. E. & NORDØY, E. S. 2017. Hooded seal (Cystophora cristata) pups ingest snow and seawater during their post-weaning fast. *Journal of Comparative Physiology B,* 187**,** 493-502.
SERGEANT, D. E. 1974. A rediscovered whelping population of hooded seals Cystophora cristata Erxleben and its possible relationship to other populations. *Polarforschung,* 44**,** 1-7.
SHAIKH, S. A., SAHOO, S. K. & PERIASAMY, M. 2016. Phospholamban and sarcolipin: Are they functionally redundant or distinct regulators of the Sarco (Endo) Plasmic Reticulum Calcium ATPase? *Journal of molecular and cellular cardiology,* 91**,** 81-91.
SIEVERS, F., WILM, A., DINEEN, D., GIBSON, T. J., KARPLUS, K., LI, W., LOPEZ, R., MCWILLIAM, H., REMMERT, M. & SÖDING, J. 2011. Fast, scalable generation of high‐quality protein multiple sequence alignments using Clustal Omega. *Molecular systems biology,* 7**,** 539.
SMITH, P. E., KROHN, R. I., HERMANSON, G. T., MALLIA, A. K., GARTNER, F. H., PROVENZANO, M., FUJIMOTO, E. K., GOEKE, N. M., OLSON, B. J. & KLENK, D. 1985. Measurement of protein using bicinchoninic acid. *Analytical biochemistry,* 150**,** 76-85.
SMITH, W. S., BROADBRIDGE, R., EAST, J. M. & LEE, A. G. 2002. Sarcolipin uncouples hydrolysis of ATP from accumulation of Ca2+ by the Ca2+-ATPase of skeletal-muscle sarcoplasmic reticulum. *Biochemical Journal,* 361**,** 277-286.
SOPPELA, P., NIEMINEN, M., SAARELA, S., KEITH, J. S., MORRISON, J. N., MACFARLANE, F. & TRAYHURN, P. 1991. Brown fat-specific mitochondrial uncoupling protein in adipose tissues of newborn reindeer. *American Journal of Physiology-Regulatory, Integrative and Comparative Physiology,* 260**,** R1229-R1234.
STAINSBY, W. N. & LAMBERT, C. R. 1979. Determinants of oxygen uptake in skeletal muscle. *Exercise and sport sciences reviews,* 7**,** 125-152.
STOFFEL, M. A., ACEVEDO‐WHITEHOUSE, K., MORALES‐DURÁN, N., GROSSER, S., CHAKAROV, N., KRÜGER, O., NICHOLS, H. J., ELORRIAGA‐VERPLANCKEN, F. R. & HOFFMAN, J. I. 2020. Early sexual dimorphism in the developing gut microbiome of northern elephant seals. *Molecular ecology,* 29**,** 2109-2122.
SYMONDS, M. E., POPE, M. & BUDGE, H. 2015. The ontogeny of brown adipose tissue. *Annual review of nutrition,* 35**,** 295-320.

THELLIN, O., ZORZI, W., LAKAYE, B., DE BORMAN, B., COUMANS, B., HENNEN, G., GRISAR, T., IGOUT, A. & HEINEN, E. 1999. Housekeeping genes as internal standards: use and limits. *Journal of biotechnology,* 75**,** 291-295.

TIMMERMANS, M. L. & LABE, Z. 2021. Sea Surface Temperature.

TOWBIN, H., STAEHELIN, T. & GORDON, J. 1979. Electrophoretic transfer of proteins from polyacrylamide gels to nitrocellulose sheets: procedure and some applications. *Proceedings of the National Academy of Sciences,* 76**,** 4350-4354.

VÁZQUEZ-MEDINA, J., OLGUÍN-MONROY, N., MALDONADO, P., SANTAMARÍA, A., KÖNIGSBERG, M., ELSNER, R., HAMMILL, M., BURNS, J. & ZENTENO-SAVÍN, T. 2011. Maturation increases superoxide radical production without increasing oxidative damage in the skeletal muscle of hooded seals (Cystophora cristata). *Canadian Journal of Zoology,* 89**,** 206-212.

WAWRZYNOW, A., THEIBERT, J. L., MURPHY, C., JONA, I., MARTONOSI, A. & COLLINS, J. H. 1992. Sarcolipin, the "proteolipid" of skeletal muscle sarcoplasmic reticulum, is a unique, amphipathic, 31-residue peptide. *Archives of Biochemistry and Biophysics,* 298**,** 620-623.

WILLIAMS, T. M., HAUN, J., DAVIS, R. W., FUIMAN, L. A. & KOHIN, S. 2001. A killer appetite: metabolic consequences of carnivory in marine mammals. *Comparative Biochemistry and Physiology Part A: Molecular & Integrative Physiology,* 129**,** 785-796.

WRIGHT, T., DAVIS, R. W., PEARSON, H. C., MURRAY, M. & SHEFFIELD-MOORE, M. 2021. Skeletal muscle thermogenesis enables aquatic life in the smallest marine mammal. *Science,* 373**,** 223-225.

WRIGHT, T. J., DAVIS, R. W., HOLSER, R. R., HÜCKSTÄDT, L. A., DANESI, C. P., PORTER, C., WIDEN, S. G., WILLIAMS, T. M., COSTA, D. P. & SHEFFIELD-MOORE, M. 2020. Changes in northern elephant seal skeletal muscle following thirty days of fasting and reduced activity. *Frontiers in physiology***,** 1295.

ZARAIN-HERZBERG, A., MACLENNAN, D. & PERIASAMY, M. 1990. Characterization of rabbit cardiac sarco (endo) plasmic reticulum Ca2 (+)-ATPase gene. *Journal of Biological Chemistry,* 265**,** 4670-4677.

ZENTENO-SAVíN, T., CLAYTON-HERNÁNDEZ, E. & ELSNER, R. 2002. Diving seals: are they a model for coping with oxidative stress? *Comparative Biochemistry and Physiology Part C: Toxicology & Pharmacology,* 133**,** 527-536.

ZOROV, D., PLOTNIKOV, E., JANKAUSKAS, S., ISAEV, N., SILACHEV, D., ZOROVA, L., PEVZNER, I., PULKOVA, N., ZOROV, S. & MOROSANOVA, M. 2012. The phenoptosis problem: what is causing the death of an organism? Lessons from acute kidney injury. *Biochemistry (Moscow),* 77**,** 742-753.

ZURLO, F., LARSON, K., BOGARDUS, C. & RAVUSSIN, E. 1990. Skeletal muscle metabolism is a major determinant of resting energy expenditure. *The Journal of clinical investigation,* 86**,** 1423-1427.